

UNIVERSIDADE DE LISBOA

FACULDADE DE CIÊNCIAS

DEPARTAMENTO DE FÍSICA



**Development of a Mechatronic Platform for Passive Tactile Stimulation
Using a Rotating Drum with Embossed Patterns**

Rodrigo Nogueira Januário

Mestrado em Engenharia Biomédica e Biofísica

Dissertação Orientador:
Professor Doutor Calogero Maria Oddo
Professor Doutor Alexandre Andrade

2023

Acknowledgments

I would like to thank each and everyone that has helped me directly or indirectly in this journey, without all these people this would not be possible.

I would like to thank first and foremost, myself, for embarking in this journey, for never giving up or saying “no” to a new challenge, for the dedication and love I showed to the project and for committing to it until the end even when the odds were not in my favor.

Secondly, I want to give the biggest and most sincere gratitude to Giacomo D’Alesio, without him this project would have never been possible. Thank you for your guidance and knowledge, for never giving up on me and enduring this journey by my side, even during weekends or your honeymoon. I will not forget I owe you one for the 4098. Big hug Giacomo <3

I want to thank Calogero Oddo and Sara Ballanti for making this opportunity a reality, for accepting me in the lab with open arms and for being always by my side if I needed anything, you never gave up on this, and I will not forget that.

I want to thank Professor Alexandre Andrade for accepting being my tutor and calming me when I was most in doubt.

I give to my family and specially my parents the most heartwarming gratitude, for the man they helped me become, for the values they thought me and for making this opportunity possible. Thank you so so much!! Darei à minha família e especialmente aos meus pais o mais caloroso agradecimento de todos, por me ajudarem a crescer e a tornar-me na pessoa que sou hoje, pelos valores que me transmitiram e por me permitirem e apoiarem nesta aventura.

They have been always here and I hope they will be forever, with no order of importance Tomas, Pedro, Marta, André, Gonçalo, Rafa, Alberto, Juja, Bibas, Kekas, João, Maria, Margarida, Tiago, não precisam de apelidos que vocês sabem que são. Thank you so so much for being here since the beginning and for never letting me down, for the laughs, the hugs, the words of affirmation, the harsh talks and the late night ones, for making me grow and seeing me grow, I will be forever thankful like I never been for something in my life.

I thank all the people that I made friends with, but couldn’t mention above, you know you were important to me, and I will never forget what we talked, did and what you taught me, I am grateful.

A huge “I miss you” hug to all the people I have met in Italy, to Garcia, Mario, Juvandes, Torrinha, Maria, Sofia, Xico, Nogueira, Enrico, Hugo, Sara, Gloria, Teresa, Marcela, Pedro, Alex, Iris, Marta, Inês, Lilah and the boring French guys, the crazy Germans, and to all the people I have come across and talked to but never got the chance to make friends with.

Just to force you to read this in English, the biggest and most important “thank you” of all goes to Mariana Tarouca, for the talks and the walks, for the hugs and snugs, and for being the best thing I could have wishes for. Thank you for being here, and I will always be here too.

I would also like to thank the small stuff: my bike, my peanut and chocolate sandwich, my mozzarellas, palestra olimpya, piazza Vettovaglie, the moreti beer, the ice cream, the bombolos, the bridge, 41 bis, my plastic 3D printed hand and the shop owners in Vetto.

Finally, I thank the Erasmus + program for giving to student’s opportunities like this which are life changing and make us grow so much, as individuals and as a community, thank you.

To all the people I haven’t mentioned, which were important but whom life made us grow apart, thank you, if you were special once upon a time, you will mean a lot forever.

Abstract

Here by it is presented Emily, an automatically controlled mechatronic platform for passive tactile stimulation using a rotating drum with different embedded textured surfaces. The stimulator has two DC motors and therefore two degrees of freedom, one from the rotating drum and one from the linear guide where the drum is mounted, which moves the stimulator along the guide changing the stimuli presented to the subject. The stimulator is a in house design built with 3D printed components with a versatile design concept allowing for a variety of experimental protocols. The platform uses a sbRIO-9637 with LabVIEW FPGA installed, which guarantees a high degree of flexibility on how the platform can be programmed to operate. The goal of this platform is to create an automatically controlled, versatile, and standardized manner of performing tactile stimulation while conducting parallel electrophysiological and psychophysiological tests to deepen our understanding of the neuronal processes underlying the human sense of touch. Emily comprises a series of advantages such as (1) automatic control; (2) small size and ease of transportation; (3) control of the motors rotation speed; (4) display of the contact force exerted by the subject in real-time by a force sensor; (5) stimulation with different topographies in short intervals; (6) the use of the sbRIO with LabVIEW FPGA embedded making the experimental protocol configurable, improvable and versatile, while allowing to view live the status of the platform with great accuracy; (7) low electromagnetic interference by the use of a linear current amplifier; (8) use of commercially available components. This thesis is a guide on how the platform was thought out, designed, and built, so that in the future other investigators can recreate, and improve upon it to further progress our knowledge of the neural processes of touch in humans.

Key words: Mechatronic, Stimulator, Passive, Touch, Psychophysics

Resumo

O tato é a capacidade inata de um ser vivo sentir o ambiente em seu redor através do contacto físico com o mesmo. Este contacto é registado por neurónios sensoriais que os animais possuem na pele que ao serem estimulados emitem informação sobre a estrutura em que tocam para o sistema nervoso central.

A utilidade deste sentido transcende variadas vezes a nossa noção basal do quotidiano humano porque é impossível “desligá-lo”, não nos permitindo compreender totalmente o impacto que tem nas nossas vidas.

As principais utilidades do tato são a comunicação e a sobrevivência. A primeira surge por diferentes meios como um abraço, um aperto de mão ou até mesmo atos violentos como um encontrão na rua ou um soco. A segunda provém da distinção empírica do que é potencialmente seguro ou perigoso, desde superfícies rugosas ou com espinhos ou matérias quentes até objetos macios e confortáveis. O tato permite ainda sentir matérias em outros estados físicos, como a água nas marés, o ar, como o vento ou vibrações causadas por objetos distantes. Durante a infância o tato apresenta ainda um importante papel no desenvolvimento, permitindo ao bebé criar uma relação afetuosa com os seus progenitores, aumentando a capacidade de sobrevivência e impulsionando o crescimento do seu cérebro.

Durante o contacto o ser humano é capaz de reconhecer e distinguir, a partir da sua enorme variedade de recetores táteis, a forma e textura dos objetos usando apenas exploração tátil. Apenas com a necessidade de haver contacto físico entre as duas matérias, não importando se a pele toca no objeto (exploração ativa) ou o objeto na pele (exploração passiva).

Contudo, existem pessoas que por razões genéticas, perda da funcionalidade dos recetores táteis, ou remoção de um membro não conseguem ter acesso a este sentido. Atualmente, a ciência procura criar próteses que consigam devolver às pessoas esta habilidade, mas para o fazer é primeiro necessário compreender como o cérebro regista a informação sobre as texturas, como as distingue e como é propagada a informação. Desta forma, esta dissertação foca-se no desenvolvimento de uma plataforma mecatrónica que realiza estimulação tátil dos dedos da mão usando um cilindro rotativo com diferentes padrões topográficos embutidos.

De forma a compreender como a estimulação tátil opera serão realizados testes neurofisiológicos em paralelo que estudam a atividade elétrica tanto durante a transmissão da informação para o cérebro, microneurografia, como a atividade cerebral durante o processamento da mensagem, eletroencefalografia. Serão também realizados testes psicofísicos para relacionar a perceção do sujeito com as características de cada estímulo (rugosidade, velocidade e forma).

O estudo da estimulação tátil desde sempre necessitou que um investigador estimulasse ativamente o paciente, o que devido a incapacidades humanas cria experiências desiguais dado que fatores como, a força aplicada e a velocidade de estimulação não são possíveis de manter constantes de experiência para experiência. Para standardizar estas experiências e as tornar mais eficientes foram criadas máquinas robóticas que fazem a estimulação pelo investigador, mantendo os parâmetros referidos constantes e tornando todo o processo mais automático e autónomo.

A Emily é uma plataforma robótica autónoma para estimulação tátil passiva do dedo com dois graus de liberdade, que usa um cilindro rotativo com padrões de diferentes texturas embutidos, esta é

suportada sobre uma guia horizontal que desloca o cilindro lateralmente alterando a topografia usada para estimular o paciente.

Esta plataforma foi construída de modo a replicar alguns avanços feitos previamente por outros engenheiros e investigadores em outras máquinas, fundindo o máximo possível de benefícios de todas as plataformas numa só. As vantagens da Emily em relação às outras plataformas contruídas são: autonomia e independência de controlo humano para realizar experiências; o tamanho reduzido e facilidade de transporte; a capacidade de controlar a velocidade de rotação do motor a qualquer momento durante a experiência e mantê-la constante; Exibição da força de contacto exercida pelo paciente em tempo real; estimulação com diferentes topografias em intervalos de tempo muito curtos; a filosofia de programação da maquina é configurável e melhorável, devido ao LabVIEW FPGA embutido no hardware que a controla, dando ao utilizador uma versatilidade quase infinita de experiências que pode realizar e permitindo ter acesso ao estado da maquina em direto e com grande precisão; utilização de um amplificador com reduzida interferência eletromagnética, de modo a não danificar os dados de testes mais sensíveis como a microneurografia; construída com materiais facilmente obtidos comercialmente, sendo fácil de recriar em qualquer laboratório.

Estruturalmente a plataforma é composta pelo suporte do cilindro, que estimula o paciente, e por uma caixa que engloba todos os componentes eletrónicos e conexões entre os mesmos.

O suporte do cilindro foi impresso em 3D e tem uma forma de “U” com dois “U’s” perpendiculares a este em cada um dos braços. No centro do suporte encontra-se o cilindro apoiado nos braços do suporte. O cilindro é formado por um prisma hexagonal carregado com vários cilindros com diferentes texturas na sua superfície lateral, sendo suportado no braço esquerdo por um motor rotativo que o controla e por um rolamento no lado direito. Na base do suporte encontram-se outras estruturas impressas que o conectam à guia linear e um medidor de força aplicada, que mede a força que o paciente aplica no cilindro durante estimulação. A guia inclui um motor que transforma o movimento rotativo em linear e desliza o suporte ao longo da mesma. Em cada um dos motores encontra-se um codificador que regista indiretamente a posição quer do suporte na guia como do cilindro no seu movimento rotativo através do número de iterações que executa enquanto gira.

A plataforma é alimentada por uma conexão com um adaptador da parede que envia 220V para a caixa que contem os componentes eletrónicos. Dai passa por um disjuntor, um mecanismo de segurança que corta a alimentação caso haja um curto-circuito, e de seguida para conversores de energia de corrente alternada para direta, cada um fornecendo uma voltagem especifica dependendo do que iram alimentar. Dentro desta caixa encontra-se o controlador da plataforma, o sbRIO-9637, com o programa LabVIEW FPGA embutido, permitindo criar, adaptar e melhorar as operações executadas pela placa e de todos os componentes ligados a esta, através de uma linguagem de programação versátil e funcional. O sbRIO receberá a informação do estado da plataforma pelos codificadores usando-a para controlar os motores sobre que operação executar a cada iteração dos mesmos.

Como intermediários para a conexão entre o sbRIO e cada motor temos o amplificador “*Linear Actuator Amplifier, LCAM-1*” que controla o motor superior responsável pelo cilindro e um conversor “*TRACO POWER CONVERTER*” de 15V que conecta a um *buffer* acoplado que conduz o motor inferior associado à guia linear. O sistema apresenta ainda ventilação de maneira a evitar o sobreaquecimento dos seus componentes.

Para controlar a plataforma foi criado um código no programa LabVIEW FPGA que utiliza cada iteração dos codificadores como um marcador para introduzir no sistema uma operação especifica. O

motor que controla o cilindro foi mantido em rotação constante, existindo para o mesmo apenas um input de voltagem no programa que permite alterar este valor em tempo real.

O motor que controla a guia terá de parar em locais específicos para o paciente entrar em contacto com o cilindro. Como tal, foram definidos marcadores onde a plataforma iria parar, se o suporte não se encontrar nesse marcador deslocar-se-ia até ao mesmo, através da indução de voltagem do buffer no motor, movendo a guia. Ao atingir o marcador o buffer passa a fornecer 0 V, o suporte imobiliza-se durante um tempo definido ocorrendo a estimulação nesse período. Com o término do tempo define-se um novo destino para o suporte e é de novo fornecida voltagem ao motor. Para definir os marcadores ao longo da guia foi desenhado um contador de iterações do codificador, a guia foi definida empiricamente como tendo 118096 iterações, logo esta medida foi usada como uma escala de 118096 pontos e daí as posições de paragem são definidas de acordo com o local real que se pretende que a plataforma pare. De modo a certificar a exatidão dos dados dos codificadores foi criado um filtro que remove as flutuações ocorrentes durante o envio do sinal, estabilizando-o.

De modo a verificar a validade dos controladores, contadores e filtros vários testes foram executados tendo o filtro e o contador provador realizar a sua função corretamente, contudo o controlador da ação do estimulador apresenta uma tendência para imobilizar o mesmo algumas iterações à frente de posição desejada (188 iterações ou 0,18 mm), este erro foi estudado e foi concluído que provem de um desfecho normal de um processo de travagem que não é feito momentaneamente, mas sim usando o atrito da guia, levando assim à diferença de posição observada.

Por fim, definimos a Emily como uma plataforma de estimulação tátil com um cilindro rotativo que é versátil, melhorável, fácil de reconstruir, e leve, permitindo ainda um controlo da velocidade de estimulação e da força de contacto aplicada no cilindro.

Palavras-chave: Mecatrónica, Estimulador, Passivo, Tátil, Psicofísica

Index

Acknowledgments	II
Abstract	III
Resumo	IV
List of Tables	IX
List of Figures	X
List of Acronyms	XIII
1. Introduction	1
1.1 Motivation and Research Objective	1
1.1.1 Dissertation Outline	1
1.2 Sense of Touch	2
1.2.1 Importance of Touch	2
1.2.2 Physiology and Anatomy of Touch	3
1.2.3 Active Vs Passive Touch	5
1.3 Electrophysiological and Psychophysical Experiments	5
1.3.1 Microneurography	5
1.3.2 Electroencephalography (EEG)	6
1.3.3 Psychophysical Experiments	7
1.4 State of the Art on Tactile Stimulators	9
1.4.1 Contributions of this Thesis to the SoA	11
1.5 NeuroRoboticTouch Lab	11
2. Emily: Platform for Passive Tactile Stimulation	12
2.1 Requirements for a Passive Tactile Stimulator	12
2.2 Purpose and Design Conception	13
3. Methodology	16
3.1 Designing and Building the Stimulator	16
3.1.1 3D Printed Components	17
3.1.2 Designing the Box Layout	26
3.2 Hardware Components	30
3.2.1 DC Motors	30
3.2.2 Force/Torque Sensor System, Load Cell	31
3.2.3 Encoder	32
3.2.4 Linear Guide	34
3.2.5 sbRIO-9637	35

3.2.6 Linear Current Amplifier Module (LCAM-1)	38
3.2.7 Buffer	43
3.2.8 Circuit Breaker	43
3.2.9 Powering the Platform	44
3.2.10 Overview of The Platform	47
3.3 Software Development to Control the Platform	48
3.3.1 LabVIEW FPGA as a coding tool and graphical Interface.....	48
3.3.2 Stimulator Control Concept	48
4. How to Perform Tactile Stimulation with Emily	54
4.1 Before Operating	54
4.2 During the Experiments.....	55
4.2.1 Instructions for the User.....	55
4.2.2 Instructions for the Subject	56
5. Results and Discussion	58
5.1 Possible adaptations and Upgrades to the Controllers.....	61
6. Conclusion	62
7. Bibliography	63
8. Appendix.....	67

List of Tables

Table 1-1 Types of tactile receptors and their respective physiological properties

Table 3-1 Parameters and their values for current operation of the sbRIO-9637.

Table 3-2 Table with all the connections made to the sbRIO's J4 and J5 port and specific pins used, as well as the purpose of each connection and the component they are connected to.

Table 3-3 User Connection Header of the LCAM displaying all its pins and their functions.

Table 3-4 Header for Power Supply of the LCAM.

Table 3-5 connection header for the load connector of the LCAM.

Table 3-6 Parameters for safe usage of the LCAM.

Table 3-7 Gain settings and the impact of each resistance in the amplifier configuration block.

List of Figures

- Figure 1-1 Diagram of an action potential in relation to the membrane voltage over
- Figure 1-2 Various tactile stimulator mentioned above [3], [13], [19], [32], [39]–[41][40]
- Figure 2-1 Emily the automatic controlled mechatronic platform for passive tactile stimulation with an incorporated rotating drum with embossed topographies, mounted on a linear guide.
- Figure 3-1 Emily the passive mechatronic tactile stimulator platform with an incorporated rotating drum with embossed topographies.
- Figure 3-2 The ultimaker S5 3D printer used to print all the components of the Emily platform.
- Figure 3-3 Drawing of base of stimulator with all the measurements.
- Figure 3-4 Drawing interface bottom of force sensor and its measurements.
- Figure 3-5 Drawing support stabilizer, and its measurements.
- Figure 3-6 Drawing filler for right arm of the drum, and all its measurements.
- Figure 3-7 Drawing of the drum support and its measurements.
- Figure 3-8 Drawing of the hexagonal prism to hold the textured cylinders.
- Figure 3-9 Stimulus 1, 2, 3 and 4. The first two are formed from 24 rectangle outdents, the third is an array of large semi spheres and the fourth a smooth surface. Stimulus 5 and 6 are formed from two different arrays, to the left is an 40x10 array of small rectangles and to the right a 40x7 array of small semi spheres.
- Figure 3-10 Drawing of drum cover and its measurements.
- Figure 3-12 Drawing of the resting mount for the electronic components and its measurements.
- Figure 3-13 Layout of the electrical connections of the hardware box. Every elongated pin has a connection with a different pin with the same name. Meaning that if two pins have the same name, they should be connected by a wire.
- Figure 3-14 Hardware box. Includes the four traco power converters, the sbRIO, the LCAM, the buffer, the ventilator, and the circuit breaker. It receives power from the wall plug, and has an on/off button to control current flow, from it exit a 4-pin and a 12-pin
- Figure 3-15 Wire box. Housed all the connections between the tactile stimulator and the hardware box. It is a hub to simplify connections and to make the machine safer for outdoor trials.
- Figure 3-16 RE35 DC motor from Maxon Motors. Used to drive the drums rotation and the movement of the guide.
- Figure 3-17 Force sensor for calculation of the contact strength between the drum and the finger. On the right is the drawing of this component.
- Figure 3-18 Inner working of an optical encoder. Light either passes through the disc or not, creating a binary sequence of square waves, the signal will be read by the sbRIO and used to control the platform.
- Figure 3-19 On the top behavior square wave of the encoders during Clockwise and Counterclockwise rotation. On the bottom behavior of the square wave of the encoder when inverting the direction of rotation.
- Figure 3-20 Pinout for the encoders attached to the DC motor. Pins 2, 3, 6, 8, 10 are extremely relevant since the first pair receives power and the last three output data.
- Figure 3-21 SKF Multitec LTP 60.180.0804-02 linear guide. On the left is the drawing of the guide with measurements and on the right a picture of the linear guide used in this project.
- Figure 3-22 1. W3, RS-485 (ASRL3) 2. W4, RS-232 (ASRL2) 3. J6, SDHC 4. J9, Power Connector 5. J10, USB Host Port 6. W1, CAN (CAN0) 7. J7, RJ-45 Ethernet Port 8. W2, RS-232 (ASRL1) 9. J5, MIO 10. J4, DIO
- Figure 3-23 On the left is the pinout of port J4 and J5 the DIO and MIO ports of the sbRIO-9637. On the right the board layout with the location of the pins in the top left corner.
- Figure 3-24 Board Layout of the LCAM-1.
- Figure 3-25 On the left is the electric circuit of the op amp and on the right the pin out of the op-amp.
- Figure 3-26 MERLIN GERIN MULTI9 C60HB 25844 B16 16A 16 AMP MCB C miniature circuit breaker.
- Figure 3-27 48V traco power converter, model TXL 100 48S.
- Figure 3-28 15 V TRACO POWER converter.
- Figure 3-29 24 V traco power converter, model TML 40124C.
- Figure 3-30 5 V traco power converter, model THN 30-2411W1.

Figure 3-31 On the top overview of all the power connections between the components inside the box and the ones attached to the stimulator. Each arrow has the direction of power flow. On the bottom overview of the data connections between all components inside the box and with the components attached to the stimulator. Each arrow has the data transferring direction as well as the name of the pins connected in both ends.

Figure 3-32 Representation of the possible changes in state and how each is counted in the counter of elapsed states code. In clockwise motion 00 moves to 10, next to 11 and after to 01, repeating the cycle and adding plus one on the counter. In the counterclockwise motion 00 moves to 01, then 11, and finally 10, always subtracting one to the counter.

Figure 4-1 Graphical User Interface, with the controls and live status displays of the random stimuli selector controller. In this interface a brief explanation on how to operate with the controller is also included in the top left corner.

Figure 4-2 Graphical Subject Interface with lights to signal the subject on what to do at each moment of the trial. Green light to touch the drum, red light to remove the finger. The interface also includes a timer to inform the user on how much time is left for stimulation.

Figure 5-1 Box Plot of the difference between current and desired positions of the stimulator for both 2V and 3V the most optimal voltage options for Emily.

Figure 8-1 Code on LabVIEW to filter to remove random fluctuation in data. This filter adds the 16 latest values outputted by the encoder and relays the states the encoder is at depending on the thresholds implemented. Sum lower or equal to 6 is a low wave, higher or equal to 10 is a high wave, in the middle keeps the previous value until a threshold is met.

Figure 8-2 Code in LabVIEW for counter of elapsed states, this code adds one to a counter if a clockwise pattern is met and subtracts one if a counterclockwise pattern in the square waves is met.

Figure 8-3 Sequence structure used in both controllers to output a signal voltage to the LCAM to power the drum motor. This sequence first enables the LCSM then powers the motor and later disables it.

Figure 8-4 Sequential stimuli selector code on LabVIEW. This code moves the stimulator forward stopping at each preselected location for tactile stimulation to occur. At the end of the slider the stimulator returns to the begging position and the cycle repeats. This image displays the case where the motor moves forward.

Figure 8-5 Sequential stimuli selector code on LabVIEW. This code moves the stimulator forward stopping at each preselected location for tactile stimulation to occur. At the end of the slider the stimulator returns to the begging position and the cycle repeats. This image displays the case where the motor stops and stimulation occur.

Figure 8-6 Sequential stimuli selector code on LabVIEW. This code moves the stimulator forward stopping at each preselected location for tactile stimulation to occur. At the end of the slider the stimulator returns to the begging position and the cycle repeats. This image displays the case where the motor moves backwards.

Figure 8-7 Sequential stimuli selector code on LabVIEW. This code moves the stimulator forward stopping at each preselected location for tactile stimulation to occur. At the end of the slider the stimulator returns to the begging position and the cycle repeats. This image displays the case where the motor stops at the last marker.

Figure 8-8 Parallel while loop used to output a signal voltage to the buffer which will power the guide motor. This code reads the values from a FIFO and depending on the value outputs a specific signal voltage to AO0. Used in “sequential stimuli selector”.

Figure 8-9 Random stimuli selector code done on LabVIEW. This code randomly selects a stimulus to be used for stimulation, after this the controller verifies if the stimulator is in the right location considering the chosen stimulus. If not, it moves the stimulator until that position and then stops the motor for stimulation to occur. After this the controller gets a new random stimulus and the cycle repeats. This case displays the “get next random stimulus” structure.

Figure 8-10 Random stimuli selector code done on LabVIEW. This code randomly selects a stimulus to be used for stimulation, after this the controller verifies if the stimulator is in the right location considering the chosen stimulus. If not, it moves the stimulator until that position and then stops the motor for stimulation to occur. After this the controller gets a new random stimulus and the cycle repeats. This case displays the “compare current desired stimulus” structure.

Figure 8-11 Random stimuli selector code done on LabVIEW. This codes randomly selects a stimulus to be used for stimulation, after this the controller verifies if the stimulator is in the right location considering the chosen stimulus. If not, it moves the stimulator until that position and then stops the motor for stimulation to occur. After this the controller gets a new random stimulus and the cycle repeats. This case displays the “stimulation case” structure.

Figure 8-12 Random stimuli selector code done on LabVIEW. This codes randomly selects a stimulus to be used for stimulation, after this the controller verifies if the stimulator is in the right location considering the chosen stimulus. If not, it moves the stimulator until that position and then stops the motor for stimulation to occur. After this the controller gets a new random stimulus and the cycle repeats. This case displays the “move stimulator case” structure.

Figure 8-13 Random stimuli selector code done on LabVIEW. This codes randomly selects a stimulus to be used for stimulation, after this the controller verifies if the stimulator is in the right location considering the chosen stimulus. If not, it moves the stimulator until that position and then stops the motor for stimulation to occur. After this the controller gets a new random stimulus and the cycle repeats. This case displays the safety measure used to both initiate the platform always in the same position and to prevent it from going moving past the workspace delimited by the limit switches (the false case push the motor back not to touch the end point and the TRUE case forces it forward to not touch the start point).

Figure 8-14 Parallel while loop used to output a signal voltage to the buffer which will power the guide motor. This code reads the values from a FIFO and depending on the value outputs a specific signal voltage to A00. Used in “random stimuli selector”.

Figure 8-15 "random number generator V4.5" code. This code generates a random number from 0 to the specified in the "number of stimuli" control in the "random stimuli selector" code. This number is then sent to the "random stimulus selector" code and used to decide the next desired stimulus.

Figure 8-16 Alternative state counter, using a Boolean array converted to number to identify the state 00-0, 01-1, 11-3, 10-2. The current states are then compared to the previous state by equal functions and depending on this comparison the code will either increases one to a counter, subtract or do nothing. This variation in behavior is dependent on the direction of rotation, since the previous state to any current state can have to options, depending on the rotation.

Figure 8-17 Manual drawing off all the power and data connections between components with the pins used for each connection.

List of Acronyms

AO - Analog Output
CNS - Central Nervous System
DIO - Digital Output
EEG – Electroencephalogram
LCAM - Linear Current Amplifier Module
LS – Limit Switch
PNS - peripheral Nervous System
STL – Single Cycle Timed Loop
VI - Virtual Interface

1. Introduction

A relationship between technology and healthcare has been developed over many years and it will continue to in the decades to come. Robotic platforms have been developed to overcome the deficits or inabilities of humans to perform specific meticulous actions. In scientific research this approach has gained a lot of notoriety and especially in the field of tactile stimulation where mechatronic platforms are currently being developed to mimic real world tactile interactions with controlled and standardized parameters to study the sensation of touch.

1.1 Motivation and Research Objective

In this rapidly evolving world, there is a constant need for improvement and learning, thus it is essential for humans to keep up with the advancements happening all around us. Even though we don't think about it this self-development is only possible due to our five major senses, thus the impairment of one of them could have major repercussions in this process. Unfortunately, and in the light of this master thesis dissertation it is possible for humans to lose their sense of touch, a major player in understanding our environment and to create bounds with other humans.

Therefore, it is essential for researchers and engineers to restore this ability to whom may have lost it, and in order to do it we must first understand how touch operates. This is currently performed by tactile stimulating healthy subject and studying how the touch sensation travels to the brain and is interpreted by it.

However, currently this task is not always performed with the required standards for proper scientific investigation, since the vital control parameters, texture, speed, and force aren't always repeatable, thus it is necessary to create a way to perform these studies where we can trust these three parameters are controlled.

Currently this is achieved through the implementation of mechatronic platforms which are able to standardize these parameters through the use of precise electronic equipment. Until now great scientific breakthrough has been achieved through this approach, however there is still more to improve in order to create a complete and controlled recreation of tactile stimulation which accurately mimics real world interactions. Thus, this thesis will be focus on the development of a mechatronic platform for passive tactile stimulation which balances two major ratios: size and ease of creation, with the implementation of the relevant features for a complete tactile stimulator, creating a complete and accessible tactile stimulator so that more scientific research can be achieved in this topic.

1.1.1 Dissertation Outline

This Thesis aims to be a detailed guide on how the Emily mechanical platform for passive tactile stimulation was thought out, designed and build, alongside leaving the necessary information on why each design choice was made.

To understand the overall thesis firstly we will introduce the sense of touch both as a sensation and theoretically by explained it physiologically and anatomically. Through this explanation the problem we are trying to solve will be set, alongside the solution created to solve it which is the tactile stimulator.

Two different types of tests will be introduced, electrophysiological and psychophysiological tests, which will be important studies to perform while using this tactile stimulator in order to better understand the underlying mechanisms of touch.

The process of building the platform will be initiated by a state-of-the-art in tactile stimulators, which will give a bases on what has been done and what needs to be improved. After, the mechanical design philosophy will be explained as well as the printing and build process. The electronic devices and

their mounting will also be discussed and explained, followed by schematics to better comprehend how the platform was built. Lastly, the software controlling the platform will be described, and also the UI of both the subject and the user, followed by the instructions of operation of the stimulator.

To conclude this thesis the stimulator will be tested through its mechanical and software fidelity, and the results from the tests displayed and explained.

1.2 Sense of Touch

Touch is the innate ability of living beings to feel their surrounding by contacting a part of their body with matter in any state, working as a sensory perception tool. This sensation is possible due to the stimulation of the mechanoreceptors in the surface of the skin, which communicates the spatial features that characterize a specific surface to the central nervous system (CNS) where the information is processed, and the sensation is perceived [1].

When humans interact with an object, we run our finger over its surface, unconsciously scanning its spatial features like shape, texture, compliance, and temperature. Information on the textures of a surface is signalled through precise temporal spiking patterns in the tactile receptors, they create a high-frequency skin vibration which stimulates the receptors [2][3]. These features are then conveyed through electrical signals from the tactile receptors on our skin to the CNS.

However, there are people who lack this ability both entirely and locally. The loss of the sense of touch can happen either due to an absence of communication between the tactile receptors on the skin and the CNS in a condition called hypoesthesia (negative sensory symptoms), which are more prevalent in densely innervated areas, such as the hands [4], [5]. Or because they lost their finger, hand, or arm.

Currently scientists are trying to develop prosthesis that can restore this ability in people who have lost it. However, first we need to understand the neuronal processes underlying the human sense of touch. This dissertation project aims to improve our understanding of how the body and the brain perceive and communicate the sense of touch, so one day, conditions like this can be answered [6].

1.2.1 Importance of Touch

Touch is one of the five senses humans possess and the first to develop [7], so its importance in daily activities as well as more complex tasks cannot be understated. Humans use touch to communicate, either with each other or with the environment around them, allowing us to understand and learn from our surroundings, express ourselves, and stay away from danger. Touch deepens our forms of communication, both verbal and non-verbal; moreover, it reduces stress by the release of oxytocin, and increases the chance of reproduction since it enhances intimacy in a relationship. As a means of survival touch keeps us away from dangerous situations, like cutting objects, hot temperatures, or as a diagnostic technique feeling our own body [7]. Touch even enables the ability to sense vibration, which is possible both in proximity of a vibrating object or further away as in an earthquake or a passing truck on the street.

It has been discovered that in touch is essential, combination with visual cues, to apprehend the weight of an object instants before it has been picked up. This is possible because we sense the fine friction created between the finger and the surface when we first touch the object, therefore this is used to guess how much strength its needed to raise it, and that why we usually do not miscalculate it [8].

Touch is also essential for infant development [9] enabling the creation an emotion bond with their caregivers which boost infants' chance of survival and increases learning rate [10].

On the other hand, a shortage of touch often carries negative connotations, such as a lack of empathy, less ability to express ourselves, and a shallower knowledge of the world.

1.2.2 Physiology and Anatomy of Touch

There are a variety of different mechanical stimuli that can excite the tactile receptors of the skin, these are stretch, vibration and tangential movements [8]. Touch is defined when the skin touches another object, which doesn't necessarily mean it must be solid, as humans can also feel the water or the wind blowing, requiring only for a force to be applied on the skin [11]. The force causes a dislocation of the skin which is perceived by mechanosensory neurons embedded in the skin. These neurons create an electrical signal which flows from the Peripheral Nervous System (PNS) to CNS. Therefore, to stimulate the tactile nerves it is required movement between the finger and the surface, independently of which surface is rubbing which, therefore whether the finger is rubbed on the surface or the surface on the finger has no real difference for pattern acquisition by our sensory nerves [12].

1.2.2.1 Physiology of Touch

When stimulation occurs and the tactile receptors are excited the mechanical stimuli is transformed into an electrical signal in a process called sensory transduction. This signal elicits a local depolarization of the afferent neurons on the skin due to an alteration in their membrane potential.

This process is called an action potential (Figure 1-1) and it is a local depolarization of the axon of the neuron, followed by a repolarization and a refractory period where that section of the axon cannot be depolarized again [13], [14], [15].

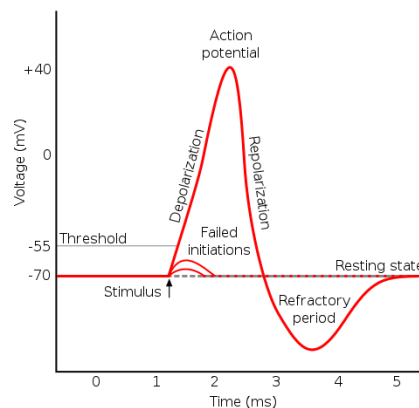


Figure 1-1 Diagram of an action potential in relation to the membrane voltage over time.

The action potential occurs locally on the stimulated neuron, however the electrical signal is intended to travel from the afferent sensory neurons on the skin to the CNS so that the information of the stimuli can be perceived and processed. This mechanism is possible because there is induced depolarization of the adjacent axonal membrane, creating an adjacent action potential, this process happens along the entirety of the axon. As the electrical signal is propagated the previous action potentials finish and enter the refractory period, this means that the action potential will not happen again and the signal travels in one direction from the tactile receptors to the CNS [14].

1.2.2.2 Anatomy of Touch

Humans' distal fingertips are innervated by four different types of tactile receptors (Table 1-1): Merkel's discs, Pacinian corpuscles, Meissner's corpuscles and Ruffini's corpuscles, all with different attributes and purposes.

Table 1-1 Types of tactile receptors and their respective physiological properties [16].

Properties	Merkel's discs	Pacinian corpuscles	Meissner's corpuscles	Ruffini's corpuscles
<i>Encapsulated</i>	No	Yes	Yes	Yes
<i>Adaptation</i>	Slow	Rapid	Rapid	Slow
<i>Strength of stimuli</i>	Light	High	Light	Heavy
<i>Receptive field</i>	Small	Large	Small	Large
<i>Response frequency</i>	20-60 Hz	100-300 Hz	60-200 Hz	20-60 Hz

Rapidly adapting receptors generate action potentials, then quickly adapt, and stop generating signals even if the stimulus continues. They respond to changes rather than static objects. On the other hand, slowly adapting receptors continue generating signals as long as the stimulus continues. They focus on signaling continuous pressure on the skin and sense object's texture, edges, and shapes [15].

One other important property is the receptive field, some mechanoreceptor families have smaller fields, meaning that a stimulus in proximity can be felt separately, as there is probably more than one receptor being stimulated, however, in the larger fields the two different stimuli are not felt separately and require the stimuli to occur further apart. The finger is normally innervated by a higher density of mechanoreceptors with small receptive field [15].

Different studies have shown that the most relevant nerve fibers for pattern recognition are the slowly adapting fibers [17], since they focus on recognizing pressure and texture continuously during stimulation, a finding congruent with the literature which has evidenced that the primate's finger is densely innervated by this type of afferents, especially the slow adapting type 1 fibers [3]. Rapid adapting fibers with small receptive fields like Meissner corpuscles also densely innervate the fingertip, however they are not as relevant to spatial acuity as slow adapting ones. Finally, fibers with large receptive fields innervate the finger with lower density [3].

Tactile perception of fine texture relies on the processing of complex high-frequency vibrations (in the range of 50–800 Hz) that propagate over the skin when we scan a surface [18]. Regarding stimulation of this receptors a study has shown [19] that slow adapting fibers respond best to stimulation frequency in the range 20-60 Hz, rapid adapting fibers on 60-200 Hz, and Pacinian fibers best defined stimuli with a high temporal frequency 100-300 Hz [20].

In conclusion, tactile receptors are stimulated by specific high-frequency vibration created by the features of the surface they are in contact with, creating local depolarizations. The electrical discharges along the neurons propagate the touch information to the CNS, in the brain this will be processed relaying a specific sensation. However, the underlying process is not well understood, hence investigators are developing mechatronic platforms like Emily to perform standardized stimulation of these tactile receptors and in parallel perform neurophysiological and psychophysics studies to better comprehend these mechanisms.

1.2.3 Active Vs Passive Touch

There are two major pipelines to perform tactile stimulation, either through active touch or passive touch. Active touch is the voluntary action to explore and scan the surface of an object, while passive touch is not voluntary. In the first alternative the subjects finger comes in contact with a texture from its willingness alone and it explores the stimulus freely, while in the latter the finger is stationary and the stimulus comes in contact with it, moving to induce the same sensation [21]. In passive touch the stimulus moves in relation to the finger, either through a horizontal sliding movement, a rotating surface with continues stimulation or the sequential activation of the tactile receptors though sharp needles which induce a touch sensation.

These two approaches are frequently considered equivalent in resultant perceptual abilities [22], [23], concluding that relative motion of the surface against the finger is the only requirement for relevant information related to surface roughness to be encoded, therefore implying information is encoded independently of exploration.

However, it is clear that the two protocols engage different mechanisms, in passive touch mainly cutaneous receptors of the skin are activated whereas in active touch the cutaneous, kinesthetic, and proprioceptive senses are engaged as well. The introduction of the motor system and thus the activation of the areas outside the somatosensory has also been found in active touch but not passive [21].

Furthermore, studies have shown there is suppression of afferent information to the primary somatosensory cortex during active movement, which is referred as “gating”. It is considered that gating is an essential aspect for efficient representation of the tactile stimulus in the presence of multiple sensory inputs [24]. This suppression would suggest better behavioral performance in passive touch, however the ability for the subject change the scanning speed at critical points and using different sensory regions to adapt to the stimulus, compensate for the drawback of the gating, resulting in an equivalent performance for patten recognition and representation in both pipelines [21].

1.3 Electrophysiological and Psychophysical Experiments

To Study the behavior of these tactile receptors and the propagations of information to the CNS and the interpretation of the stimulus in the brain Electrophysiological and Psychophysical Experiments like microneurography, electroencephalography and psychophysical tests must be performed.

1.3.1 Microneurography

Microneurography is an electrophysiological technique used to record nerve impulse traffic in nerve cells directly from human peripheral nerves. This technique can be applied either for single or multiunit analyses of nerves. It yields information about physiological and pharmacological mechanisms as well as insights into diseases related to the nervous system. Studying electrical signal traffic allows us to better understand how the spatial features of an object and their perception by tactile receptors guides human behavior in common and novel tasks like in social environments, around dangers objects or while touching new things [25], [26].

For this project microneurography is relevant since it provides information on sensory physiology, including the identification of threshold for stimulus, perception of spatial features, and the specificity and quality of the pictured concepts or percepts created by the fingertip. As the subject is stimulated by different topographies, parallel microneurography display how tactile receptors electrically encoded textural information which they relay to the brain for processing.

The technique is performed by inserting the metal tip of a tungsten microelectrode into an accessible peripheral limb nerve of the sympathetic nerve system. For this study the most relevant nerves are the peripheral nerves in the upper's limb such as the median, ulnar, and radial nerves which innervate the distal fingertip. Neural activity is recorded by the difference in potential between the recording electrode placed inside the nerve and a reference electrode inserted near the recording electrode [26].

After the electrodes are inserted, the subjects should be asked to place their arm on the arm rest with their palm facing up, and after following the experimental protocol detailed by the investigator to perform tactile stimulation by touching the rotating drum.

Parallel to recording electrical impulses, it is possible to perform micro neurostimulation through the recording electrode, exploring the effects of impulse trains in an afferent nerve fiber [25].

1.3.2 Electroencephalography (EEG)

Electroencephalography (EEG) is a non-invasive technique used to measure brain electric activity, existent due to the electrical current neurons create to communicate with each other [27].

Although EEGs measure electrical activity, they do not register action potentials, instead they assess postsynaptic potentials, which are the result from slow currents after neurotransmitter release at the axon's terminals [20], [28]. This activity comes from the current dipole created between the excitatory postsynaptic potential at the dendrite (positive) and the extracellular current sink or negativity at the soma.

The electrical activity measured is the summation of currents from the neuronal populations firing simultaneously. The current then is conducted in an isotropic manner, first throughout the brain matter followed by the vascular system, after through the cerebral spinal fluid, dura matter, skull, muscles, fat, and skin and finally to the electrodes [28]. The magnitude of the signal recorded depends on the angle subtended at the electrode and the distance from the electrode. Therefore, the EEG is a "spatiotemporal average of synchronous postsynaptic potentials arising in radially oriented pyramidal cells" [27].

EEG is performed by placing several electrodes on the scalp which record voltage from current flow in and around neurons. Electrolytic gels or salts are normally used to improve contact between the electrode and skin, therefore improving the data from the EEG [28].

In touch studies EEG has an important role. For instance, this easy-to-use and economical technique allowed the discovery of the somatosensory cortex role in representing and processing tactile information originating from the contralateral side of the body [29]. However, recent studies have also considered the role of the ipsilateral side of the brain to form a complete representation of the tactile stimulus [30].

Tactile stimulation has been linked with long-latency potentials such as P50, N70, P100 and N140, where the last two were found with higher amplitudes in the contralateral hemisphere and with delayed latency in the ipsilateral side, revealing its overall impact in touch perception. Other keys aspects found from EEG in parallel with mechanical stimulation have been the discovery of a late potential elicited around 200 ms after the stimulation was stopped, likely marking the end of the stimulation [31].

It has also been found an initial synchronization in the theta waves (4–7 Hz) for 500 ms after the stimulation starts in the contralateral cortex, followed by a desynchronization in the alpha band (8–15 Hz) that lasted for the remainder of stimulation. This decrease was relevant in the somatosensory cortex and equal in both contralateral and ipsilateral hemispheres [31].

This versatile and accessible technique has also been long used for clinical diagnostics by correlating brain activity with different pathologies (e.g. epilepsy, sleep disorders, strokes or seizures, brain tumors, neurodegenerative diseases such as Alzheimer's or Parkinson Disease [27]) and for the characterization of neurophysiologic pathways, states of consciousness or sleep, and the dynamics of brain function [28]. For this project the purpose of the EEG stems from the need to study brain activity during stimulation, so that a correlation can be made between various spatial features and a specific kind of brain activity.

This study starts by first explaining to the subject the study and the tasks they will be required to do. After their consent the investigator should set up the EEG helmet, placing the electrode and incorporating the gel to improve contact between the scalp and the electrode. After this the cerebral activity of the subject should be recorded at rest and subsequently perform simultaneously the stimulation using the mechatronic platform. Emily should therefore be used in future scientific researcher for stimulation alongside the studying the electrical activity of the brain through EEG.

In healthy subjects, the main EEG frequency content is comprised in the range of 1-40 Hz with amplitudes in the order of magnitude of μV . The observed frequencies are subdivided into five groups: delta (0.5–4.0 Hz), theta (4.0–7 Hz), alpha (8.0–13 Hz), beta (13–30 Hz) and gamma (>30 Hz). Alpha is common in relaxed states, beta waves in more intense mental activity, delta and theta are not usually record during wakefulness, and if they are present usually indicating the presence of a disorder [20], [27]. So, during stimulation we expect to see frequencies in the beta range, with higher activity during stimulation due to the increased brain activity.

Examples of electrophysiological tests using EEG relate the electrical activity of the brain during stimulation and the perception of the subject. Pleasantness of touch with parallel EEG can output a correlation between various brain waves and patterns and how pleasant a stimulation may feel [32].

1.3.3 Psychophysical Experiments

As the name suggests psycho-physic relates the phycological interpretation of something physical happening to a subject. Psychophysical experiments seek to determine the relationship between a physical stimulus and the sensations and perceptions they produce, for example if the subject can detect and identify a stimulus or differentiate between various stimuli, or even express the extent or nature of this difference [33].

A psychophysical experiment consists of the following elements: stimulus, task, method, analysis, and measurement. The stimulus is individually tailored to the specific question about sensory function being asked, which in this study is the rotating drum and its different topographies. The task is the action the subject must perform, like selecting which stimulus is more pleasant. The method is the way the stimuli are presented and how the observer's responses are recorded, for example selecting which stimulus is more pleasant or to grade how rough it feels in a numerical scale. The analysis refers to how the data is converted into a measurement, such as a threshold for unpleasantness or an ELO ranking of pleasantness [34], [35].

The classical psychophysical methods are: (1) method of limits where the stimuli are gradually increased from a point where it is not recognizable to where it is apprehended. After this, the same test is done but in a decreasing order. To prevent habituation a staircase procedure to zero in on the threshold; (2) method of constant stimuli where the subject is presented stimuli at random with no connection to the previous or next one, this in turn circumvents the problem of habituation; (3) in the methos of adjustment

the subject itself regulates the stimulus until it is barely noticeable, however this last method is not applicable to Emily [36].

For this project the psychophysical experiments performable are based on the perception of the different textures by the subject, and how it differentiates the topographies from one another.

There are a variety of tests that can be performed, such as threshold tests, where the subject is presented a smooth surface at first and as the trial progresses is stimulated by more and more rough topography until he is able to identify a change in smoothness. This procedure can also be performed on a start case procedure where the subject is presented a rough surface and subsequently smoother ones until it makes the mistake of confirming a harsh topography when it should not be felt, then the topography is increased in roughness until the subject answers correctly [37].

Test of compared magnitude can also be performed, where the subject signs a number to indicate how unpleasant or rough a stimulus is and a power scale can be done to evaluate the results. On the other hand, just a simple comparison of pleasantness between two or more topographies can also be performed.

Previously mentioned studies were typically performed with the same rotating drum velocity, however scientific studies have shown that humans are able to accurately judge the speed of a moving object through touch by a combination of factors such as the ratio of specific stimulus and in turn the distance travel between stimuli as well as the duration of stimulation [18]. Therefore, one alternative psychophysical test with varying velocities would be to apprehend and compare the different speeds of a moving stimulus and interpret which was fastest and which sensations are invoked by changing the scanning speed with the same stimulus.

Research reports that the estimations of the speed of a moving object are influenced by the physical properties of the object. Revealing that increasing the spacing between outdents influences the participant's estimates of speed, if the dents are further apart subjects think the stimulus is moving slower and vice-versa. Hence the opposite can be theorized, increased speed creates the sensation of denser stimulus. Which is an interesting experiment to perform with Emily [18].

This is confirmed in [3] where the spiking patterns created by the high frequency vibration of the skin dilate or contract depending on the scanning speed. They also theorize that this process can be reversed achieving perceptual constancy by varying speed and spatial features of the surface.

This temporal/spatial relation greatly extends the range of obtainable textures with only one printed stimulus.

It is possible that prolonged stimulation might create numbness, or that the sensation provoked by one stimulus carries over affecting the next. To prevent this a period of rest between trials can be implemented to improve the results.

1.4 State of the Art on Tactile Stimulators

To induce controlled stimulation of the tactile receptors to perform this experiments a mechatronic tactile stimulator must be developed.

Currently there are three main approaches to perform passive tactile stimulation, the first is by generating motion through a horizontal plane rubbing the finger with a stimulus, the second involves activating tactile receptors in a sequence to generate simulated motion using fine needles, and the third is a rotating drum. In this section a series of platform will be mentioned and discussed so to grasp what has been achieved and what has been lacking to develop a complete platform to mimics human interactions with its environment.

[12] created an automated linear stimulator that selects one stimulus at a time which is then stroked across the skin in a defined trajectory. Although this machine was a pioneer for tactile stimulation in 1983, it was too bulky, making it hard to transport and used old digital electronics which are not as efficient.

[38]presented a horizontal plane stimulator which moved sinusoidally across the skin with a scotch yolk method. It was simple, robust, and reliable and had an open loop design for contact strength. However, it had some cross over of tangential forces making their way into the value of the contact force, which was not ideal. It also had a lack of flexibility of the experimental protocol.

[19] developed a rotating drum to stimulate a monkey's finger. Even though contact force was controlled via a counterweight in the opposite end, the strength applied by the finger on the drum was not. Therefore, contact force was kept in open loop meaning there was no feedback for correction automatically. This machine also used a damper to cancel sporadic vibrations.

[39] was great inspiration for this project. It is a rotating drum mounted on the end of a counterbalanced pivot beam. The embossed patterns on the drum are lowered onto the skin using gravity as a controller for contact strength. This machine also performs lateral movement controlled by a servo motor, just like Emily, however Johnson and Phillips incorporate this movements for lateral stimulation while Emily only uses them to change to the next stimulus. It uses a counterweight to balance out the angular moment created by the drum, however it also had an open loop to control contact strength. This machine is much smaller compared to other platforms and it uses an air suspension table which isolates the stimulator and subject's hand from mechanical vibration.

[32] was also a huge inspiration for this project since it was developed in the NRT Lab by my tutor and his team. Even though it is a horizontal sliding stimulator I used it as a basis for the approach I needed to develop my own platform. This machine has many perks, like the ability to control the speed of the sliding motion as well as the contact strength. In the design concept of this platform the finger is kept still during the experiments while the stimulus is pressed onto the skin until it reaches a specified contact strength, measured by the same force sensor used in Emily. The machine also produces scarcely any vibration due to the inertia of the motor which absolves all the vibrations. The machine produces little electromagnetic interferences because it uses two liner current amplifier, one on each converter, just like Emily, to power its motors. Moreover, it is relatively light and easy to transport. However, it required the stimuli to be changed manually which took at least 10 seconds between trials. Years later this machine was upgraded, adding a vertical position encoder, and encapsulating the platform inside a dense metal structure, which reduced its vibrations even more, but made it too bulky.

Other platforms use different approaches to present the stimuli to the subject, [2] uses gravity to push down a weight that lifts a rod which will stimulate the subject, this gives a constant contact force since the finger is kept in place; [40] performs a multi finger stimulation, with a unit for each finger, the

major perk of this platform lies on being the smallest stimulator found during the research gathered to write this dissertation. It also allowed for stimulation with different hand positioning and spacing between fingers and even multi digit stimulation which is not something widely done.

Even though many researchers have created platforms with rotating drum, most only have one degree of freedom [41], the one driving the rotating the drum, restricting motion to two opposite directions clockwise or counterclockwise, limiting the number of experiments possible. Emily, on the other hand incorporates two degrees of freedom one for the rotating motor and one for the lateral movement, enabling the possibility of stimulation in two different directions, separately or at the same time.

One platform which took this even one step further was [41], which created a visual-tactile stimulator for cross-modal sensory experiences, relating the impact of vision in tactile exploration. Their platform was designed with three degrees of freedom: one for the drum's rotation; one to raise and lower the drum to increase the relative indentation depth by increasing the force the drum applied into the finger; and one to turn the drum side to side in its z axis. Each degree of freedom was controlled by a specific stepper motor, which gave It incredible versatility for experiments. To add to the perks of this platform it was also capable of controlling the rotation speed as well as the contact strength due to the implementation of the vertical motion.

Now that a state of the art in the field of mechatronic platforms for tactile stimulation has been established, we can move over to the development of Emily, a mechatronic platform for tactile stimulation which is inspired by the platforms mentioned above trying to improve upon them by fusing some of the best characteristics. Emily fulfils all the requirements for a standardizable robotic stimulator studies created for electrophysiological, psychophysical experiments on different tactile surfaces.

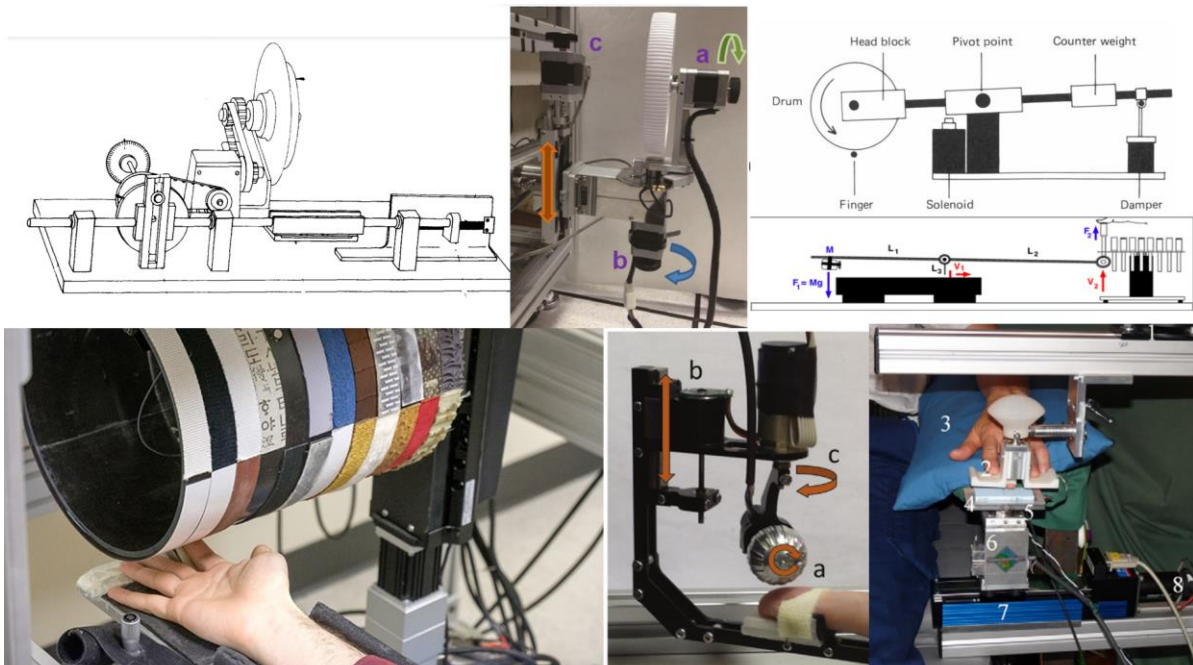


Figure 1-2 Various tactile stimulator mentioned above [3], [13], [19], [32], [39]–[41][40]

1.4.1 Contributions of this Thesis to the SoA

As a master thesis for the creation of a mechatronic platform for tactile stimulation the major goal was to build a simple, versatile tactile stimulation, which was reliable and independent from human input. Therefore, the contributions provided by this tactile stimulator are as follows:

1. A good relationship between portability, and the versatility of the platform: the more versatile a device tends to be the bigger it gets since it must comprise more structures and devices inside it, hence Emily, was designed with the most important features in mind, while trying to make it at small and light as possible.
2. Easy to Replicate: Emily was built from accessible material and structures to design, and 3D print. The electronic equipment used are also more accessible and only the most important ones were implemented.
3. Versatility of experimental protocols: From the implementation of an sbRIO board we acquired the ability to program the behavior of the platform through an intuitive coding language, which opened the possibility for almost limitless experimental protocols.
4. Implementation of many textures at the same time: The lengthier drum allows for the implementation of up to 7 different stimuli at one time, which enables more versatile experiments and different study protocols as well as it reduces the experimental time.

As a whole package Emily doesn't include any new stand out feature that previous stimulators don't already have, however it comprises many of them in one single stimulator and all inside a smaller platform which is configurable and enables more experimental protocols.

1.5 NeuroRoboticTouch Lab

The NeuroRoboticTouch Lab is the laboratory where this project was developed, personally speaking it was a pleasure working here since it provided the necessary conditions for a safe and healthy work environment, with a great open and clean space and an amazing team of engineers always keen to help me.

The laboratory is located in Pontedera in the BioRobotics Institute, it belongs to the Sant'Anna School of Advanced Studies in Pisa, and it specializes in the engineering of an artificial tactile sense in parallel to the investigation of human touch.

The main goal of the laboratory is to analyze neural data to unveil the neuronal processes underlying the human sense of touch, characterizing the perception of tactile features. The data and knowledge acquired through all the projects inside the lab converges then in a key application domain in upper limb neuroprosthetics, with complementary interests stemming towards safe human-machine co-work, tele-presence for medical robotics and hand-held consumer electronics [42].

The Emily project fits perfectly inside the interest of the lab and my owns, since it focuses on biomechanics and the human perception of touch, moreover the creation of the mechatronic robot gives the lab another tactile stimulating platform for experimental purposes, not only for the making of my thesis but also for the future of the lab, being it an asset in the road to better understand the underlying neural connections that create the perception of different textures inside the brain.

2. Emily: Platform for Passive Tactile Stimulation

2.1 Requirements for a Passive Tactile Stimulator

Robotic platforms for tactile stimulation have many requirements to be considered suitable for scientific application since they must allow repeatable and standardized experiments [32].

First it is mandatory to create repeatable experiments with standardized conditions, requiring accuracy and precision in the control of stimulation parameters such as rotating velocity, and a low deviation of contact force amongst all trials [32].

Second, the device must guarantee the application of a range of different forces and velocities covering those that would mimic real world exploration [32]. With normal and tangential forces being recoverable for later data analyses.

Third, spurious vibrations must be removed so not to have external factors stimulating the tactile receptors of the subject [32].

Fourth, electromagnetic interference from the robotic system must be minimized not to damage the data of electrophysiological methods such as microneurography and EEG [32].

Fifth, the experiments require the subject to sit in a natural position and to remain relaxed during the trials [32]. Hence, the platform must be created with the specific proportions to make it as comfortable as possible [43].

Sixth, the program controlling the machine is simple, flexible, and easily upgradable [32].

Seventh, the physical components printed can be easily substituted and upgraded [32]. The machine should be easily dismantled, and they can be upgraded or changed if needed.

Finally, the platform must follow safety regulations such as heat control and dissipation, reduce the likelihood of electrical faulting, short-circuits or the possibility of electrocuting someone, and most importantly be designed in a way to impede the user or the subject from harming themselves or anyone [32].

2.2 Purpose and Design Conception

Frequently tactile stimulation is performed manually, which is time consuming, requires effort and concentration from the investigator, and leaves many stimulus parameters uncontrolled [2]. Due to the inconsistencies of manually stimulating subjects, robotic stimulators that enable detailed analyses of both the electrical activity of the neurons and the receptor response of the CNS were created to achieve equal, standardized, and repeatable experiments protocols. These stimulators can either stimulate the finger actively or passively. In the active protocol the subjects explore the stimuli, and in passive studies tactile stimuli are presented to the fingertip[44], [45]. The latter case will be the focus of this project.

A passive stimulator must allow controlled variation of stimulation parameters such as the materials used, their spatial features, the scanning speed by the finger and the contact force between stimuli and finger to make comparisons between participants and trials meaningful [32].

Previous platforms for tactile stimulation had a few drawbacks, they either were too big, produce too many vibrations and electromagnetic interference, used old digital electronic component, or had low flexibility for the number of performable experiments.

With this project most of these problems will be tackled and solved, aiming to build a complete, versatile, and portable mechatronic platform for passive tactile stimulation.

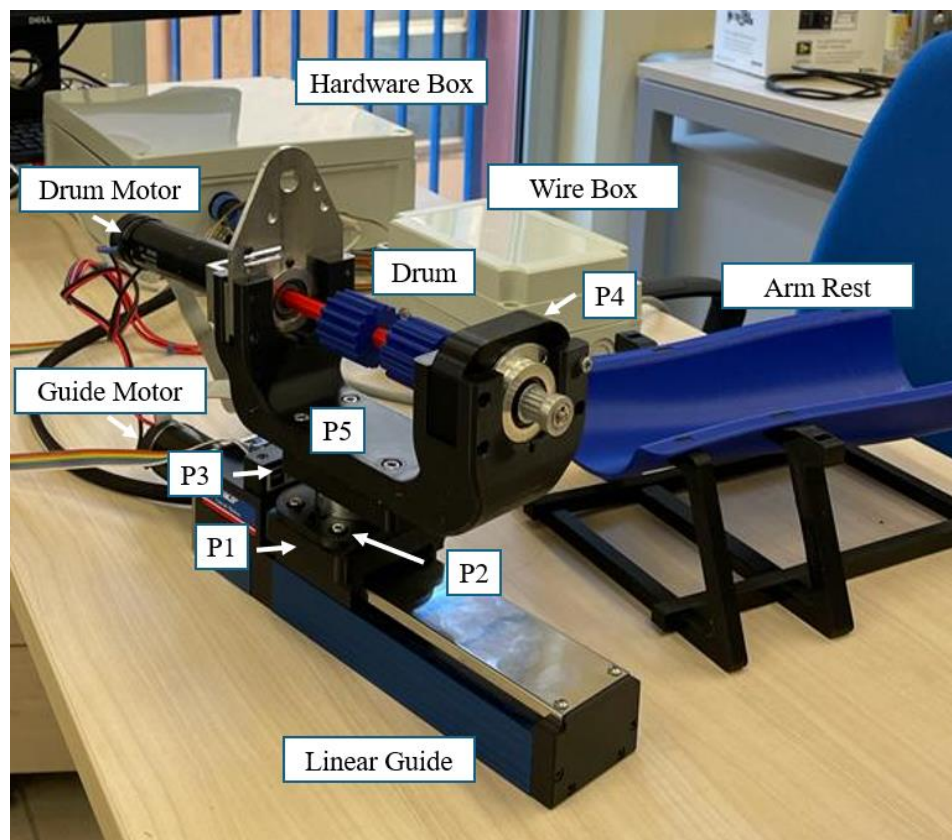


Figure 2-1 Emily the automatic controlled mechatronic platform for passive tactile stimulation with an incorporated rotating drum with embossed topographies, mounted on a linear guide.

Emily (Figure 2-1) is an automatically controlled mechatronic platform for passive tactile stimulation with a rotating drum with different embossed topographies. The drum is mounted on a linear guide that moves it laterally along its rail in order to change the stimuli presented to the subjects. Therefore, the platform has two degrees of freedom, one for the drum which can rotate either clock or counterclockwise and one for the lateral movement along the guide, enabling the possibility to change stimuli during the trial and even perform lateral stimulation alongside the stimulation longitudinal to the finger. The different topographies are incorporated on the curved side of the drum by loading it with different small 3D printed cylinders, each with a predefined texture. The stimuli are introduced one at a time and swapped by the slider which moves the drum to the next desirable topography. The linear guide has a magnetic limit switch in each of its poles, to delimit the safe working space of the slider.

To expand the possibilities for as many different study protocols, Emily was built with an open design approach using LabVIEW FPGA embedded in the sbRIO-9637 board, which guarantees a high degree of flexibility on how the platform can be programmed to operate, also enabling its design upgradability, and restructuring for future experiments. In its design concept Emily was created to have an automatic control independent from human interaction, hence the stimulation can be performed with no user input other than the selection of the variables like scanning speed and stimulation time. LabVIEW also enables the live display and control of the status of the platform, with controls and information for variables such as the scanning velocity, the position of the platform and the contact force applied.

To ensure the platform was suitable for any neurophysiological study, a Linear Current Amplifier Module (LCAM) was used, since it produces little electromagnetic interference making Emily especially viable for microneurography studies.

To control the contact force between the finger and the drum a force sensor was implemented in the design, below the drum. This device displays live on the LabVIEW interface the contact force applied by the finger on the drum, however in the current version only a phantom sensor was used. Since it was already incorporated in the mechanical design, this opens the possibility for an accessible future upgrade, making it a more complete tactile stimulator.

Emily was also built with an efficient design to make it as light and cheap to build as possible, moreover with commercially available components so that a platform like it can be replicated anywhere in the world.

The robotic platform was built with 3D printed components following an in-house design with a “U” shape support attached to the linear guide and the drum in the middle. The two degrees of freedom are each controlled by a DC motor with an encoder associated for position tracking. The slider is driven by the guide motor attached to the side of the guide which induces linear motion through a wheel bearing, and the drum is controlled by the drum motor attached to the left side of the support which rotates it in both directions. Between the support and the guide sits the force sensor and inside the guide the limit switches. These electronic components communicate with the rest of the components controlling the platform which are stored inside an adjacent box for safety reasons. The stimulator was also designed ergonomically with its size in mind to create a comfortable and natural positioning of the arm during experiments. This was achieved by introducing an armrest and a hand holder to insert the finger and keep it stationary.

Inside this box is the controller of the entire platform the sbRIO-9637, which requires a connection to a PC with LabVIEW FPGA installed. Alongside this board is the LCAM and a buffer which are controlled by the RIO board and outputs the voltage to the drum motor and guide motor, respectively.

The box also incorporates a circuit breaker to cut power in the chance of a short circuit and fan for ventilation.

The platform is powered directly from the wall plug and its current is then converted into DC by the different TRACO POWER converters also placed inside the box. These respectively power different components of the platform such as the LCAM, the buffer, the sbRIO and the encoders.

In conclusion Emily platform is an in house built mechatronic platform for passive tactile stimulation which doesn't have many groundbreaking advancements when compared with other past tactile stimulators, however it boosts countless benefits by merging some of the qualities of prior machines. The prior requirements were answered with following implementation.

- Autonomous and independent from human input to perform experiments.
- Size, and ease of transportation.
- Ability to control the speed of rotation of the drum live during trials, and to keep it constant.
- Live display of the contact strength applied by the subject during the trials. With the ability to calculate normal and tangential forces and store the data.
- Ability to stimulate with different topographies in short periods.
- Open software approach making it easy to program and to create a limitless variety of steps that it can perform. Furthermore, the ability to have live feedback of the status of the machine with high precision.
- The use of a linear amplifier with low electromagnetic interference, so not to damage the data of more sensitive recording electrophysiological techniques.
- The adaptability of the physical components, which can be easily improved. Moreover, the simplicity to create and swap stimuli for the drum.
- The speed at which the stimuli can be changed during the trial.
- Comfortable and ergonomic for extended periods of stimulation.
- Built with commercially available devices, making it easy to recreate in other labs.
- Addition of a circuit breaker, fan, and cover for the drum for safety reasons.

Such as the focus of the lab, the aim of this platform is to improve our knowledge over the neural processes behind the human sense of touch. So, to generate relevant information for this common goal, electrophysiological and psychophysiological experiments must be performed parallel to the stimulation of the human finger by the machine. Data from EEG, microneurography and psychophysical test regarding pleasantness of touch are great examples of what can and should be studied with this machine.

The objective is then to understand how each texture stimulates the brain through its electric activity or by the sensations it produces.

3. Methodology

3.1 Designing and Building the Stimulator

For future referencing and better comprehension of this thesis, the stimulator should always be visualized like in Figure 3-1, therefore the left side is the one with the DC motors and the other side is the right since. From this we also conclude the rotational directions clock and counterclockwise.

Emilys design and structure are composed by two main parts, the stimulator, and a box to house all the electronic components. Which will be discussed thoroughly in this chapter.

The stimulator is a “U” shaped 3D printed component mounted along the length axis of the guide in with the rotating drum in the middle, parallel to this same axis. It is 25 cm high, 35 cm long and 6 cm wide. Since the drum is mounted on the middle of the support the DC motor driving it must be placed along the same axis, as well as the encoder, therefore the drum motor and encoder were attached to the drum on the left side of the stimulator, with the motors metal tabs inserted on a spacing created in this arm. In this space a metal sheet was added to strengthen the arm of the support. On the opposite end of the support a ball bearing was added to create another rotating support point for the drum. The same spacing was created here to hold the bearing inside the arm of the support. The support is opened from the top so to facilitate placing and removing the drum.

However, this design created an imbalance in the center of mass of the stimulator tilting it to the left because of the extra weight of the motor and longer length of this component compared to the bearing. This counterclockwise angular momentum induced huge stress on the base of the support which was attaching the support to the guide. To solution this problem the support was designed asymmetrically with a longer right side and thicker structure, countering some of the imbalance. Following this improvement, a separate component (P3) was designed with the intent of moving the stimulator to the right, away from the center of the base, moving the center of mass closer to the center. Alongside these alterations, the previously mentioned metal sheet was added on the left arm of the support to increase its strength, since the angular momentum of the motor will also inflict extra tension of the arm itself.

The force sensor was added bellow P3, in the axis of the center of mass of the platform and bellow it, a 3D printed base was added to attach the simulator to the linear guide.

The linear guide gave the stimulator another degree of freedom, moving it along the axis of the drum. It has a DC motor incorporated with an encoder, to drive and follow the stimulator along its movement. The guide also included a magnetic limit switch at each pole to delimit the safe working space of the guide.

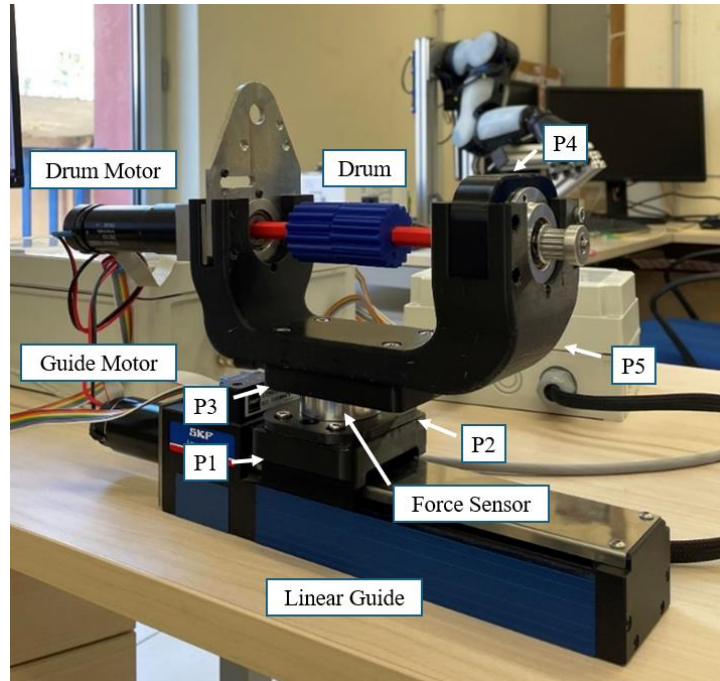


Figure 3-1 Emily the passive mechatronic tactile stimulator platform with an incorporated rotating drum with embossed topographies.

This design concept has three main advantages: first it allows for stimulation with the hand facing up and down, leaving enough space between the support and the drum for either experimental choice; secondly it permits the introduction of a force sensor below the drum, giving a live display of the strength applied to the drum during stimulation, as well as the position along the drum where that force is applied. Lastly, it allows the implementation of a lengthier drum with many different integrated topographies since there are two support points, one in each arm of the “U”. This last perk comes at the cost of a bigger and bulkier stimulator, however while other tactile stimulators must manually change their stimulus every time, Emily doesn’t and enables the possibility of a completely autonomous platform.

During the design and mounting process all the screws used were lodge inside the components so that they would not protrude to the outside, so not to cause injury if touched and to comply with the specifications of safety for these kinds of platforms.

3.1.1 3D Printed Components

Emily is an in-house design created from several 3D printed components, these components were designed in the CAD software Fusion 360 and subsequently turned into STL files so that they could be used in the slicing software Cura, posteriorly these files were sent to the Ultimaker S5 3D printer (Figure 3-2) to be printed.

The material used for printing was either black, blue, or red PLA, and white PLA for the breakaways and supports. The printer resolution was set to fine - 0.1 mm and all the other setting were left as the default values for this resolution.

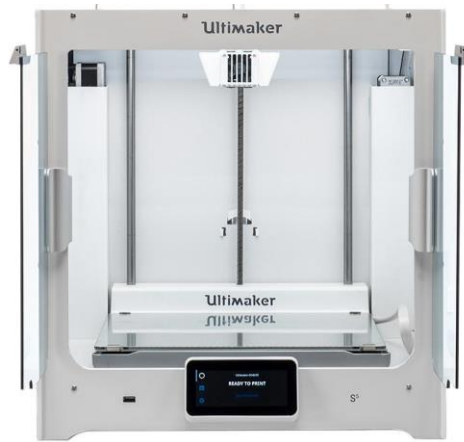


Figure 3-2 The ultimaker S5 3D printer used to print all the components of the Emily platform.

The following chapters will focus on explaining in detail the design and purpose of each 3D printed component.

3.1.1.1 Base of the Stimulator (P1)

This component Figure 3-3 was created as an interface between the slider and the force sensor, working as the base of the stimulator. It attaches directly to the guide with four M4 screws faced downwards and on top of it there is a thin piece P2 which is screwed to P1 by the same screws.

P1 was created with a bridge like shape on the bottom to create an opening for the stimulator to freely ride along the guide without any friction. On the top face there are three holes where the head of other screws will rest so that there is no spacing between pieces.

The following drawing shows the piece and its measurements.

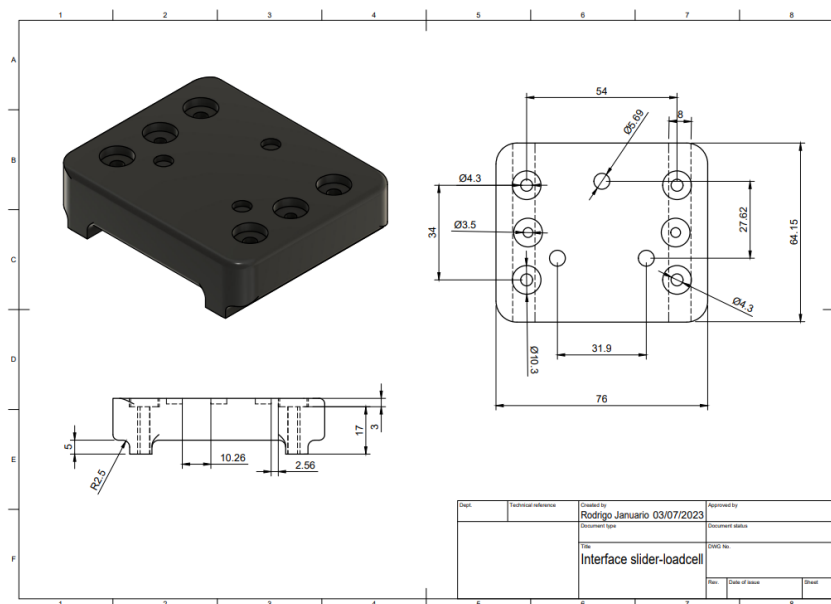


Figure 3-3 Drawing of base of stimulator with all the measurements.

3.1.1.2 Interface bottom of the force sensor (P2)

This component (Figure 3-4) is an interface between the base of support and the bottom of the force sensor, attaching them together, it is fixed to the sensor by three M3 screws pointed upwards starting from the bottom face of P2, and fixed to P1 by the 4 M4 screws mentioned above.

This piece was developed so not to make P1 fragile, since if P3 was directly screwed to P1 the huge holes would span the entire height of P1 making it less durable, and since the base must be robust to withstand the weight of the platform and the angular moment it created, P2 was developed in order to create a stronger P1. This component also elevated the drum in 5 mm which was needed for the comfort of the subject during the experiment.

The following drawing shows the piece and its measurements.

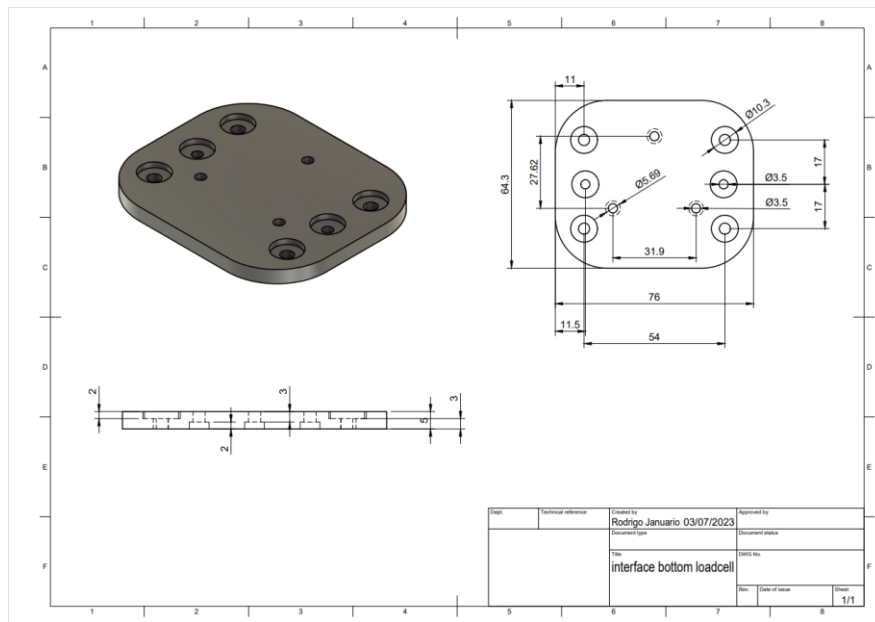


Figure 3-4 Drawing interface bottom of force sensor and its measurements.

3.1.1.3 Support Stabilizer (P3)

This component (Figure 3-5) is an interface between the top of the force sensor and the support for the drum. P3 was created with an array of M3 holes for the user to choose where to fix this piece to the sensor. Their purpose comes from the need to balance the weight of the stimulator, since it isn't evenly distributed because the motor in the left side creating a huge amount of angular moment tilting the platform counterclockwise (CCW). By moving the center of mass of the stimulator to the right we compensate this angular momentum.

The three M3 screws used to attach it to the sensor are lodged deep inside the piece because the recommended screws designed by the manufacture had a smaller length so to be in compliance with the maker this design was implemented. P3 is fixed to the support of the drum with four M5 screws faced downwards with a nut on the other end.

The following drawing shows the piece and its measurements.

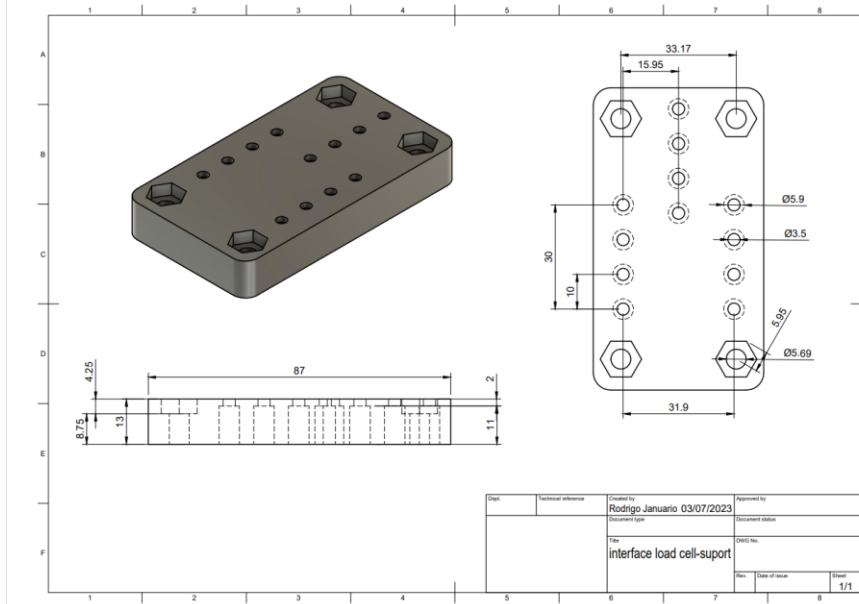


Figure 3-5 Drawing support stabilizer, and its measurements.

3.1.1.4 Filler for right arm of the support (P4)

This component (Figure 3-6) was created to fill in the space not occupied by the bearing in the right arm of the drum support (P5). Its purpose is to ease the mounting of the drum (P7) onto the support (P5) because the drum is mounted from the top, so the support has to have an opening in both arms to place it, moreover this round piece fixed the bearing on the right arm in place creating a leveled and fixed holding point.

This piece is fixed in the right arm of P5 by 4 M4 screws facing the inside of the drum. The following drawing shows the piece and its measurements.

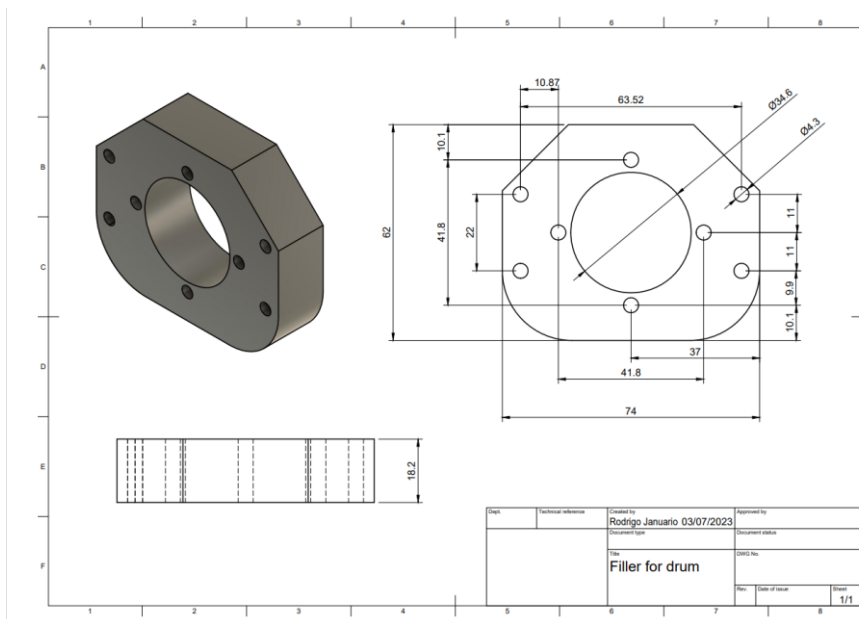


Figure 3-6 Drawing filler for right arm of the drum, and all its measurements.

3.1.1.5 Drum Support (P5)

The drum support (Figure 3-7) houses three very important components, the drum motor, the drum encoder, and the drum itself. This piece was created with a “U” shape collinear with the guide and a “U” shape hole on each of its sides, perpendicular to the main support, and opened on the top so that the drum could be mounted by dropping it in from the top. In each arm of the support sits the two resting points of the drum with the drum motor on the left and a bearing on the right side. On the left side there is a metal sheet to strengthen the support due to the forces created by the angular moment caused by the weight of the motor.

The metal tabs of the motor and the metal sheet are housed inside the spacing created in the left arm and fixed with four M3 screws faced to the inside of the support, the bearing in the right side and P4 are placed inside the same spacing but in the right arm and fixed to the support with four M4 screws faced again to the inside. There are no protrusions of this screws to that the subject is not injured during trials.

The drum spans along the inside length of the support leaving both space on the top and bottom part for the subject to place the finger during stimulation, explaining the U like shape of the design. This support can also house a cover for the drum.

The following drawing shows the piece and its measurements.

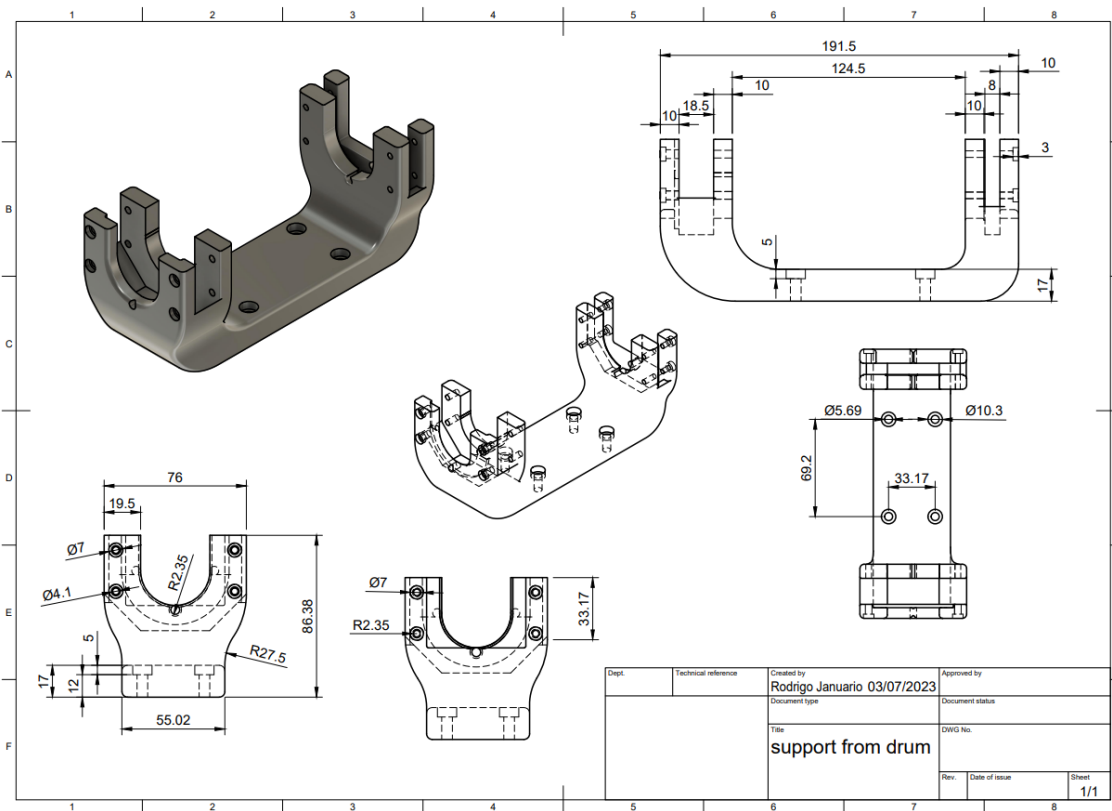


Figure 3-7 Drawing of the drum support and its measurements.

3.1.1.6 Hexagonal Prism to Load with Stimuli (P6)

The drum is composed of various small cylinders each with a textured surface. To hold them all together a hexagonal prism (Figure 3-8) with the shape of a pencil was created. The tips of this piece were made to fit in the axial of the motor and the bearing on the other side. This allows for future implementation of other stimuli and to rearrange their order without needing to print a completely new drum.

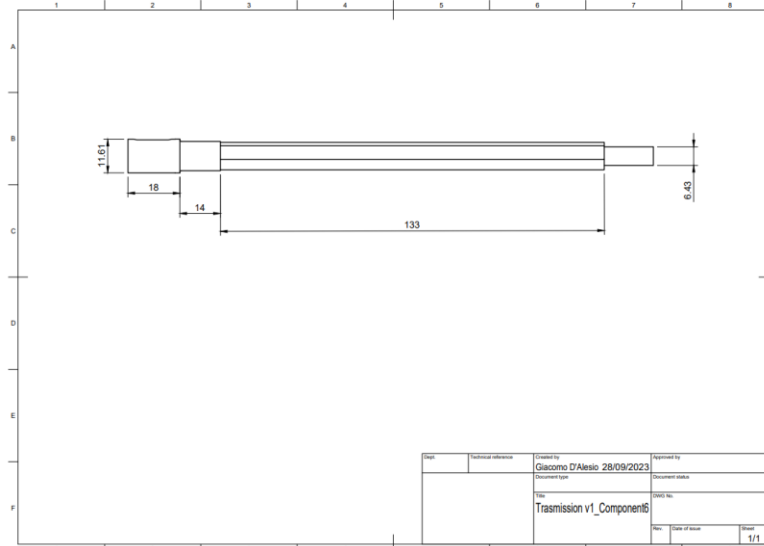


Figure 3-8 Drawing of the hexagonal prism to hold the textured cylinders.

3.1.1.7 Drum for Stimulation (P7)

The rotating drum (Figure 3-9) is created by loading a hexagonal prism with a variety of small cylinders each with a specific texture on its curved side. The drum was initially intended to have 6 stimuli, however the user can print and add as many as it pleases as long as they fit inside the length of the prism. It is easily loaded and unloaded, meaning this machine is adaptable and capable of stimulating the subjects with a different stimulus in rapid succession.

The rotating drum is used for tangential stimulation of the finger along its x axis, even though due to the versatility of this platform, it can also be used for lateral stimulation along the y.

To decide which topographic designs were to be implemented, inspiration from other tactile stimulators was taken [3], [17], [18], [41]. First, we created two drums with 24 outdents along the z axis, one with wider and higher dents than the other, the outdents followed a square wave structure with a wavelength of 4.96 mm and amplitude of 1.01 mm for the more robust and a wavelength of 4.83 mm and amplitude of 0.48 mm for the other one. Secondly, two drums with spherical outdents, one with three lines of dents the middle one with 18 semi spheres and the edge ones with 15, the fourth stimulus has an array of 40x7 semi spheres along the z axis. The fifth stimulus is an array 40x10 rectangles in the z axis. The final stimulus is a smooth surface cylinder with no texture.

All stimuli were created on top of a 20 mm radius cylinder excluding there outdents, and with an inscribed hexagonal hole in the middle to insert the hexagonal prism that holds all the stimuli together.

The following figure shows the drawings of all the stimuli:

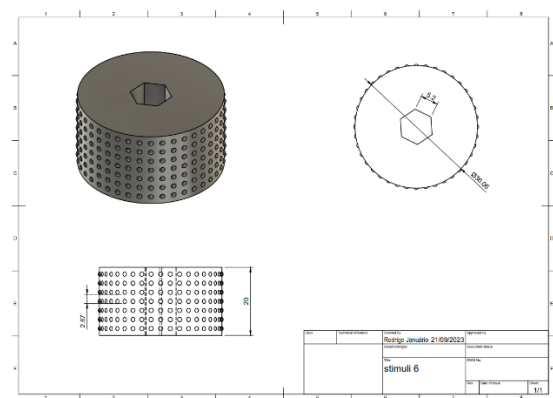
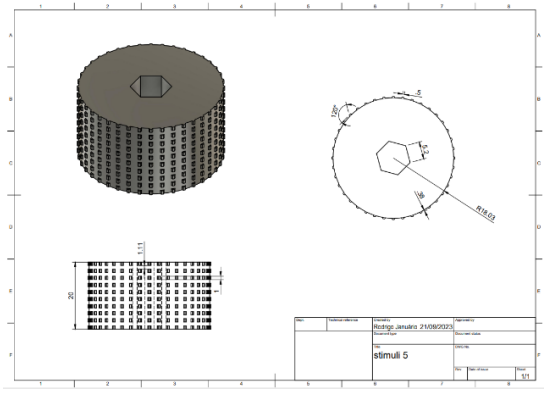
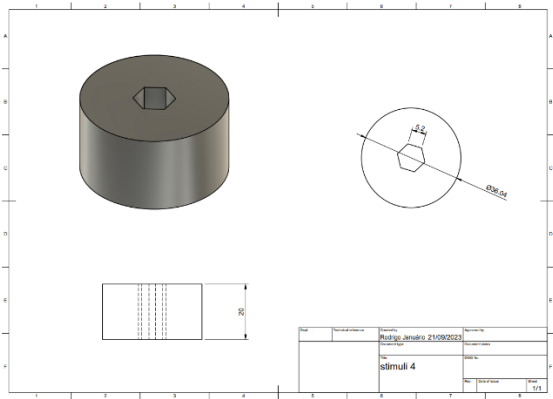
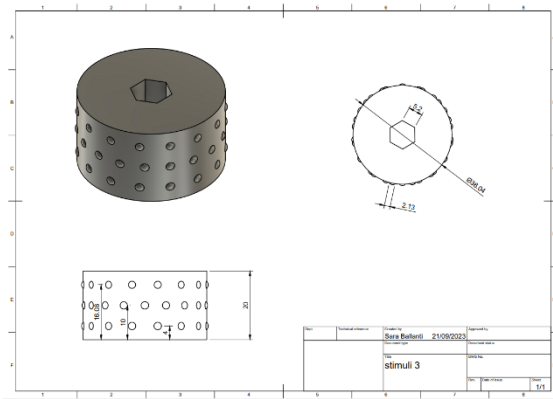
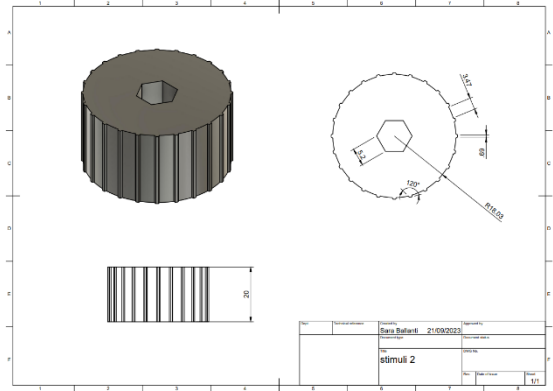
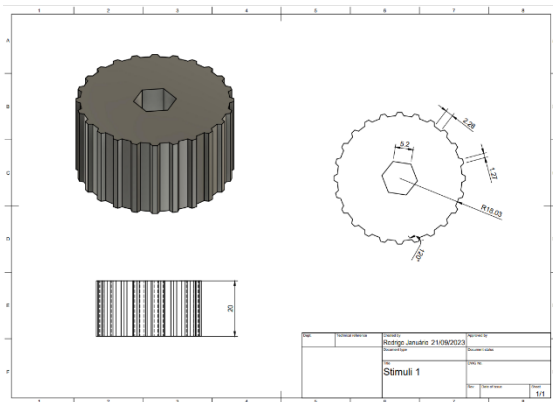


Figure 3-9 Stimulus 1, 2, 3 and 4. The first two are formed from 24 rectangle outdents, the third is an array of large semi spheres and the fourth a smooth surface. Stimulus 5 and 6 are formed from two different arrays, to the left is an 40x10 array of small rectangles and to the right a 40x7 array of small semi spheres.

3.1.2 Designing the Box Layout

The box design had two major requirements: to make it compact, and to keep it hazard free. Since the goal of this project is to create a portable tactile stimulator, the box needed to be as small as possible, so the layout must be efficient. On the other hand, the smaller it is, the easier it is to heat up and damage the internals of the components. One other disadvantage of the smaller size is that if an electrical connection is detached from a component, it could create a short circuit damaging once again the electronic devices.

To prevent these occurrences a few measures were taken. First, the box size was increased from the first one considered because it could fit everything in a safe manner, secondly a fan was added which extracted the heat inside the box and finally a circuit breaker was used to cut the power supply if any ground faults, or short circuits occurs.

The layout considered for the machine also kept in mind space between components and that they had sufficient surface area to extract the heat produced during activation.

3.1.2.1 Eagle Software

After the layout of the machine was set, all the connections between components needed to be planned, certified, and registered to correctly power and transfer data between components. Thus, the Eagle software was used to create a guide of all the connections between all the components so that this information could be saved and given to other people that could one day try to build Emily Figure 3-13.

Eagle is an electronic design automation (EDA) software that lets printed circuit board (PCB) designers connect schematic diagrams, component placement, PCB routing. Although it was not used to directly build a circuit board, it was the best way to inform an outside source on how to build the box.

Even though this platform was developed by me, it is still a joined venture between a lot of other engineers, and to build it there are some tasks I couldn't perform myself. After designing the layout with all the connections, the platform was sent to a technician who followed the instructions in the designed layout and built the entire platform, screwing the resting mount (P9) to the box, as well as the components and creating all the connection between the components, and between the box and the stimulator.

The following figure is the layout designed on Eagle. Drawing of the connection in the appendix.

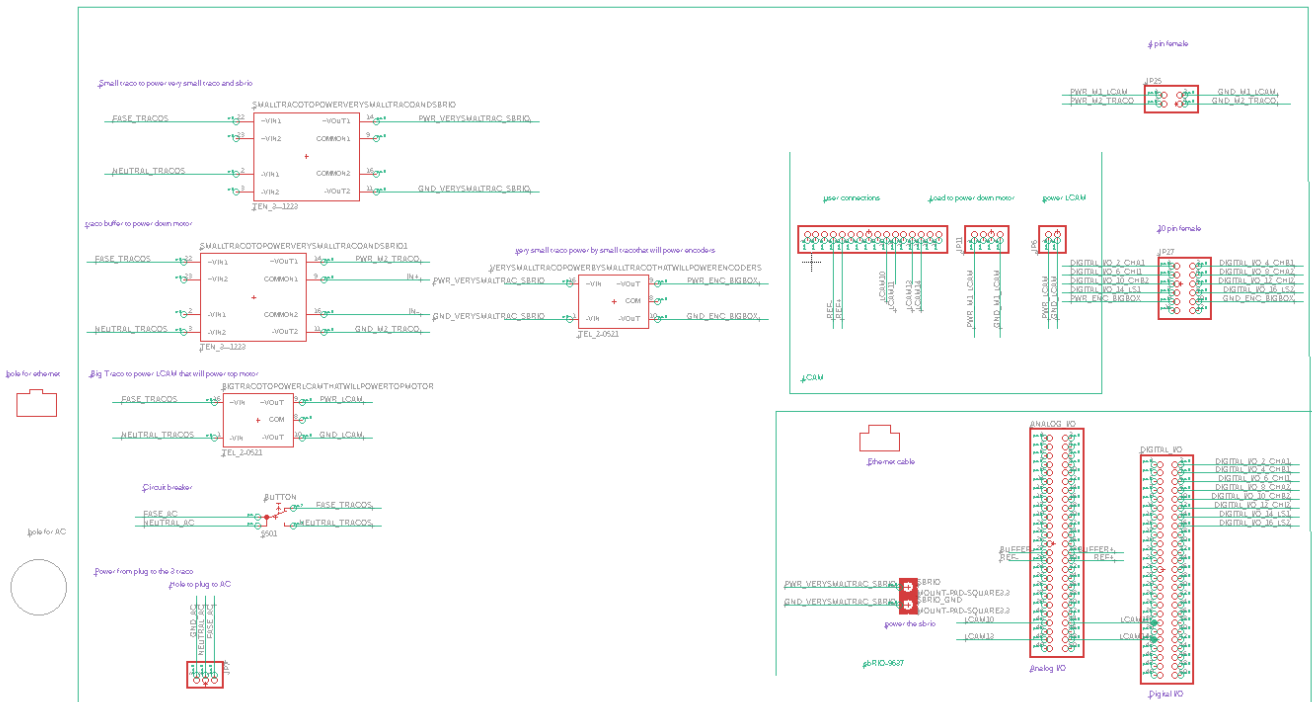


Figure 3-13 Layout of the electrical connections of the hardware box. Every elongated pin has a connection with a different pin with the same name. Meaning that if two pins have the same name, they should be connected by a wire.

3.1.2.2 Hardware Box

The Hardware Box (Figure 3-14) is the biggest of the two boxes and it comprises the four TRACO POWER converters, the sbRIO-9637, the LCAM-1, the circuit breaker, the buffer and the fan for ventilation. This box drives the platform, receiving the data, operating on it, and outputting it as the user defines it to. In this chapter an overview of the connections and the workings of this box will be done, however all this information will be further explained in the following chapters dedicated to each of the specific components.

The hardware box receives power from the wall plug as a 220 VAC, this current flows through a circuit breaker which works as a safety measure in case of any current malfunction, the current then splits into three paths one for each TRACO POWER converter that transforms the power into DC and outputs each with a specific voltage according to the needs of the component they are powering. The 48 V TRACO powers the LCAM which will power the drum motor connecting to the 4-pin cable that goes to the wire box. The 15 V TRACO will power the buffer which will in turn drive the guide motor connecting to the same 4-pin cable. The 24 V TRACO will power both the sbRIO-9637 and the 5 V TRACO with the latter powering the encoders and the Limited Switch (LS) connecting to the 12-pin cable which also goes to the wire box.

The control part of the stimulator is done inside the hardware box, and it uses the sbRIO as its central component. The buffer is connected to the sbRIO which uses a function inside LabVIEW to pilot the power output from the buffer which will then power the guide motor of the slider. The LCAM is also connected to the RIO board as it drives the power output to the drum motor. Finally, the encoders and LS arrive in the hardware box by the 12-pin and have their data channels connected to the the DIO's of the sbRIO, allowing the user to view in their data in the pc.

At last, the Hardware box as a hole for the ethernet cable which connects the sbRIO to the host pc, a fan for ventilation powered by the buffer and a ON/OFF switch to turn on or shut down the flow of current to the box.

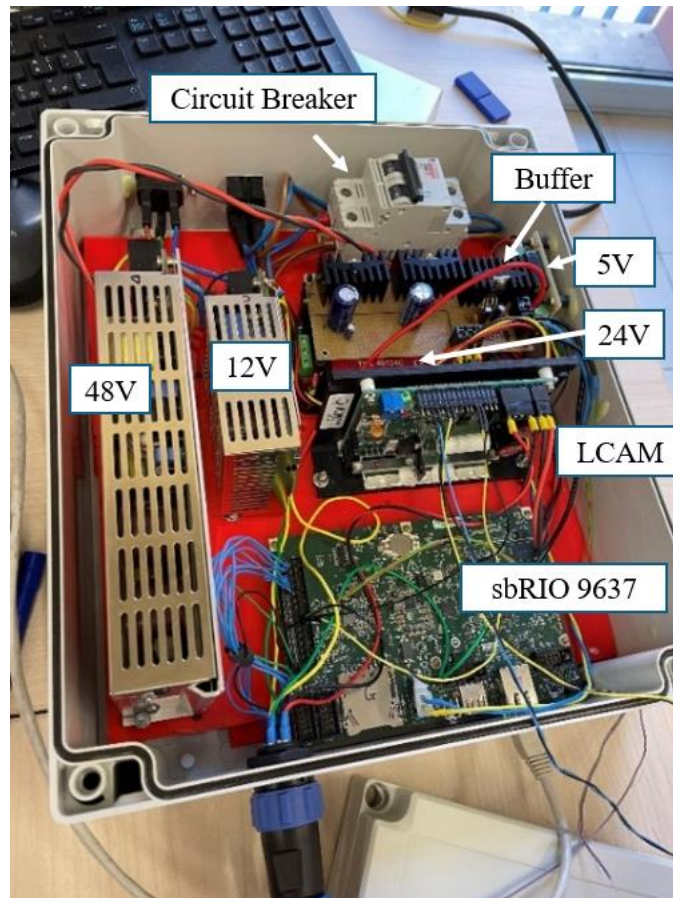


Figure 3-14 Hardware box. Includes the four traco power converters, the sbRIO, the LCAM, the buffer, the ventilator, and the circuit breaker. It receives power from the wall plug, and has an on/off button to control current flow, from it exit a 4-pin and a 12-pin

3.1.2.3 Wire Box

Until now this box has not been mentioned since its purpose doesn't affect the behavior of the platform, making it only more confusing to explain. The wire box (Figure 3-15) is the smaller of the two and its purpose is to arrange the cables and the connections in a safer and more organized manner.

To this box connects the encoders associated to each motor in a DB9 port (encoder has ten pins however the first is useless so it was discarded), where pins 2, 3, 6, 8, 10 of each were followed with a wire. The Limited Switch was also connected to the box in a DB9 port using only pins 2, 5, 7, 9 which were followed with a wire. All these wires were fixed together and from this box exited a single cable with all of them inside as a 12-pin cable (only 10 were used), six pins for the channels of both encoders, two for the LS and two for 5 V powering the encoders and the LS. This single cable is an input in a 12-pin female in the hardware box.

To this box is also connected a 4-pin cable with the two positive and two negative wires of the motors for power. These cables enter the box separately, and inside are turned into a single cable which exits the wire box as a 4-pin cable and reaches the hardware box in a 4-pin female port.

In the following chapters explaining in more detail all the connections of the components, this box or the cable leading to it will not be mentioned to make it easier to comprehend and to visualize for the reader. This box has no direct effect on the workings of the platform only creating a hub for all the wires to make the platform easily mountable and movable so there is no need to mention it. From now on the connections will be referred as if they were directly done without the use of this box.

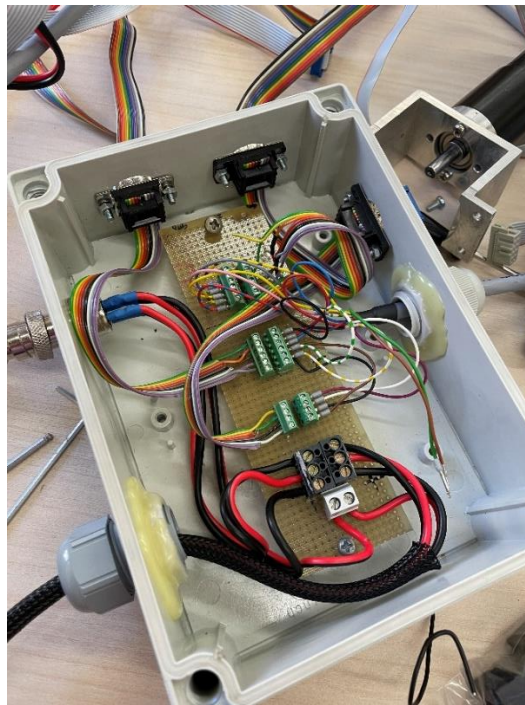


Figure 3-15 Wire box. Housed all the connections between the tactile stimulator and the hardware box. It is a hub to simplify connections and to make the machine safer for outdoor trials.

3.2 Hardware Components

3.2.1 DC Motors

The two DC motors used for this project were a RE35 from Maxon Motors Figure 3-16 [46]. Which will from now on mentioned as drum motor, for the motor driving the drum and mounted higher up, and guide motor, for the one controlling the movement of the stimulator along the guide, mounted bellow the other.

Each DC motor controls one of the degrees of freedom: rotation to create a linear movement on the linear guide which will move the stimulator back and forth to change the stimuli presented during the trial; rotation of the tactile stimulating drum with various vertically embedded textures along its length axis. All the motor specifications can be verified here [46].

Each DC motors is control by a VI in the LabVIEW code on the host pc, after performing all the tasks programmed by the user the code will output a number for each IO which will be relayed to the sbRIO. When controlling the drum motor, the RIO sends this number to the LCAM and thus makes the drum motor rotate with the same voltage as the number specified in the IO. On the other hand, when controlling the guide motor, the RIO transmits the number to a controller on the buffer which will feed the guide motor with the same voltage as determined by the number the IO communicated to the RIO.

When using LabVIEW to control the behavior of each motor, there is complete freedom in the way the platform operates, allowing it to start, stop, go back or forward or even increase or decrease its speed as the user pleases. This creates a versatile platform that can be used to perform a variety of pipelines for tactile stimulation and many different neurophysiological and psychophysical experiments.

To have valid and comparable data between trials the motors must produce a controlled and constant speed of rotation, which is possible because to the output from the LCAM. One major aspect to have in consideration is the friction caused by the finger touching the drum which can change the speed of rotation. However, thanks to the inertia of rotation of the motor when unpowered (67.9 cm^2) the force applied by the user, which only amounts for a few grams, will not be strong enough to affect the speed of rotation of the drum.

Power connections were very simple, the drum motor was connected to the load connector on the LCAM, and the guide motor to the power output of the buffer (top right corner of the board) which in turn is powered by the 15 V Traco.



Figure 3-16 RE35 DC motor from Maxon Motors. Used to drive the drums rotation and the movement of the guide.

3.2.2 Force/Torque Sensor System, Load Cell

The current design of the stimulator houses a force sensor bellow the drum support collinear with the center of gravity of the stimulator. However, only a design implementation was achieved. Therefore, a phantom sensor was used which served as a place holder to validate its implementation in the design structure and for a future introduction of a functional cell.

The sensor aimed to be used was a Nano43, ATI IA, (Figure 3-17) with all its specification here [47].

Its purpose would be to measure the force applied by the subject onto de drum during experiments, and to locate the finger along the drum, since it can register where the force is applied, displaying this information live on the LabVIEW interface shown on the PC. However, its future implementation will not be able to automatically keep the contact strength constant which is one essential requirement for standardized and repeatable experiments. To achieve this, the user or the subject must compensate with human input attempting to keep this value stationary by tracking the applied force in the graphical interface on the PC and adjust it during the trial. This design concept is called an open loop control since the measured contact force doesn't have any effect on the behavior of the stimulator. To close this loop an idea inspired by [41] would be to incorporate movement on the vertical axis with a third DC motor, which used the data from the force sensor to move the stimulator vertically controlling the contact force between the finger and the drum. This would even expand the applicable pipelines for experiments, as well as increasing the number of sensations provoked by the same stimulus, since increasing the contact force mimics the increase in indentation depth of the stimulus [41] basically invoking new sensations from the same stimulus.

With the implementation of the third motor a finger support could even be added to keep it stationary, therefore removing any required action from the subjects.

Despite the lack of this third degree of freedom, it is still possible to control the indentation depth by asking the subject to do a specific amount of force onto the drum and validate it with the value from the sensor.

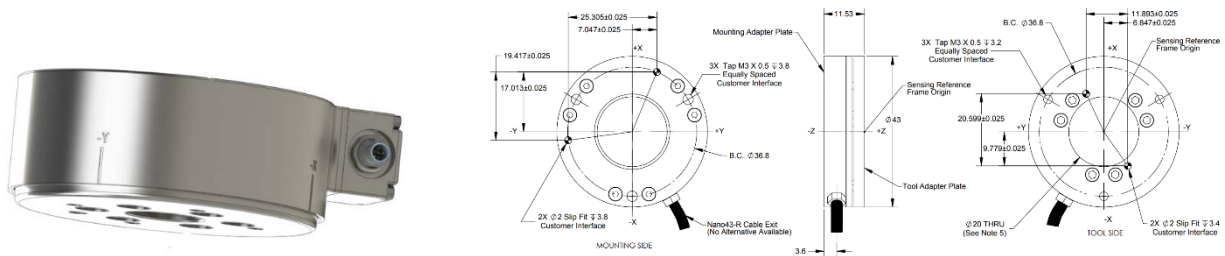


Figure 3-17 Force sensor for calculation of the contact strength between the drum and the finger. On the right is the drawing of this component.

3.2.3 Encoder

To build an autonomous tactile stimulator which moves inside its workspace it is required precise position monitoring and control. To achieve this an encoder attached to each motor was used to track the rotation of the motors and indirectly calculate the position of the stimulator using this data. They are precise sensor that converts mechanical movement into an electrical signal that can be read by a control system like a counter.

These devices rotation follows the motors rotation and produces periodic square waves which can be used as a measurement of how much each motor has rotated. The drum encoder is responsible for calculating where in the rotation the drum is located, and the drum encoder responsible for localizing the stimulator along the linear guide. Each passing of the square waves produced by the encoder is considered an iteration, or state, therefore the program controlling the machine can be set to automatically do a specific task as each iteration of the encoder, giving the user freedom to control it in a variety of ways.

The encoders used are the MR type L, 265-1024 CPT, 3 channel, with line driver [48], meaning it has a rotating disk with 1024 openings. The encoder has a resolution of $0.98\mu\text{m}$, thus each transition/iteration is $0.98\mu\text{m}$ of linear distance. The 3 channels are “A”, “B” and “I”, “A” and “B” form two different sets of square waves with the same frequency and amplitude (either 0 or 1), however they have a 90° phase shift, thus they are misaligned and change states at different times. “I” is a mono square wave which only registers a positive value when the encoder does a full rotation, its amplitude is the same as the others, but the frequency is different.

There is a variate of different encoders, in this project we will be using an optical sensing encoder that provides feedback based on the existence of photo stimulus.

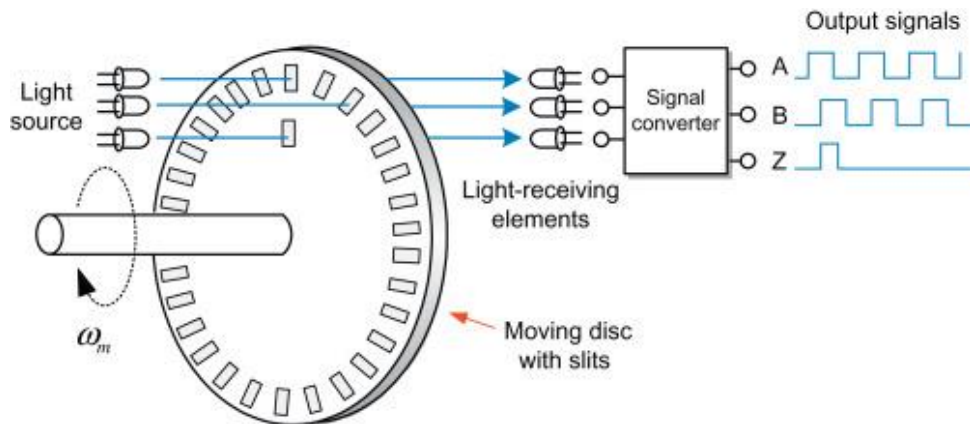


Figure 3-18 Inner working of an optical encoder. Light either passes through the disc or not, creating a binary sequence of square waves, the signal will be read by the sbRIO and used to control the platform.

Like shown in Figure 3-18 the rotating optical encoder has three LEDs that emit a beam of light that is received by three photodetector, however, between these two there is a code disk with opaque spaces, as the encoders shaft rotates the light beam either is interrupted or it gets through, creating a pulse signal like a square wave, were it is either on or off (1 or 0).

The three-square waves, A, B and I, are therefore created by reception of light in the photodetector, and the phase shift created from misaligned LED's.

When either wave A or B changes its value, a new state is achieved, and since A and B have a phase difference of 90°, they will never change states at the same time, resulting in 4 possible states (A=0, B=0); (A=1, B=0); (A=1, B=1); (A=0, B=1), hence this encoder has 1024 opening but 4096 iterations/states per rotation.

The states produced by the encoder follow a pattern depending in which direction the shaft is rotating (Figure 3-19), either clockwise or counterclockwise. In either orientation the encoder can start in any state, but we will consider “00” to be the first. In the clockwise rotation the encoder starts from “00” then since both states can never change at the same time it swaps to “01”, then “11”, then “10” and finally “00”, repeating the cycle, the counterclockwise does the opposite, it starts in “00”, moves to “10”, then “11”, “01” and finally “00”.

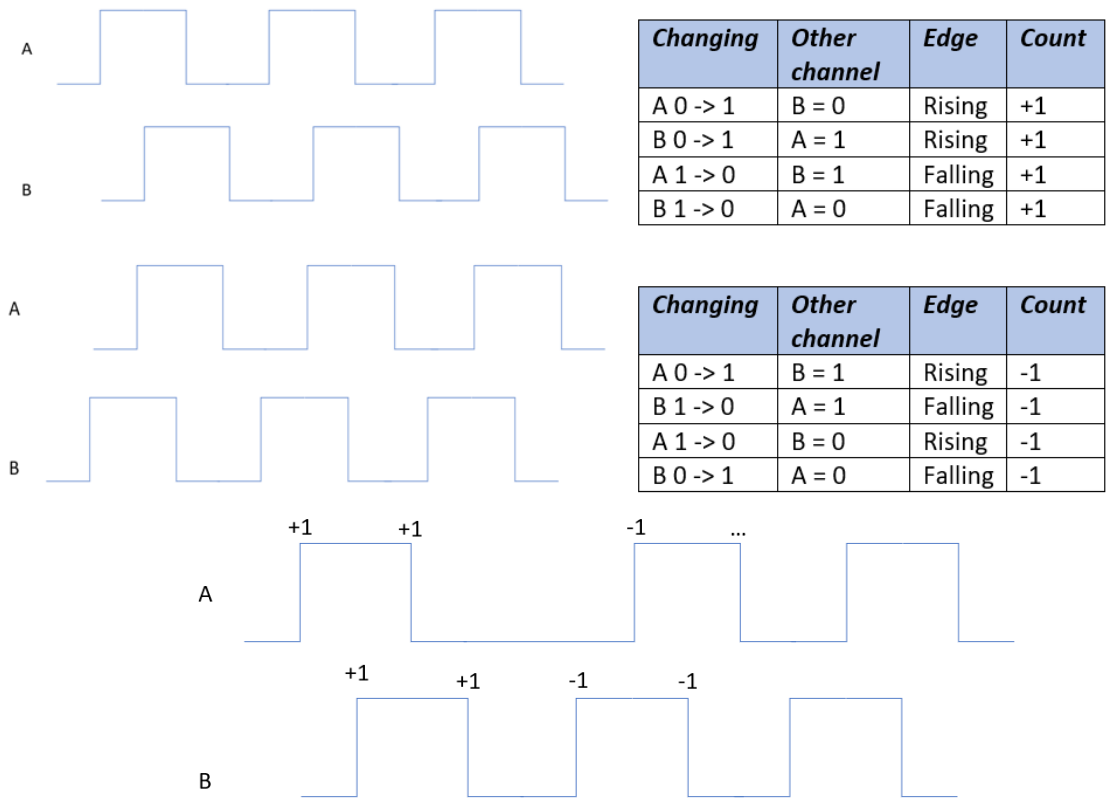


Figure 3-19 On the top behavior square wave of the encoders during Clockwise and Counterclockwise rotation. On the bottom behavior of the square wave of the encoder when inverting the direction of rotation.

To reiterate the encoders used have 1024 counts per turn of the shaft, since channel A and B have a 90° shift between them this created 4096 states per rotation and a linear distance of 0,98 µm per state. These values will be important for validation purposes of the codes created and described in the following chapters.

Even though it isn't relevant for the development of the software, the drum encoder, has an 86x multiplier, meaning that the count in the state counter is multiplied by 86, however this data will not be necessary since the stimulation drum will always be rotating during the experiment.

The encoder has a supply voltage of 5 V given by the, a current draw of 14 mA, a phase shift and impulse width of $90^\circ \pm 45^\circ$ and it operates at a maximum frequency of 80 KHz or 18750 rpm. The pins of the encoder are as follows.

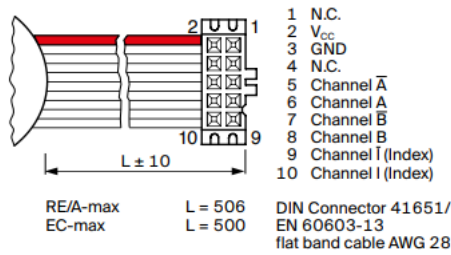


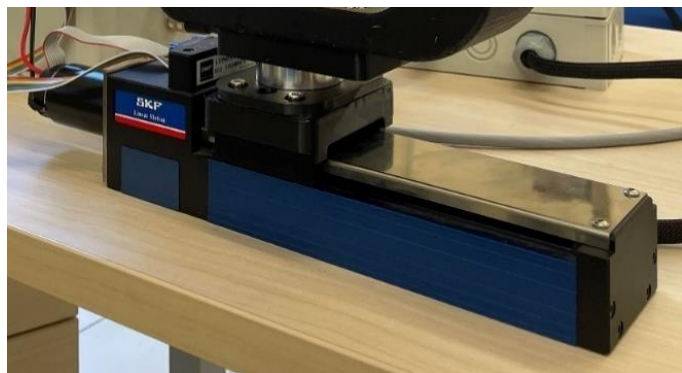
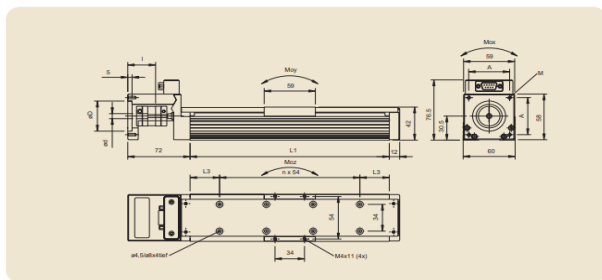
Figure 3-20 Pinout for the encoders attached to the DC motor. Pins 2, 3, 6, 8, 10 are extremely relevant since the first pair receives power and the last three output data.

The pins used for this project were pin 2 and 3 (V_{cc} and GND) which were connected to the power from the 5 V TRACO (chapter 3.2.9.5), and pins 6, 8 and 10 (channel A, B and I) which were connected to the sbRIO (chapter 3.2.5) to build the counter for the elapsed states in LabVIEW.

3.2.4 Linear Guide

Many rotating tactile stimulators only have one degree of freedom [41] however, Emily introduces the addition of a second movement direction by the usage of a linear guide. This guide is a SKF Multitec LTP 60.180.0804-02 linear guide (Figure 3-21) [49] driven by the guide motor with the sliding motion applied through a 4 mm pitch ball bearing screw that translates rotating motion to linear motion, meaning that each full rotation of the bearing corresponds to 4mm of linear travel distance. This guide is 180 mm in length with an attachment of 59 mm to plant the base of the support.

The addition of this guide introduced the ability to rapidly, and with the correct controller, automatically change the stimuli presented to the subject by moving the stimulator along the drum's length axis. Most platform change it manually [32], [43], and there are some that do it very quickly [39], [40] however none of them can do it this quickly and autonomously at the same time. Even though it is not currently implemented a controller could be developed to have stimulation from the motor with parallel lateral stimulation induced by the movement along the slider.



Designation	Size	Stroke ²⁾	Mass	Screw data	$I_{ref}^{2)}$	a_{max}	n_{max}			
-	L_1 mm	L_2 mm	n	S	d_s mm	p	$kgmm^2$	m/s^2	1/min	
LTP60.180.0804-XX	180	9	3	110	1,5	8	4	2,8	3,2	4 500

Figure 3-21 SKF Multitec LTP 60.180.0804-02 linear guide. On the left is the drawing of the guide with measurements and on the right a picture of the linear guide used in this project.

Since the goal is to create a controllable automatic stimulator, the data from the encoders will be implemented in the program philosophy, enabling the ability to track and in turn manage its behavior. Since the encoder produces square waves following the motors rotation, a parallelism can be created between counted elapsed waves (chapter 3.3.2.2) and the linear movement created from the rotation. A comparison can then be made between a ruler and the slider, where the ruler measures centimeters the slider measures elapsed states, therefore the elapsed states can be counted and used as a marker to command the platform to do a specific task at a specific marker. Since the encoder has a resolution of $0,98\mu m$ each counted state corresponds this measurement, thus we can now choose a position measured in cm and turn it into states and make the stimulator move to that location.

At the extremities of the linear guide two magnetic limit switches were integrated for delimitating the workspace. This will be implemented in the controllers developed in LabVIEW to delimit the beginning and end positions of the slider by using them as Boolean constants which turn TRUE if the stimulator as reached on of the positions.

The connection is made in the top left part of the linear guide where there is a DB9 pin. Power comes from the 5 V traco (Figure 3-30), the same source as the encoders.

During movement there are vibrations caused by the motor's rotation, friction from the slider, some looseness from the platform itself since it is not one solid piece. The propagation of these small vibrations was not filtered with a damper or with metallic structures like other platforms have done, hence this is another aspect for future improvements.

3.2.5 sbRIO-9637

The sbRIO-9637 [50] is an embedded controller developed by National Instruments that integrates a real-time processor running NI Linux Real-Time, a user-reconfigurable FPGA, and I/O on a single printed circuit board (PCB). This controller features Gigabit Ethernet, CAN, USB, serial, and SDHC ports and an operating temperature range that can handle the most demanding environments. The sbRIO-9637 has sixteen 16-bit analog inputs, four 16-bit analog outputs, and 28 3.3 V digital lines.

The processing power of this board associated with the configurability given by LabVIEW FPPA permits the user to extract different types of data from components connected to the sbRIO, as well as it allows to control other components behavior.

The sbRIO was implemented on this platform to enable the creating of a configurable controller to manage the behavior of the entire platform. Due to the installed LabVIEW FPGA the user can create different operating pipelines with a high degree of flexibility to meet the needs of any experimental protocol. This is possible also because the RIO board is able to communicate directly or indirectly with all the other components of the platform, controlling their behavior through the programmed designed on LabVIEW. Therefore, the sbRIO can receive the data from the encoders use it to process a response and output this response to the LCAM and the buffer to indirectly drive the two motors. The sbRIO also allows for live feedback on the status of the stimulator with great precision.

3.2.5.1 Board Layout of the sbRIO-9637

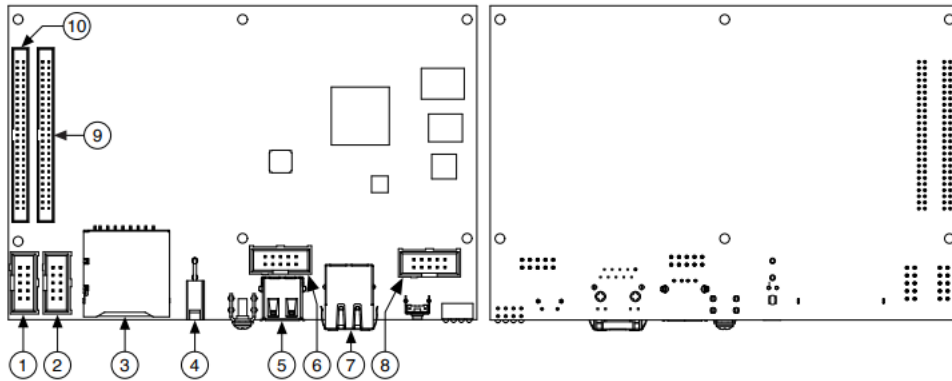


Figure 3-22 1. W3, RS-485 (ASRL3) 2. W4, RS-232 (ASRL2) 3. J6, SDHC 4. J9, Power Connector 5. J10, USB Host Port 6. W1, CAN (CAN0) 7. J7, RJ-45 Ethernet Port 8. W2, RS-232 (ASRL1) 9. J5, MIO 10. J4, DIO

3.2.5.2 Technical Specification of the sbRIO-9637

Table 3-1 Parameters and their values for correct operation of the sbRIO-9637.

Parameter	Value	Unit
Operating temperature	85	Celsius
Supply voltage	9 min – 30 max	Volts

3.2.5.3 Power Connection and Data Transferring

The sbRIO-9637 requires a voltage input between 9 V and 30 V Table 3-1, this power is supplied by a TRACO POWER that outputs 24V (Figure 3-29), which is inside the operation range of the device. The powering is done through port J9.

The sbRIO-9637 has a tri-speed RJ-45 Gigabit Ethernet port. This connection transfers data from the host PC to the RIO, for example the LabVIEW VI created to control the platform and from the RIO to the PC such as information from the encoders. This connection is done in port J7.

3.2.5.4 Controlling the platform through DIO and MIO Ports

The sbRIO-9637 has two main ports for data connections (Figure 3-23), port J4 with all the digital outputs (DIO) and port J5 with the analog inputs (AI) analog outputs (AO) and some DIO's. We will only be using DIO's and AO's for this project. There are two major differences between these two pin types: first the analog pins use continuous signals that vary in magnitude, such as voltage, current, or resistance while digital pins use discrete signals that have only two states, such as on/off, high/low, or 1/0; secondly Digital output exists when a voltage is applied to a pair of digital output leads. While AO output an electronic non-digital signal processed by a control system, in this case the sbRIO, on the other hand digital output exists when a voltage is applied to a pair of digital output leads, thus when an encoder registers a positive spike in its square wave [51], [52].

From the above-mentioned examples, we can apprehend that to properly connect each component to the RIO it must be connected to the right pin type. Hence the encoders will be connected to the DIO's to receive the digital discrete signals and the LCAM and buffer to the AO's to receive the continues voltage output to drive the motors.

In port J4 the pins 6,8,10 (channel A, B, I) from each encoder will connect to the pair pins 2 throw 12 of the sbRIO. Alongside them pins 2 and 5 (LS beginning, end) from the limit switch must be connected to pins 14 and 16 of the RIO.

To this port also connect the LCAM which will connect pins 10 (ground, 0 V), 11 (enable LCAM if at 0 V), 13 (5 V pin), 14 (enable LCAM if at 5 V) from the user connection header of the LCAM to pins 43, 43, 47, 48, respectively.

In port J5 are the connections responsible for powering the motors, therefore the two different components connected are the LCAM and the Buffer. The LCAM connects its pins 4 and 5 (REF±) of the user connection header to pins 29 and 30 of the RIO, while the buffer connects its control pins in the top right of the PCB board to pins 27 and 28 of the RIO.

The following figure (Figure 3-23) shows the pin location in both J4 and J5 as well as the IO's to be implemented on LabVIEW code to control the information inputted and outputted to the sbRIO. The right image is a reference to locate J4 (left array) and J5 (right array) on the board.

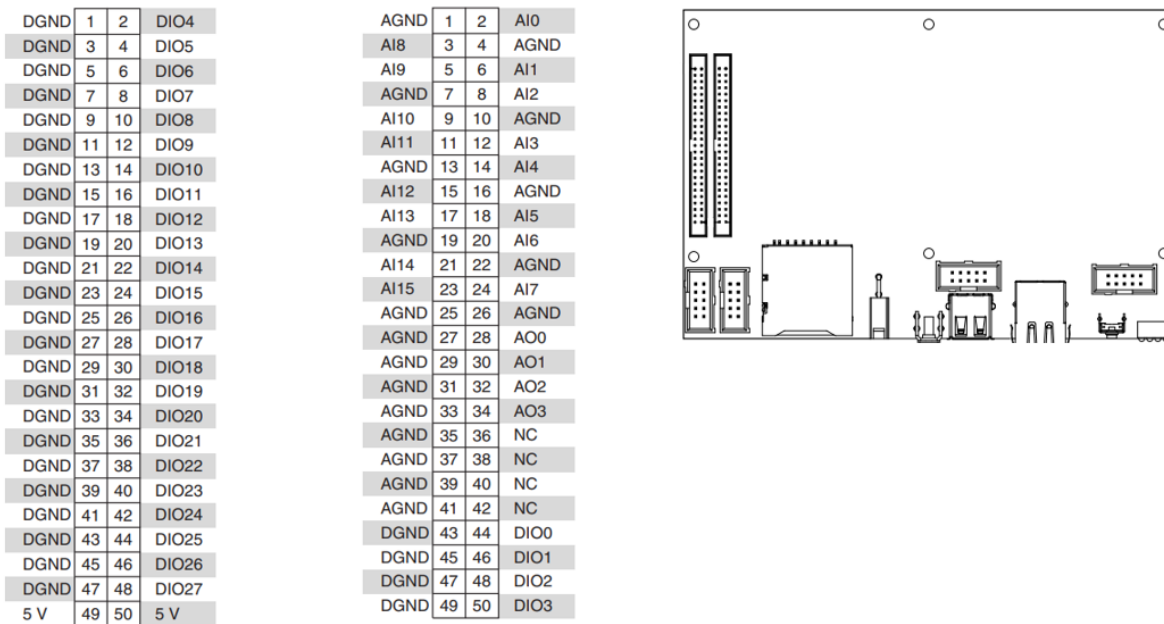


Figure 3-23 On the left is the pinout of port J4 and J5 the DIO and MIO ports of the sbRIO-9637. On the right the board layout with the location of the pins in the top left corner.

The followig table (Table 3-2) shows all the connections perfomed with the sbRIO, explaining each connects purpouse and where to connect it.

Table 3-2 Table with all the connections made to the sbRIO's J4 and J5 port and specific pins used, as well as the purpose of each connection and the component they are connected to.

<i>Port</i>	<i>Pin</i>	<i>Purpose</i>	<i>Component</i>	<i>Pin of component</i>
J4	2, 4, 6 (DIO4,5,6)	Data channel A, B, I	Top encoder	6, 8, 10
J4	8, 10, 12 (DIO7,8,9)	Data channel A, B, I	bottom encoder	6, 8, 10
J4	14, 16 (DIO10,11)	Data reach beginning and end of slider	Limiter Switch	2, 5
J5	43, 44 (DIO0, DGND)	Enable LCAM	LCAM	10, 11
J5	47, 48 (DIO2, DGND)	Disable LCAM	LCAM	13, 14
J5	27, 28 (AGND, AO0)	Chose how much voltage to output	Buffer	PCB board top right
J5	29, 30 (AGND, AO1)	Chose how much voltage to output	LCAM	4,5

3.2.6 Linear Current Amplifier Module (LCAM-1)

The Quanser Power Amplifier [53] is a linear power amplifier which produces low electromagnetic interference. It is designed to drive leads in either voltage or current mode. The unit displays low noise, wide bandwidth, and an offset voltage adjustable to zero. Designed to run from a single supply, the amplifier's features include accurate current sensing, selectable fixed gain configurations, current limiting, and thermal protection.

The purpose of the LCAM is to power the drum motor while producing the least electromagnetic interference possible. Since the power supply used inputs 48 V, the range of the output is between +20 V and -20 V which means the LCAM can move the DC motor back and forth as it was needed for the development of the platform.

Other hardware components like a normal power supply could have been used for this task however, since the platform will be used for microneurography experiments low electromagnetic interference is mandatory because the data is easily damaged. During the making of this platform, it was also discussed the possibility of a second LCAM to power the drum motor, however, since this motor would not be rotating during any tactile stimulation trials, its noise and interference will not damage the data of the experiment. Currently, this possibility as risen in our considerations once again, and in the future it would be an important upgrade to incorporate lateral stimulation without compromising the data of more sensible studies.

The LCAM will be controlled by the sbRIO-9637 by the means of a LabVIEW FPGA VI in the host PC that will enable it and control the voltage it outputs.

3.2.6.1 Board Layout of the LCAM

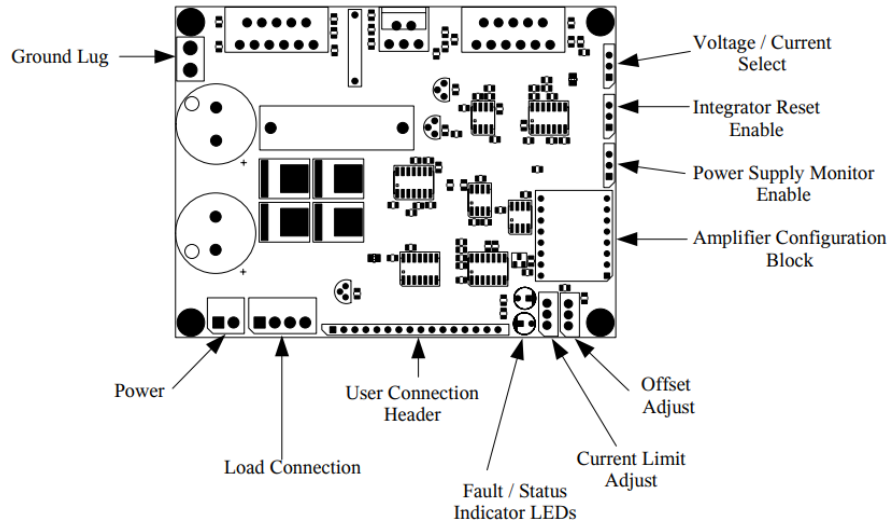


Figure 3-24 Board Layout of the LCAM-1.

3.2.6.2 Configurations of the LCAM

To setup the LCAM there are many modes, headers, and pins to be chosen for the specific purpose of the component, so the following options were selected.

3.2.6.2.1 Mode Selector

In the amplifier mode selector, the jumper J1 was set in the 1-2 position, meaning it is in the voltage mode rather than the current mode. This makes it function as a voltage amplifier since in this mode it adjusts the current automatically independently from external forces like the force of the finger when the stimulation occurs, meaning the velocity or rotation is kept constant even though a force like drag is applied. In this configuration, the amplifier accepts a command signal and outputs a voltage proportional to the command signal. The signal can be amplified by the configurable gain setting of the amplifier.

The Power Supply Monitor Enable jumper (J2) was set in the 1-2 position allowing for the safety measures built in the amplifier to be applied. This header employs a voltage monitoring system to ensure that the safe startup and shutdown conditions of the amplifier are met. This feature limits surge currents that may be sent to the load at startup or shutdown. A delay of approximately 0.5 seconds is used when the amplifier is turned on disabling it until the power supply has reached the minimum voltages of 27 volts. To disable this feature, install the jumper in the 2-3 position.

The Integrator Reset Enable jumper (SW EN) was set in the 1-2 position enabling the integrator reset feature. enables / disables resetting of the integrator of the amplifier. With this jumper in the 1-2 position, the integrator used for the current feedback loop is cleared or reset to zero when the amplifier is first powered up, or when the amplifier is disabled. In the 2-3 position, this feature is disabled.

3.2.6.2.2 User Connection Header

One very important part of the LCAM is the user connection header (Table 3-3), this 1D array of pins allows the user to control the behaviour of the amplifier and to control other devices. The following section and table explain the purpose of each pin in the user connection header and what they were used for in the making of Emily.

Since the LCAM as a safe switch toggle on and off option, to turn it on it is required to enable its system through pins 11 and 13, pin 11 is mandatory to be at 0 V and 13 at 5 V. The voltage required was extracted from the LCAM user connection header, since pin 10 is a ground, meaning 0 V and pin 14 a 5 V output, therefore if pins 10 and 14 are set to TRUE in the LabVIEW code the LCAM turn on, and if they are set to FALSE it turns off.

These four pins were connected to the sbRIO: pins 10, 11, 13, 14 of the LCAMs user connection header to pins 43, 44, 47, 48 of port J4 respectively of the RIO. The IO's used in the VI were DIO0 and DIO2.

To power the drum motor pins 4 and 5 (REF \pm) were used to output a signal from the RIO to the LCAM making the latter output to the drum motor the same voltage as the signalled value sent from the RIO. These two pins were connected to the sbRIO in pin 29 and 30 of port J5 respectively. By using a control on the IO function used in LabVIEW to drive the motor the user can change the voltage output from a range of ± 20 V making the motor rotate faster or slower or even backwards.

Table 3-3 User Connection Header of the LCAM displaying all its pins and their functions.

<i>Pin Number</i>	<i>Signal</i>	<i>Comments</i>
1	+5 V	Available for signal conditioning circuitry, 10 mA max.
2	GND	Ground connection.
3	-5 V	Available for signal conditioning circuitry, 10 mA max
4	REF -	Command signal negative or ground reference.
5	REF +	Command signal positive or signal.
6	Current Limit Monitor	Output of current limit setting.
7	GND	Ground connection.
8	Not used	Do not make connections to this terminal.
9	Current Monitor	Current measurement output, 0.5V/A
10	GND	Ground connection.
11	/ENABLE	Amplifier Enable input. This line must be at 0V for the amplifier to operate.
12	GND	Ground connection.
13	ENABLE	Amplifier Enable input. This line must be at 5 V for the amplifier to operate.
14	+5 V	Available for signal conditioning circuitry, 10 mA max.
15	FAULT OUTPUT	Fault indication for the amplifier, external LED connection
16	GND	Ground connection

3.2.6.3 Power Supply and Load Connector

The LCAM must be powered in the power supply port with a voltage between 27 V and 60 V (Table 3-4). Power must be applied to these pins with the correct polarity, otherwise the amplifier may be damaged. Only isolated-secondary type power supplies should be used. The power supply should be a floating type of supply, and not referenced to ground on the secondary.

This power is given by the 48V TRACO POWER CONVERTER which inside the safe power range and just enough to enable the LCAM to output a voltage range between ± 20 V.

Table 3-4 Header for Power Supply of the LCAM.

Pin Number	Function
1	POWER + (27 – 60 Volts)
2	POWER -

To give power to other components the LCAM has four pins, two positives and two negatives, these will be used to supply the drum motor, controlling it via the sBRIO.

Table 3-5 connection header for the load connector of the LCAM.

Pin Number	Function
1	Motor -
2	Motor -
3	Motor +
4	Motor +

To power the top motor the LCAM connects pin 1 to the negative cable (black) of the motor and pin 4 to the positive cable (red).

3.2.6.3 Technical Specifications of the LCAM

Table 3-6 Parameters for safe usage of the LCAM.

Parameter	Value	Unit
Supply Voltage	27-60	V
Input (command) Voltage with 48V of supply	± 20	V
Operating Temperature	50	$^{\circ}\text{C}$
Voltage Mode	>10	KHz

3.2.6.4 Voltage Mode and Gain function

The LCAM was used in the voltage mode (jumper J1 in the 1-2 position). In this mode the amplifier accepts a command signal inputted digitally in the LabVIEW code and outputs a voltage proportional to the command signal which is amplified by the configurable gain setting of the amplifier. The gain was configured to be at 32,143 which means that if 1 V was applied the LCAM would output 32,143V $output = input \times gain$. This value was obtained through the following equation $G_t = G_1 \times G_2 \times G_F$, where G_F is the final gain stage of the amplifier and is fixed to a value of 20.

Table 3-7 Gain settings and the impact of each resistance in the amplifier configuration block.

Row	Function	Value
A	This resistor with D sets the first gain stage of the amplifier. The resulting gain is $G1 = D/A$	5,6 k Ω
B	Current loop feedback gain resistor	15 k Ω
C	Sets the gain in voltage mode for the amplifier. The resulting gain for this stage is $G2 = C/1k$.	0,5 k Ω
D	With A, this resistor value sets the first gain stage for the amplifier. The resulting gain for this stage is $G1 = D/A$.	18 k Ω
E	Current loop error feedback integration capacitor	100 nF
F	Current loop feedback compensation capacitor – typically use factory value of 2.2nF.	$1 \times 10^{-7} F$
G	Do not make connections in this position.	open
H	This enables the integrator clearing circuitry and must be installed for it to function properly.	short

The maximum output voltage the amplifier will be able to provide is close to the supplied voltage on the power supply port.

To know what to input to the LCAM as a voltage measurement for it to power the bottom motor simple math is required.

$$Input_{LCAM} = \frac{V_{Bottom\ motor}}{Gain} \quad 3.1$$

With this we know what to code in LabVIEW in order to power the bottom DC motor with a specific voltage.

3.2.7 Buffer

The buffer is responsible for powering the drum motor, through the control of the sbRIO to which it connects. The purpose of this component is to store power given by the 15 V traco and apply it to the drum motor when the sbRIO demands it [54].

The buffer is composed by a heat dissipator, four capacitors, and an op-amp. The op-amp is a OPA547t [54] with a supply voltage of 8-60 VDC thus the 15 V traco is inside the range. The OPA547 is a low-cost, high-voltage/high-current operational amplifier. The 15 V traco connects to V+ and V- and in Vin the sbRIO. The output of the buffer connects to the drum motor and the control pin to the sbRIO in pins 27 and 28 (AGND, AO0).

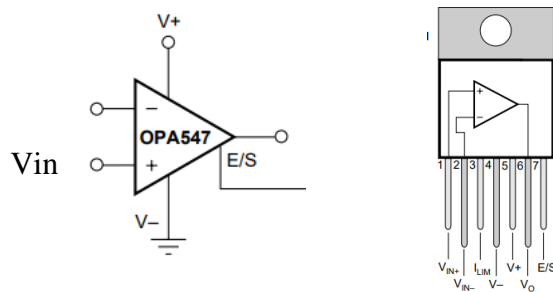


Figure 3-25 On the left is the electric circuit of the op amp and on the right the pin out of the op-amp.

A buffer was used to control the drum motor since in the experimental protocol this motor was not meant to be moving during stimulation, therefore it would not create interference and damage the data of the electrophysiological tests. However, to expand the catalog of possible pipelines to be executed by Emily a second LCAM should be implemented allowing for lateral stimulation as well. Tho the buffer is simpler to implement and less expensive, so it has its advantages.

3.2.8 Circuit Breaker

In this project the *MERLIN GERIN MULTI9 C60HB 25844 B16 16A 16 AMP MCB C* miniature circuit breaker was used (Figure 3-26) [55].

A circuit breaker is an electrical safety device, a switch that automatically interrupts the current of an overloaded electric circuit when a ground faults, or short circuits occurs.

In this project a miniature circuit breaker (MCB) was used, which is a normal practice when there is a low-energy requirements, like home wiring, offices, or small electronic circuits.

MCBs are equipped with two tripping mechanisms: the delayed thermal tripping mechanism for overload protection and the magnetic tripping mechanism for short circuit protection [56].

The MCB was connected directly to the power from the wall plug, working just as a safety switch closing the circuit of the hole platform if something were to malfunction. From the MCB exit three phase cables (blue) and three neutral cables (brown) and a pair of each goes each traco power converter which will power all the components of the platform.



Figure 3-26 MERLIN GERIN MULTI9 C60HB 25844 B16 16A 16 AMP MCB C miniature circuit breaker.

3.2.9 Powering the Platform

The platform is powered by an AC power outlet source from the wall which outputs 220V and is connected directly to the box.

The connection is done with a three-phase electrical system composed by three wires: phase, ground and neutral. Phase conducts the electric current flow; neutral creates a closed loop for the circuit working as a return path for the current and ground is a safety mechanism to reroute the current in case of an accidental contact of the phase wire to any metal part, basically a low resistance path for fault current to flow to ground. One important thing to note is that the neutral and the ground are bonded together so that neutral is referenced to earth, this doesn't however mean that neutral has no current flowing.

If at any point phase contacts, a metal component, the current flows through the ground wire to the ground (earth) avoiding an electrical shock by activating the circuit breaker [57].

For identification purposes the blue wire is phase, the brown is neutral and the yellow and green is ground.

After the current enters the platform, it reaches the circuit breaker later splitting into three parallel pathways which all lead to an AC-DC power convert from the TRACO POWER company. The three converts will be mentioned by their voltage output level.

3.2.9.1 TRACO POWER Converter

The traco power converters used in this project aim to transform the AC current from the wall outlet into DC current to be used by the rest of the components, outputting a specific voltage each depending on what they are powering. Basically, a power converter is an electrical circuit that changes the electric energy from one form into the desired form optimized for the specific load.

This conversion phenomenon works using transformers that change the voltage of the AC, rectifiers to save it from AC to DC and a filter that removes noise from the peaks and troths of the AC power waves.

The process of converting AC current into DC is called rectification. It starts by stepping down the AC voltage, which is normally much higher than the DC output pretended, which changes the 240 AC into the specific output of the converter, 48 V for example, also in AC. To convert this new voltage value into DC a rectifier must be used, which is four diodes connected as a bridge that allow for current flow in only two diodes at a time depending on the polarity of the AC at that same time. Following this the DC must be transformed from a pulse wave into pure DC waveform by using capacitors, these store energy while the voltage increases and discharge it while the input voltage is decreasing, basically creating a constant output rather than a pulse.

Finally, to change the output voltage to the desired value a voltage regulator is used [58], [59].

3.2.9.2 48V TRACO Power Converter (TXL 100 48S)

The 48 V traco (Figure 3-27) is used to power the LCAM, which will subsequently power the drum DC motor driving the rotating drum. This converter requires an input of 88-264 VAC and outputs 48VDC which is inside the supply range of the LCAM (27-60 V) and exactly the voltage required for it to output between ± 20 V to power the top motor.

The input is done by connecting the phase (blue cable) from the circuit breaker to the IN port on the traco, the neutral (brown cable) to the L and the ground (yellow and green cable) to the ground of the traco. The output connects the traco to the LCAM binding the V+ port of the traco with the POWER+ in the supply power port of the LCAM and the V- with the POWER- of the LCAM.



Figure 3-27 48V traco power converter, model TXL 100 48S.

3.2.9.3 15 V TRACO Power Converter

The 15 V traco (Figure 3-28) is used to power the buffer which drives the guide motor that moves the stimulator. The converter requires an input of 80-264 VAC and outputs 15 VDC which is inside the input range of the buffer 8-60 V.

The converter receives power from the circuit breaker connecting “IN” with the phase cable, “L” with the neutral and “ground” with the ground cable. The output from the traco connects to the voltage input in the right side of the buffer.



Figure 3-28 15 V TRACO POWER converter.

3.2.9.4 24 V TRACO POWER Converter (TML 40124C)

The 24 V traco (Figure 3-29) is used to power both the sbRIO-9637 and the 5 V traco. The converter requires as input between 90 and 264 VAC and outputs 24VDC, which inside the supply voltage of the sbRIO 9 V to 30 V and the input voltage in the 5V traco of 9-36 VDC.

The input connections were done just as in the previous two cases, phase (blue) in IN of the traco and neutral (brown) in the L and ground in the ground connection. The output of the 24 V traco connected the positive pin to the positive input of the 5 V and the negative to the ground; in the sbRIO the connection was done in port J9.



Figure 3-29 24 V traco power converter, model TML 40124C.

3.2.9.5 5 V TRACO POWER Converter (THN 30-2411WI)

The 5 V traco (Figure 3-30) is responsible for powering the encoders and the limited switch.

This traco requires 9-36 VDC of input and outputs 5 VDC. Since this traco is very expensive other options were considered to power the these components , like the 5V from the sbRIO or the 5 V from the USB port of the PC, however these options either were not powerful enough to power everything at the same time or required extra holes in the box each would lead to more problems trying to certify its safety, so it was decided to use a traco to power them because it was also already available in the lab.



Figure 3-30 5 V traco power converter, model THN 30-2411WI.

3.2.10 Overview of The Platform

Following the detailed overview of all the components Emily incorporates and all connections between them, a simplified and general overview of both the relative location of the components inside the box, and the power and data connections between them can be demonstrated.

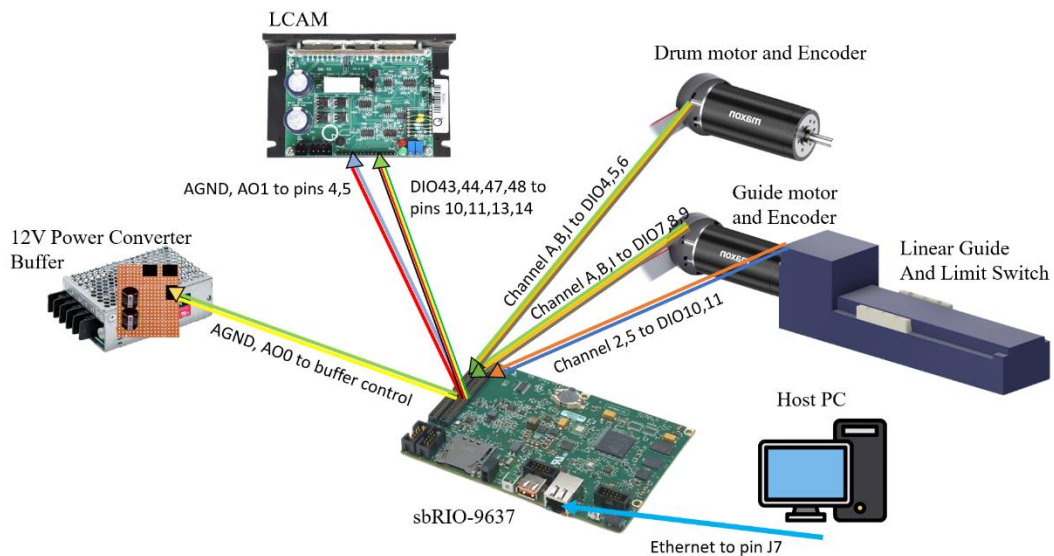
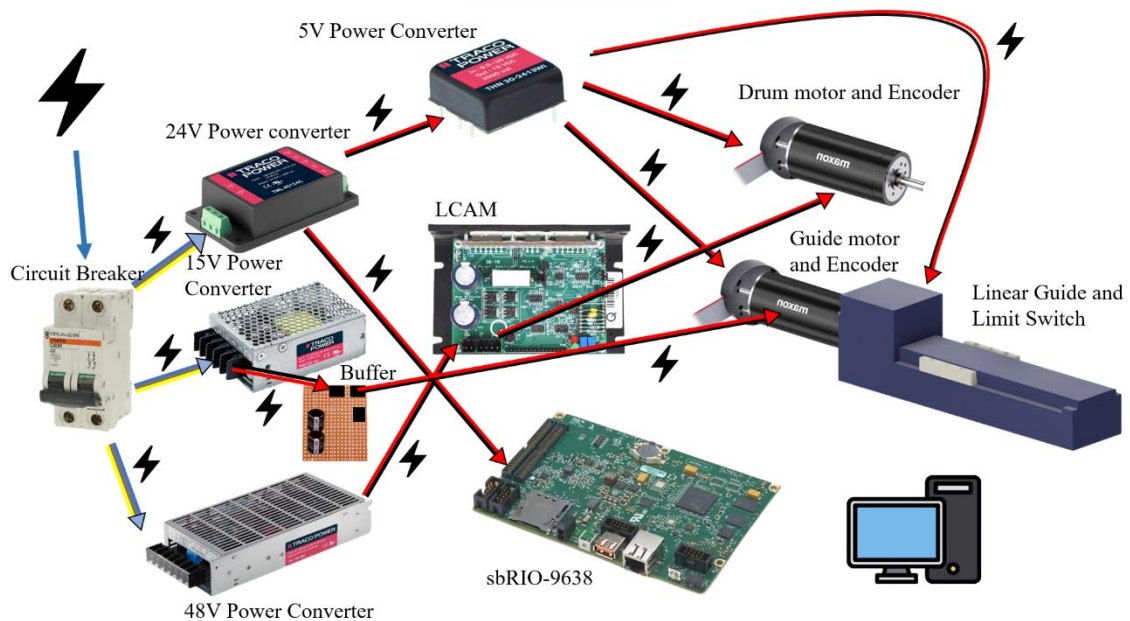


Figure 3-31 On the top overview of all the power connections between the components inside the box and the ones attached to the stimulator. Each arrow has the direction of power flow. On the bottom overview of the data connections between all components inside the box and with the components attached to the stimulator. Each arrow has the data transferring direction as well as the name of the pins connected in both ends.

3.3 Software Development to Control the Platform

3.3.1 LabVIEW FPGA as a coding tool and graphical Interface

The robotic system has been devised with an open design approach, this means the software controlling the platform is not embedded directly in it, but instead on the sbRIO board which is programable via LabVIEW FPGA. This coding tool offers endless possibilities for how to control the platform, making it versatile as well as upgradable after it has been completed. With LabVIEW the user can have many protocols set inside the board and operate the platform in a variety of ways in rapid succession, allowing for quick and multifunctional experiments.

The perks of using the sbRIO as well as LabVIEW to program the platform were to in the future upgrade the architecture by installing on the FPGA additional soft-core processors, peripherals, custom digital hardware modules and to achieve via hardware-software codesign a variety of experimental protocols. However, the biggest drawback is the necessity to perform a 5-to-10-minute compilation of the code every time a change is made, reducing the time efficiency of the programmer coding the machine since it is a task usually done by trial and error, and every error is a heavy time investment.

3.3.2 Stimulator Control Concept

The purpose of this mechatronic platform is to perform tactile stimulation of the finger by rotating a stimulation drum with different topographies along the skin. To operate the machine two conditions are required, for the drum to rotate, and to move the stimulator along the linear guide to change the stimuli presented to the subject. The first task is relatively simple, since the drum will be rotating the entirety of the trial, it is only necessary to power it in the beginning and to stop at the end. However, the second task is much harder because the stimulator must move to a specific location in the guide with great accuracy and to be there for as long as the trials is occurring, and after moving to a new location for the experiment to continue.

The three main components necessary to control the sliding motion of the stimulator are the encoder, giving position data, the motor, rotating the bearing in the shaft moving the platform, and the power supply of this motor, which in this case will be the buffer.

To program this task three codes were created, the first to filter the data from the encoders removing fluctuations, the second is a counter which will use the filtered data and count how many states have occurred inside the encoder, and finally a controller that will use the counted states as an input and in turn give it specific tasks at each marked iteration.

In LabVIEW the codes are created in a Virtual Interface (VI), composed of the block diagram, where the code is developed, and the front panel, where all the indicators, graphs and sliders of inputs and outputs are visualized. LabVIEW also allows the creation of subVI's, a tool to simplify the code, which can be called by higher level VI. It is similar to any other individual function of LabVIEW but instead it comprises a portion of coded created by the user inside it.

In this software the higher-level code is the controller, followed by the state counter, which is a subVI inside the controller, followed by the filter which is inside the counter. With this, the logic of the code created follows the route of inputting the data from the encoder into the RIO, after the RIO board uses all the codes compile inside it, first applying the filter to the data, then counting the passing of the states and then using them as info to control the behavior of the platform.

In the next chapters each code will be explained extensively to understand the inner working of how the sbRIO controls the platform. Pictures of the codes will be left in the appendix.

3.3.2.1 Filter to Remove Random Fluctuations in Data

The platforms functionalities depend on the validity of the data it outputs, so its behavior depends on the values of the encoders which will be used to control it.

As previously mentioned, the data acquired from the encoders and the LS are square waves with different phases, and frequencies. However, due bounces when sending the signal, random events, or spikes, are created where a change in state happens even though physically no change has occurred, this corresponds to a false transition which can in the long run lead to incorrect positioning of the platform during trials. These events can be corrected, and the signal stabilized with a filter which only allows a change in state if a certain strict condition is met (Figure 8-1).

During each state there is a certain number of iterations where no change is supposed to occur, with this in mind in order to compensate for random events where spikes happen, an adder function adds the last 16 values given by the encoder (1's and 0's), and a low and high threshold is applied to differentiate states. If this value is lower or equal to 6 the state is considered low/down, if the value is higher or equal to 10 it is considered high/up, with a minimum of 0 when all values are 0 and 16 when all values are 1. The case in between keeps the previous state until the sum crosses one of the thresholds.

These binary values are given by the IO function in LabVIEW that outputs a Boolean value, True or false, which is then converted to numerical, 1's and 0's.

This technique allows the filter to remove random fluctuations and prepares the data to be used for further achievements.

To validate the filters efficiency, it is required to first build the counter of elapsed states. Therefore, these tests will be performed along with the implementation of the state counter and discussed in chapter 5 "Results and Discussion".

3.3.2.2 Counter for Elapsed States

For stimulation to occur the stimulator must stop in specified markers along the linear guide, meaning that to stop it first it is necessary to acquire its position. To track this information a counter of the elapsed states was built that used each change in state as an increment or decrement, depending on the orientation of rotation, in the position of the platform along the horizontal slider (Figure 8-2).

For the making of these code four combinations/states will be considered for channel A and channel B, which will be called A and B for reading purposes. A and B equal to 1, A and B equal to 0, A equal to 1 and B equal to 0, and A equal to 0 and B equal to 1. Every time the wave changed from one combination to another the LabVIEW code would do an increment of 1 if the motor was rotating in the clockwise (CW) direction, or a decrement of 1 if rotating in the counterclockwise (CCW) direction (Figure 3-32). This code was created (Figure 8-16), however, an alternative state counter was developed that demanded less from the board, making it more resource efficient. This code used a pattern created from the difference in phase between wave A and B (Figure 3-19), (Figure 3-32) in the CW rotation a falling edge of A (changing from 1 to 0) corresponds to a low state of B (B=0), and the rising edge of A (changing from 0 to 1) corresponds to the high level of B (B=1), the falling edge of B corresponds to a low state of A and rising edge in B with a high state of A. In the CCW motion, the opposite happens, falling A – high B, rising A – low B, falling B – high A and rising B – low A.

The falling and rising edges for each channel were acquired comparing the current iteration to the previous one, if the value is greater in the current, it is a rising edge, if lower it is a falling edge.

With this pattern, a logical scheme was created where every time a CW condition was met the code would add 1 to a counter, and every time a CCW condition was true it subtracted 1 to the same counter, this counter would in turn be able to tell the user where the machine was located in the slider giving an accurate position even when the motor changes orientation midway.

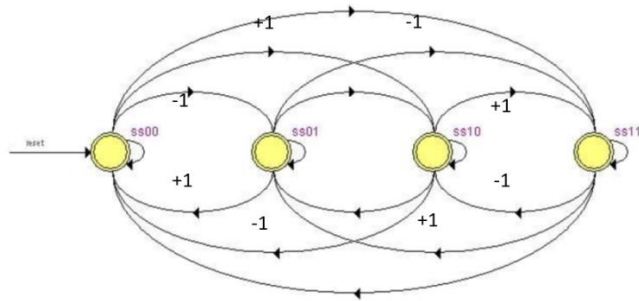


Figure 3-32 Representation of the possible changes in state and how each is counted in the counter of elapsed states code. In clockwise motion 00 moves to 01, next to 10, and after to 11, repeating the cycle and adding plus one on the counter. In the counterclockwise motion 00 moves to 01, then 11, and finally 10, always subtracting one to the counter.

To validate the data two tasks were performed, one where the platform was repeatedly forced to move the full length of the slider, yielding an average of 117553 states, and using the channel I (full rotation of the encoder) to see if at every positive iteration of this channel the counter would give 4096 counts per turn.

This code returns the exact position of the platform inside its working range, moreover with this data it is possible to create a state machine where the user can control the behavior of the platform depending on where it is located, which will be mentioned in the following segment.

To verify the counter, a comparison should be made between the counts per turn of the encoder with the theoretical value of a full rotation of 4096 states. These results will be explained in chapter 5 “Results and Discussion”.

3.3.2.3 Controller for the Platform

Now that it is possible to acquire the exact location of the platform along the encoder, the only step left is to use this information to control the behavior of the platform by giving it a specific task at each iteration on the linear guide.

Two different pipelines were created for this task, one sequential where the platform moves from stimulus 1 to 6 in order and returns to initial position, and one random where the platform moves to a random stimulus every time.

Incorporated in both controllers is a safety measure using the limit switch impeding the support from moving past the position where the switch mark the beginning and end of the slider, because forcing the movement past this point could damage the switches. These points are signaled by a positive output of voltage, shown as a positive Boolean indicator in LabVIEW, one when the support reaches the beginning and other for the end. The limit switch was also used as a guarantee that the platform only started counting

the position of the encoder when both switches were off, so in this way it was guaranteed that the platform always started in the same position (when the beginning switch turned off).

In both modes the controller was created inside a single cycle timed loop (STL) which doesn't allow for analog outputs inside, to circumvent this signal values were written inside a FIFO. Parallel to this STL a normal while loop had these signals be written to a selector function which would, depending on the signal, output a specific voltage value to the AO in a normal while loop running in parallel to this STL while loop. In both controls there is also a safety button that brings the machine back to the begging position (where the begin switch of the LS turns on) and the experiment can be stopped or restarted there at any moment.

All the values selected and mentioned, like voltage values, timer for stimulation, and the positions selected to stop the machine can be chosen before each trial, giving the user the freedom to perform the experiments as it best suits its goals.

The sequential stimuli selector is not the main pipeline for Emily, therefore all the results, interfaces, and considerations for the future of the platform will be done using the random controller.

3.3.2.3.1 Sequential Stimuli Selector

In this mode the platform moves in order, from the first to the last stimulus, returning to its initial position and repeating this movement until told to stop.

This mode was created using the state counter a point to stop the stimulator, an output for the LCAM either to power the motor or not and a timer for stimulation.

This code starts by verifying if the stimulator has reached one of the stop positions, if not it enters a case structure (Figure 8-4) which will output a signal to a FIFO (a memory function) this FIFO will then read this value to an AO0 (Figure 8-8) and power the motor. While the stimulator moves the counter increases until it reaches a stop marker, with this the case structure changes (Figure 8-5) and now a different signal is outputted to the FIFO which will go to the AO like before and send 0 V to the buffer, because now the stimulator must stop for stimulation to occur. During this time a 10 second timer is running (converted in MHz because that is the internal timer of the cycle) and after these ten seconds the stimulator starts moving again to the next stop marker, repeating this cycle. At the last marker the case changes again (Figure 8-7) to write the 0 V signal in the FIFO indefinitely. After this the platform can be manually pulled to the start position by pressing a button (Figure 8-6) and after it is pressed again the process repeats.

In parallel the drum motor is receiving controlled voltage ordered by AO1. The LCAM is also enabled by making TRUE DIO0 and DIO2 and turned off at the end by making them FALSE (Figure 8-3).

This mode however does not yield the most scientific significant results since the stimulus follows an order, and it is possible that with repeated trials the subject expects a certain texture, making the data worthless. To prevent this occurrence an alternative mode was created.

3.3.2.3.2 Random Stimuli Selector

Many restrictions and considerations must be accounted for when performing any experiment, one very important one is to remove any external factors that could influence the results of the trial, and the previously described controller had this exact flaw. The flaw was that since the stimuli were presented in order, after many trials the subject could more easily memorize the sensations created by each texture and have this prior knowledge influence the data of the neurophysiological tests. To mitigate this occurrence a random mode selector for stimuli was created.

The first approach implement for this controller was similar to the one described above, however it required more than 15 case structures, which was hard to debug, too heavy for compilation and inefficient, so a new strategy was implemented.

This strategy uses 4 major case structures each one with a specific goal: the first selects randomly the next stimuli; the second compares the current location of the platform to the desired location; the third stops the guide motor for a specified time, by writing 0 in a FIFO, while the drum motor rotates and the subject is stimulated; and the fourth signals the stimulator to move in either direction depending on where the following stimulus is located.

The controller starts with a shift register, a memory function that stores a value from the previous loop, this register was set to initial at 0 forcing the code to the case 0 (get new random position) (Figure 8-9), here a random number is selected from a parallel code running on real-time (random number generator v4.5) from a range between 0 and the pre-selected value in the control “number of stimuli”. This value is used as an index in an array with all the position the machine can stop at, which depend again on the input in the number of stimuli control. The value from the array with that index is selected becoming the new desired position, and the case forces the controller to enter case 1 next by writing this value in the shift register which will output 1 in the new loop. Now in case 1 (compare current to desired position) (Figure 8-11), the desired position is compared to the current position, given by the state counter, with an equal function, if TRUE the shift register gets a 2 to enter in case 2 in the next loop, if not it gets a 3. Considering the machine has not moved yet, the current position is obviously different than the desired, forcing the controller to case 3. In case 3 (Figure 8-13), a “higher than” function is used to compare the current to desired position, if it is TRUE, a “003” will be written in a FIFO, if not “001”, “003” represents a positive voltage output and “001” a negative voltage output. Parallel to this an equal function is also used, if this function outputs FALSE, the controller is kept in case 3, if it is TRUE the shift register will receive a 2, which will force the next loop to case 2. Depending on the direction the support as to move it will write “003” or “001” and move forwards or backwards, respectively. When it reaches the desired position, the equal function mentioned above forces the controller to case 2, initializing the stimulation. In case 2 (Figure 8-12), the same FIFO as in case 3 now receives “000A” and in parallel a 10 second timer is running, for the first 8 seconds a green light is turned on signaling the subject it can touch the drum, and in the last 2 seconds a red-light switches warning it to remove the finger from the drum. During the 10 seconds the controller is forced to stay at case 2, and when the timer finishes it changes to case 0 to get a new random position and this cycle repeats.

Parallel to this STL the values written in the FIFO are read to a selector function which writes the voltage specified to the AO0 controlling the buffer and in turn the guide motor. “003” corresponds to the positive value inserted on the “voltage slider motor control”, “001” to the symmetric of the previous number, and “000A” to 0 volts (Figure 8-14).

Also, parallel to this two while loops is a sequence structure with three sequences, the first activates the LCAM by enabling the 0v and 5v with a TRUE constant in DIO0 and DIO2, the second is the while loop that controls the voltage output to the LCAM with the control in AO1, and the third disables the LCAM with a FALSE constant in DIO0 and 2 (Figure 8-3).

Although the random mode reduced the likelihood of the subject memorizing the sensation evoked by each topography, it doesn't completely prevent it, especially in psychophysical experiments where the subjects asked to compare the pleasantness between all stimuli, since in this kind of tests they are asked to remember.

3.3.2.3.3 Random Number Selector

This code (Figure 8-15) was developed in real-time in contrast to all the previous codes which were done on FPGA. The advantage of FPGA is that it can receive and send data from other components by the implementation of the DIO's and AO's functions, unavailable in real-time, and that it uses a faster clock compared to real-time. However, these advantages have a drawback which is the unavailability of some functions like the coefficient or the possibility to insert a random number generator, which is a normal function on real-time. To circumvent this problem a code was created which generates a random number every 10 seconds, from a range between 0 and the "number of stimuli" control present in the "random stimuli selector". This value is then sent through a read/write function to the FPGA code and after it is used to signal the platform of where to move the stimulator.

4. How to Perform Tactile Stimulation with Emily

4.1 Before Operating

The stimulator was developed to be used in the two modes mentioned prior: the sequence mode where the drum is constantly rotating and the subject is stimulated from the first stimulus to the last, in order, removing its finger seconds before the stimulus changes waiting for the platform to move and placing the finger after this step is executed; the random mode where the subject behaves just like in the mode mention prior, however this time it is stimulated by a randomly selected topography of the drum every time, decreasing the impact of expectation in the data.

To operate the platform in either mode it is necessary to know how many stimuli were loaded onto the drum, and where it is intended for the finger to touch the drum at each topography. With this information it is possible to calculate where the platform should stop so that the correct stimulus can be applied in the right spot at the right time.

First, from many trials it was averaged that the full length of the linear guide is 117553 states, knowing the number of stimuli that were loaded and considering all the cylinders have the same length we can divide the number of states by the number of cylinders, and after divide this number by two since we want the finger to be placed in the middle of the cylinder, not the edge. At every multiple of this number, *Stop Constant*, we code the platform to stop when that exact amount of state changes has been counted.

$$Stop\ Constant = \frac{Lenght_{LG}}{N^{\circ}Stimuli} \quad Stop\ Positions = [1, N^{\circ}Stimuli] \times Stop\ Constant \quad 4.1$$

One other alternative to calculate the stop markers is with the rule of three, where we use the resolution of the encoder $0.98\mu m$ which corresponds to one elapsed state and the distance intended to travel from the begging point to the desired marker in centimeters. This will then calculate the number of states needed to be counted to arrive at that location, and therefore be the new stop position.

$$\frac{Resolution_{cm}}{1\ state} = \frac{Stop\ Position_{cm}}{?} \quad 4.2$$

After the stop points are discovered, they are placed in the LabVIEW VI and after compiling the code, which takes approximately 7 minutes, the platform is adapted to the new drum and ready for use.

Before the trial the user must also explain to the subject the experimental protocol and select a value for the controllers' inputs.

Before the trials the subject should find the most comfortable siting position in accordance with the height of the platform and use the armrest and the hand support not to tire the arm during the experiment. The experiment can be performed either with the finger bellow the drum or above the drum, so the set up should change accordingly to keep the subject's comfort.

4.2 During the Experiments

4.2.1 Instructions for the User

The main control developed for this mechatronic platform was the “random stimuli selector”, in this mode, the program randomly selects one of the stimuli and moves the support to the pre-selected location where it stops so that the subject can rest its finger on the drum and be stimulated by the selected stimulus.

To use this controller first the user must access the “Variables to define before trial” section and decide: the number of seconds which the subject will be stimulated at each step; the number of stimuli loaded onto the drum (all must have the same length); the voltage of both the DC motor driving the drum and the DC motor controlling the linear guide (for the drum motor any voltage value between $\pm 20V$ is possible and relevant for different types of studies; for the guide motor a voltage value of 2-3V is recommended).

After all these variables are selected the user should start the code in the white arrow in the top left corner of the screen and press the “STOP THE MACHINE” button. After this the user must open the real-time code “random number selector V4.5” and run this code by pressing the white arrow again. Now return to the controller and a number should appear on the “random number” indicator on the “state and position of the platform” section, this number is the next stimulus the platform will move to, so press again the “stop the machine button” and now the support will move to the desired location. Since the platform was programmed to be completely autonomous, no further action is required from the user for the experiments to occur.

If at any point the user intendeds to stop the platform it can be done by either pressing the “Stop the machine” button, which stops it but keeps the code running, or the “stop code” button which stops the machine as well as the code itself.

The user can also return the platform to its beginning position on the slider by pressing the “reset position” button, when this button is switched off the stimulator will continue to operate normally and go to the current randomly selected stimulus.

During operation the status of the platform can be followed live by the “state and position of the platform” section, which displays the current position and the desired position (both in counted states), a countdown for the time in Mhz left for the stimulation to stop, and the randomly selected stimulus at any given moment. There is also an indicator for the difference between current and desired position, displayed only when the platform stops in the new position, this notifies the user if the support has stopped in the wrong position hence if the subject will be stimulated by the wrong stimulus. Only values higher than 3061 states of difference are considered critical (explained in the results and discussion chapter).

The following figure shows the graphical user interface of the random stimuli selector.

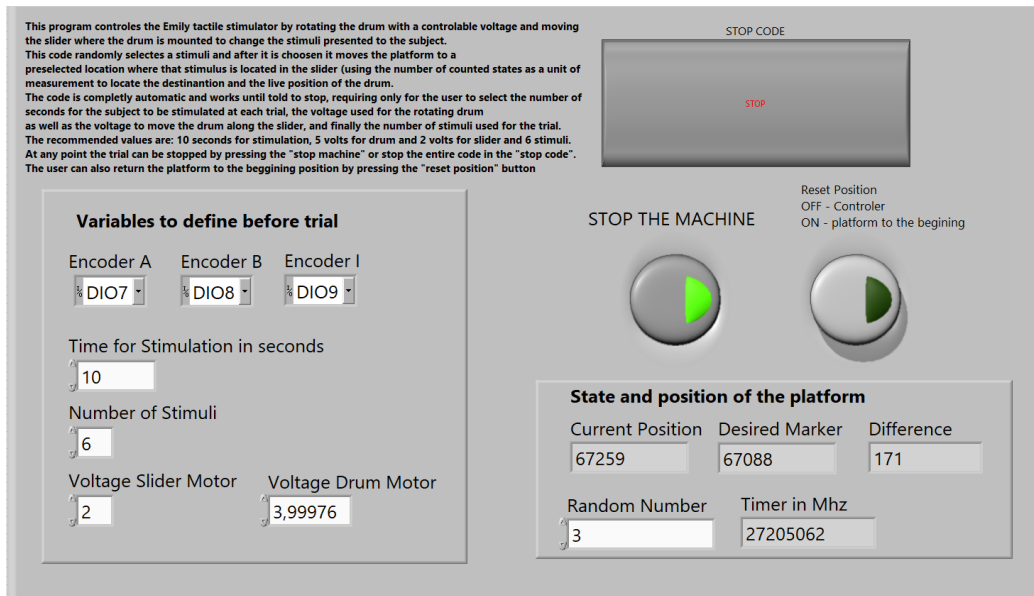


Figure 4-1 Graphical User Interface, with the controls and live status displays of the random stimuli selector controller. In this interface a brief explanation on how to operate with the controller is also included in the top left corner.

4.2.2 Instructions for the Subject

The task of the subjects during the experiments is simple. However, first the user must explain them what the purpose of the experiment is and what they should do during the trial.

The user must explain that the experiment has the goal of gaining knowledge over the underlying neurological processes behind touch and sensorial stimulation through touch. Moreover, that to further develop our understanding of these processes the subject will be stimulated through touch by coming in contact with a rotating drum with different textured surfaces which will grant a sensorial sensation, and that during these experiments they could be asked questions about the different stimuli or be evaluated with neurophysiological tests like EEG or microneurography.

After the goal of the experiment is clarified, the user must explain to the subjects what they should do during the trial. First, they should be prepared to place their right index finger in the first stimuli, the one most to the left, away from the DC motors, and look to the PC screen, when the green light “place finger” is turned on, then when it turns off the red “remove finger light” will turn on the subject must remove its finger in a vertical motion, and wait until the green light turns on again, placing then the finger in the drum again. The user must also clarify that the subject should only move its finger during the trial in a vertical motion, since the correct stimuli will always be below its finger and not to the sides. To ensure the patients do not move their finger laterally the armrest and a hand support can be used to keep the hand in place.

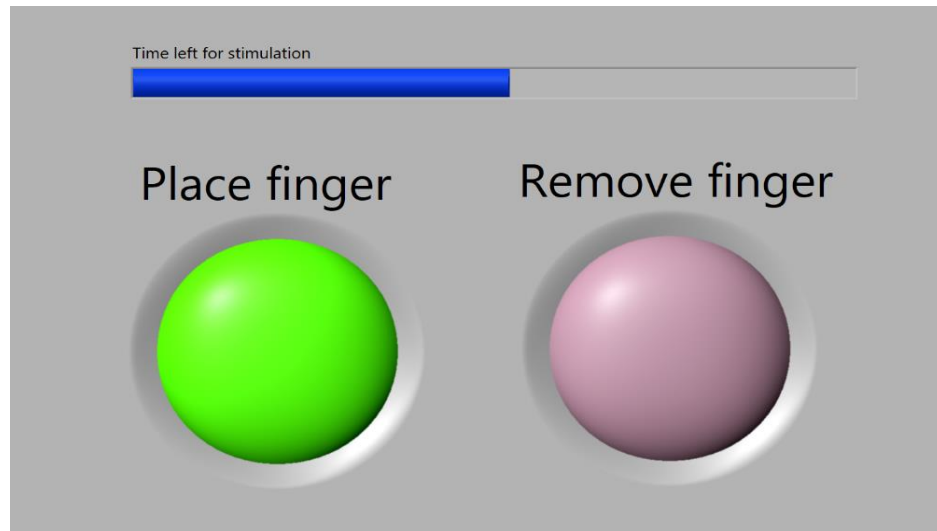


Figure 4-2 Graphical Subject Interface with lights to signal the subject on what to do at each moment of the trial. Green light to touch the drum, red light to remove the finger. The interface also includes a timer to inform the user on how much time is left for stimulation.

To recap, during stimulation the subject must follow the instructed guidelines given in the screen of the PC, which are simple, either a green light will light up when to touch the stimuli or a red light to stop touching the drum and to wait for the next stimuli to be ready.

To acquire representative and valid data the exploration or presentation of stimuli should be replicated several times in the same conditions.

The parallel neurophysiological experiments require extra setup procedures as well as further explanations to the subject, however, none of this test were performed for the realization of this dissertation, therefore they will not be mentioned.

5. Results and Discussion

After the platform was designed, built, and programmed to operate, the following step was to test if it was correctly constructed.

Firstly, manual testing was done to ensure it the stimulator was robust and did not break during operation, for this stress test were done applying force directly to the machine in all three spatial directions, as well as applying extra force to the drum motor, to verify if the base of the support would give in and break. The results were positive as the platform did not break or even tilt when light to medium forces were applied, meaning that the build was solid, and all the bolts and nuts were tightly holding the stimulator together.

Secondly endurance tests were performed, where the platform was left operating with both DC motors constantly rotating for more than 2 hours, this did not result in any collapse either mechanical or of the code used to control it, revealing the machine can be used for tactile stimulation for extended periods of time. Temperature was also verified, and box was sufficiently cool for safe operation due to the heat extraction from the fan.

Finally, accuracy tests were executed to test the behaviour of the drum motor, validation of both the filter and the state counter were performed, moreover measurements of the length of the guide as well as comparisons between the desired and actual position where the drum should stop where executed. All tests were performed with the slider motor operating at 2 V, which we latter define to be the best setup for Emily, although some other voltage values were experimented with. To properly explain the following section, I will take this opportunity to remind the reader that the position along the slider is measured in elapsed states, meaning that the slider is seen like a ruler, except it doesn't use centimetre rather measures counted states, which empirically has 117553.

The first accuracy test was to validate the efficiency of the filter, while at the same time verify the correct implementation of the state counter. To do this, an extra code was built which counted the number of states elapsed until the drum motor, and therefore the drum encoder, did 20 full rotations. Using “A” and “B” channels to count the states and the “I” channel to calculate the full rotation. However, since the first rotation is an arbitrary value because the encoder could be left in any position after its last utilization, it was acquired the value of elapsed states after the 1st rotation was done, and after the 21st rotation, later subtracting the values and dividing them by 20. The result was constantly 4096, equal to the theoretical value and confirming the correct execution of the counter. The alternative state counter (Figure 8-16) also passed this test.

To test the filter, the same test code mentioned prior, with the logic of subtracting the 21st counted states to the 1st was used, however without the filter applied to any channel, and with the filter applied to channel “I” only. The results were unexpected, when applying no filter, the values for the counted states in both instances were completely off, always random, and never more than a thousand. However, when applying the filter only to the “full rotation” channel (to see the real counted states after the encoder did 1 and 21 rotations) the results were spot on with the two previous state counters with the filters applied to all channels. Therefore, the filter greatly corrects the “I” channel, but no correction is needed for the other two channels. These tests were repeated 20 times each, thus we can confidently say both the state counter and filter are functional and correctly do their desired goal.

Following this validation, it was measured the full length of the linear guide, for this a simple code which moved the platform back and forth was designed. The platform yielded an average of 117553 states (115.18mm) with a standard deviation of 38.71. However, when moving the platform to the start position the counter shows an average of 65.5 extra states when it should be 0, with a standard deviation of 38.7. This was unexpected as both the filter and the state counter were coded symmetrically, meaning that there should not be a tendency for the code to count more states in the clockwise motion (adds 1 to the counter at each iteration of the encoder) compared to the counterclockwise motion (subtract 1 to the counter at each iteration of the encoder). This counting error relates to a miscalculation in millimetre of only 0.064mm which is negligible. A possible reason for this error could be the fact that the walls of the linear guide aren't a solid marker, rather they are a rubberized surface which is mouldable, therefore when moving the stimulator against the end of the guide the longer we force it the more it moves and when the power is shutdown this surface forces the stimulator back placing it in this 65.5 position. This was theorized since when continuously forcing the platform past the edges of the slider the counter registers an average of -498 states in the start position and 118101, both beyond the correct value of 0 and 117553 respectively, and when the power is shut down the platform returns to the more comprehensive value of 65.5 and 117553, explaining the "bounce back". Therefore, the platform could possibly stop near the correct value but never in the right location since the extremities are not a solid impeding marker which bounce the stimulator back.

With the value of 117553 states for the full length of the guide, and using the resolution of the encoder we can calculate empirically the length of the slider in cm, which is $length = 117553 \times 0.00098mm = 115.18mm$, since each state is 0.00098mm or 0.98 μ m.

Following this verification, the accuracy of the platform was once again tested, although this time for the precision of the stop markers along the guide where the drum should stop for stimulation to occur. For this test all combinations of voltage and number of stimuli were experimented with, however changing the number of stimuli and in turn the location to stop did not have any effect on the performance.

To do this task an indicator was implemented in the LabVIEW code which displayed live the position of the platform in elapsed states, this value was then subtracted to the desired stop position also in elapsed states and the absolute values of this subtraction emerged.

For 1 volt the average displacement between desired and real position was of 53 states (0.052 mm) with a standard deviation of 10.65 and variance of 113.42. However, this voltage was too low, moving the stimulator very slowly and taking up to 15 seconds to do the full length of the slider, and since quick stimulation is one of the perks of Emily 1 volt would be enough. Alongside this, one volt sometimes resulted in the machine being stuck mid movement due to insufficient power to overcome friction from the guide.

For two volts the average difference was of 188 (0.18 mm) with a standard deviation of 16.4 and variance of 268.76. With two volts the drum is much quicker taking only 7 seconds from start to finish and being powerful enough to not get stuck.

For three volts the average variation was 329 states (0.32 mm) with a standard deviation of 20.44 and variance of 417.69. With this power output the slider takes 4 seconds to move between the poles of the guide.

Lastly, for six volts the error was of 1144 states (1.12 mm) with a standard deviation of 45.76 and variance of 2093.87.

These trials with different voltage outputs show that the platform always overshoots the stopping position, independently of the direction of movement, moreover the higher the voltage used the higher the overshoot is.

To correct this issue a thorough reevaluation of the filter, state counter and controller were performed. Since the filter and state counter were working properly, no alterations were made, even when applying the alternative state counter no improvements were seen. Later the reasoning was focused on the limitations of both the board and the LabVIEW coding tool. However, the LabVIEW FPGA code was done using a single cycle timed loop (STL) which works with a 40 Mhz clock hence each second corresponds to 40 million iterations, much quicker than the speed at which the physical rotation of the encoder occurs. Moreover, even though the code also has a non STL to output the voltage to the AO's (these functions can't be placed inside a STL because they take more than one cycle to operate) this would not slow down the code enough that the encoder would be rotating quicker than the code could register, missing the stop marker timing and outputting 0 V latter than desired. The last tough out possibility was a mechanical and physical problem related to properties of momentum of an object with mass. The support is driven by a DC motor which rotates at speeds proportional to the voltage given by the buffer, higher the voltage higher the speed, furthermore as it is described by the Newtons first and second laws of motion [60] an object tends to stay in its state of motion unless a force is applied. Therefore, during powering the net force is in the direction of the movement, resulting from the combination of the force executed by the motor and the drag of the slider. When the platform reaches a stop marker the buffer stops outputting voltage to the motor, impeding its rotation and the net force now is only the drag (opposite to the movement) which slows down the support, however this unconservative force is likely not strong enough to instantly stop the support and due to the momentum the support its carrying and the inertia to change its movement, it will keep on moving until drag completely stops it, hence the stimulator always stops ahead of the desired location for either direction of rotation. This explanation also acknowledges why higher voltage creates bigger overshoots in counting, since objects with higher speeds will carry extra momentum therefore inertia to stop will be higher and drag will take longer to stop the support, increasing the delta between desired and current position even more.

Although these inconsistencies are present in every action performed by the platform, the average difference between the desired and actual position was only of 188 counts (0.18 mm), which when put in perspective to the 20 mm of length of each stimulus seems insignificant. However, the margin for error is smaller than this. Considering the human finger has an average of 19mm in width, and only uses 12 mm to touch surfaces, (value increases with strength applied to the surface in a range between 9 mm and 13 mm) and the finger is positioned in the middle of each textured cylinder we are left with a margin of 4 mm for each side of the cylinder ($\frac{20mm-12mm}{2}$) [61], [62]. Comparing now the 0.18 mm of error to the 4mm of margin, it is a 22 times difference, hence the error is small enough to validate the accuracy of the Emily platform for tactile stimulation.

Considering the nature of the error, the results from the accuracy tests and the margin for variation to not have the subject be stimulated by the wrong stimulus, it was decided that the output voltage that best suits the platform is 2 or 3 volts, since it is the best compromise between overshoot with only 0.18 mm/0.32 mm, much lower than the 4mm margin speed with 7s/4s to traverse the length of the guide, and it is strong enough to not have the support stop midway through the movement. Of course, even with higher voltage outputs the error would not be big enough to invalidate the accuracy of the platform since even with 6 volts the error is only of 1.13 mm when the margin is 4mm, but voltages this high tend to exert too much force in the stimulator without great benefits for the experiment, therefore since the extra speed doesn't provide benefits that outweigh the cons there is no need for voltages higher than 3 volts. With high voltages the stimulator also is too quick changing stimuli not leaving enough time for the subject to rest the finger between stimulations.

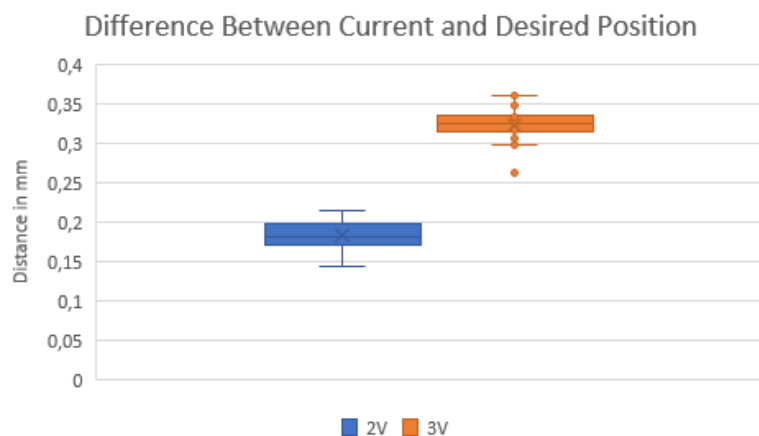


Figure 5-1 Box Plot of the difference between current and desired positions of the stimulator for both 2V and 3V the most optimal voltage options for Emily.

A possible alternative to reduce the impact of this error would be to subtract to the desired stop marker the average of difference to each specific voltage. For examples, if we use 2 V we subtract to all desired position 188 states, since the stimulator will most likely stop 188 states ahead, making it then stop closer to desired position first intended.

5.1 Possible adaptations and Upgrades to the Controllers

In order to correct or understand some of the inconsistencies of the controllers a code where the state counter stops counting when the slider motor is cut of power would be interesting to implement, to test if the extra states due to inertia and momentum would disappear or not, since even if the platform overshoot its position, the counter would count this extra states.

In the voltage controls of both DC motors, voltage is not a well-defined measurement for speed, therefore later versions of this controller should let the user decide both the speed of rotation and speed of movement of the support in m/s rather than voltage which is ambiguous.

6. Conclusion

The design, construction, and experimental validation of the mechatronic platform Emily was presented. This autonomous passive tactile stimulator with an incorporated rotating drum with embossed textures is an in-house design built from 3D printed components, the machine is a “U” shaped design with the drum sitting in the middle of the support, enabling both stimulation of the finger with the hand facing up or down. The platform incorporates two degrees of freedom, one from the drum which can rotate either clock or counterclockwise, and one from the linear guide used to laterally move the entire support and the drum, changing the stimuli presented to the subject from a 1D array of 6 preprinted stimuli. This last degree of freedom also opens the possibility for lateral stimulation alongside the already frequently applied stimulation in the length axis of the finger. To drive the platform two DC motors were used, both associated to an encoder to relay their position.

One major goal for this project was to create a portable, easy to build and versatile tactile stimulator, to establish these objectives only commercially available components were used, the physical design was kept simple and efficient and a sbRIO-9637 board with LabVIEW FPGA was used. This last component enabled the ability to personalize the behavior of the platform with two different tailored controllers.

To ensure the ability to perform sensitive electrophysiological studies Emily uses a linear current amplifier with low electromagnetic interference to reduce the likelihood of damaging the data.

The performance of the platform was tested through stress, endurance and accuracy testes, these tests revealed positive results validating the implementation of the platform for prolonged, automated and precise passive tactile stimulation.

However, further improvements need to be made, the first is to create a closed loop control for contact strength, currently only a phantom force sensor was built into the design, nevertheless its implantation is simple, and the platform is prepared both mechanically and electronically. Following its application, a third degree of freedom should be implemented, using a DC motor to move the support vertically controlling the contact strength calculated from the force sensor.

In the end, Emily fulfills almost all target goals of a complete passive and autonomous tactile stimulator, being a huge asset for the NRT Lab, for scientific research and hopefully one day for the wellbeing of Humanity.

7. Bibliography

- [1] B. A. Jenkins and E. A. Lumpkin, “Developing a sense of touch,” *Development*, vol. 144, no. 22, pp. 4078–4090, Nov. 2017, doi: 10.1242/dev.120402.
- [2] D. Goldreich, M. Wong, R. M. Peters, and I. M. Kanics, “A Tactile Automated Passive-Finger Stimulator (TAPS),” *Journal of Visualized Experiments*, no. 28, Jun. 2009, doi: 10.3791/1374.
- [3] A. I. Weber *et al.*, “Spatial and temporal codes mediate the tactile perception of natural textures,” *Proceedings of the National Academy of Sciences*, vol. 110, no. 42, pp. 17107–17112, Oct. 2013, doi: 10.1073/pnas.1305509110.
- [4] K. Stylianos, G. Konstantinos, P. Pavlos, and F. Alik, “Brachial branches of the medial antebrachial cutaneous nerve: A case report with its clinical significance and a short review of the literature,” *J Neurosci Rural Pract*, vol. 07, no. 03, pp. 443–446, Jul. 2016, doi: 10.4103/0976-3147.182772.
- [5] M. Gupta and A. Gupta, “Cutaneous Sensory Disorder,” *Semin Cutan Med Surg*, vol. 32, no. 2, pp. 110–118, Jun. 2013, doi: 10.12788/j.sder.0010.
- [6] C. Oddo and *et.al.*, “Intraneural stimulation elicits discrimination of textural features by artificial fingertip in intact and amputee humans,” *Elife*, 2016.
- [7] A. Gallace and C. Spence, “The science of interpersonal touch: an overview,” *Neurosci Biobehav Rev*, vol. 34, no. 2, pp. 246–259, Feb. 2010, doi: 10.1016/J.NEUBIOREV.2008.10.004.
- [8] H. Johansen-Berg, “The physiology and psychology of selective attention to touch,” *Frontiers in Bioscience*, vol. 5, no. 3, p. A558, 2000, doi: 10.2741/A558.
- [9] E. L. Ardiel and C. H. Rankin, “The importance of touch in development,” *Paediatr Child Health*, vol. 15, no. 3, p. 153, 2010, doi: 10.1093/PCH/15.3.153.
- [10] I. Bretherton, “The origins of attachment theory: John Bowlby and Mary Ainsworth.,” *Dev Psychol*, vol. 28, no. 5, pp. 759–775, Sep. 1992, doi: 10.1037/0012-1649.28.5.759.
- [11] Roger Cholewiak and Amy Collins, “Sensory and Physiological Bases of Touch,” in *The Psychology of Touch*, 1st ed., Psychology Press, 1991, pp. 1–38.
- [12] [LaMotte RH, Whitehouse GM, Robinson CJ, and Davis F, “A tactile stimulator for controlled movements of textured surfaces across the skin,” *J Electrophysiol Tech* , pp. 1–17, 1983.
- [13] M. H. Grider, R. Jessu, and R. Kabir, “Physiology, Action Potential,” *StatPearls*, May 2023, Accessed: Sep. 06, 2023. [Online]. Available: <https://www.ncbi.nlm.nih.gov/books/NBK538143/>
- [14] Aarushi Khanna, “Action Potential,” TeachMePhysiology. Accessed: Sep. 29, 2023. [Online]. Available: <https://teachmephysiology.com/nervous-system/synapses/action-potential/>
- [15] Gillian Pocock, Christopher D. Richards, and David A. Richards, *Human Physiology*, 4th ed. Oxford University Press, 2013.
- [16] J. Dargahi and S. Najarian, “Human tactile perception as a standard for artificial tactile sensing—a review,” *The International Journal of Medical Robotics and Computer Assisted Surgery*, vol. 1, no. 1, pp. 23–35, Jun. 2004, doi: 10.1002/rcs.3.
- [17] D. T. Blake, S. S. Hsiao, and K. O. Johnson, “Neural Coding Mechanisms in Tactile Pattern Recognition: The Relative Contributions of Slowly and Rapidly Adapting

- Mechanoreceptors to Perceived Roughness,” *The Journal of Neuroscience*, vol. 17, no. 19, pp. 7480–7489, Oct. 1997, doi: 10.1523/JNEUROSCI.17-19-07480.1997.
- [18] J. Yang *et al.*, “Brain networks involved in tactile speed classification of moving dot patterns: the effects of speed and dot periodicity,” *Sci Rep*, vol. 7, no. 1, p. 40931, Feb. 2017, doi: 10.1038/srep40931.
- [19] I. Darian-Smith and L. E. Oke, “Peripheral neural representation of the spatial frequency of a grating moving across the monkey’s finger pad.,” *J Physiol*, vol. 309, no. 1, pp. 117–133, Dec. 1980, doi: 10.1113/jphysiol.1980.sp013498.
- [20] Beatriz Caleiro, Carolina Pereira, Chloé Vaz, Joana Aguiar, and Mafalda Cavalheiro, “FISIOLOGIA HUMANA.” Faculdade de Farmácia da Universidade de Lisboa, pp. 497–520, 2017.
- [21] C. E. Chapman, “Active versus passive touch: factors influencing the transmission of somatosensory signals to primary somatosensory cortex,” *Can J Physiol Pharmacol*, vol. 72, no. 5, pp. 558–570, May 1994, doi: 10.1139/y94-080.
- [22] S. J. Lederman, “Tactual roughness perception: Spatial and temporal determinants.,” *Canadian Journal of Psychology / Revue canadienne de psychologie*, vol. 37, no. 4, pp. 498–511, Dec. 1983, doi: 10.1037/h0080750.
- [23] R. T. Verrillo, S. J. Bolanowski, and F. P. McGlone, “Subjective magnitude of tactile roughness,” *Somatosens Mot Res*, vol. 16, no. 4, pp. 352–360, Jan. 1999, doi: 10.1080/08990229970401.
- [24] C. E. Chapman and S. A. Ageranioti-Böhlanger, “Discharge properties of neurones in the hand area of primary somatosensory cortex in monkeys in relation to the performance of an active tactile discrimination task,” *Exp Brain Res*, vol. 87, no. 2, Nov. 1991, doi: 10.1007/BF00231849.
- [25] Å. B. Vallbo, “Microneurography: how it started and how it works,” *J Neurophysiol*, vol. 120, no. 3, pp. 1415–1427, Sep. 2018, doi: 10.1152/jn.00933.2017.
- [26] A. Shamsuzzaman, “Microneurography,” in *Encyclopedia of the Neurological Sciences*, Elsevier, 2014, pp. 6–10. doi: 10.1016/B978-0-12-385157-4.00504-2.
- [27] C. D. Binnie and P. F. Prior, “Electroencephalography.,” *J Neurol Neurosurg Psychiatry*, vol. 57, no. 11, pp. 1308–1319, Nov. 1994, doi: 10.1136/jnnp.57.11.1308.
- [28] A. Biasiucci, B. Franceschiello, and M. M. Murray, “Electroencephalography,” *Curr Biol*, vol. 29, no. 3, pp. R80–R85, Feb. 2019, doi: 10.1016/J.CUB.2018.11.052.
- [29] R. Nieuwenhuys, J. Voogd, and C. van Huijzen, *The Human Central Nervous System*. Berlin, Heidelberg: Springer Berlin Heidelberg, 2008. doi: 10.1007/978-3-540-34686-9.
- [30] T. Hansson and T. Brismar, “Tactile stimulation of the hand causes bilateral cortical activation: a functional magnetic resonance study in humans,” *Neurosci Lett*, vol. 271, no. 1, pp. 29–32, Aug. 1999, doi: 10.1016/S0304-3940(99)00508-X.
- [31] C. Genna *et al.*, “Spatiotemporal Dynamics of the Cortical Responses Induced by a Prolonged Tactile Stimulation of the Human Fingertips,” *Brain Topogr*, vol. 30, no. 4, pp. 473–485, Jul. 2017, doi: 10.1007/s10548-017-0569-8.
- [32] C. M. Oddo, L. Beccai, N. Vitiello, H. B. Wasling, J. Wessberg, and M. C. Carrozza, “A mechatronic platform for human touch studies,” *Mechatronics*, vol. 21, no. 3, pp. 604–613, Apr. 2011, doi: 10.1016/j.mechatronics.2011.02.012.
- [33] G. A. Gescheider, *Psychophysics*. Psychology Press, 2013. doi: 10.4324/9780203774458.
- [34] Nigel Holt, Andy Bremner, Ed Sutherland, Michael Vliek, Michael Passer, and Ronald Smith, *Psychology: the Science of Behaviour*, 4th ed. 2019.

- [35] S. J. Lederman and R. A. Browse, “The Physiology and Psychophysics of Touch,” in *Sensors and Sensory Systems for Advanced Robots*, Berlin, Heidelberg: Springer Berlin Heidelberg, 1988, pp. 71–91. doi: 10.1007/978-3-642-83410-3_4.
- [36] W. H. Ehrenstein and A. Ehrenstein, “Psychophysical Methods,” in *Modern Techniques in Neuroscience Research*, Berlin, Heidelberg: Springer Berlin Heidelberg, 1999, pp. 1211–1241. doi: 10.1007/978-3-642-58552-4_43.
- [37] G. K. Essick, A. James, and F. P. McGlone, “Psychophysical assessment of the affective components of non-painful touch,” *Neuroreport*, vol. 10, no. 10, pp. 2083–2087, Jul. 1999, doi: 10.1097/00001756-199907130-00017.
- [38] A. W. Goodwin, J. W. Morley, C. Clarke, B. Lumaksana, and I. Darian-Smith, “A stimulator for moving textured surfaces sinusoidally across the skin,” *J Neurosci Methods*, vol. 14, no. 2, pp. 121–125, Jul. 1985, doi: 10.1016/0165-0270(85)90124-4.
- [39] K. O. Johnson and J. R. Phillips, “A rotating drum stimulator for scanning embossed patterns and textures across the skin,” *J Neurosci Methods*, vol. 22, no. 3, pp. 221–231, Jan. 1988, doi: 10.1016/0165-0270(88)90043-X.
- [40] Y.-C. Pei, T.-C. Lee, T.-Y. Chang, D. Ruffatto, M. Spenko, and S. Bensmaia, “A multi-digit tactile motion stimulator,” *J Neurosci Methods*, vol. 226, pp. 80–87, Apr. 2014, doi: 10.1016/j.jneumeth.2014.01.021.
- [41] Y.-C. Pei *et al.*, “Cross-Modal Sensory Integration of Visual-Tactile Motion Information: Instrument Design and Human Psychophysics,” *Sensors*, vol. 13, no. 6, pp. 7212–7223, May 2013, doi: 10.3390/s130607212.
- [42] Calogero Oddo, “Neuro-Robotic Touch Laboratory.” Accessed: Sep. 29, 2023. [Online]. Available: <https://www.santannapisa.it/en/institute/biorobotics/neuro-robotic-touch-laboratory>
- [43] I. Birznieks, P. Jenmalm, A. W. Goodwin, and R. S. Johansson, “Encoding of Direction of Fingertip Forces by Human Tactile Afferents,” *The Journal of Neuroscience*, vol. 21, no. 20, pp. 8222–8237, Oct. 2001, doi: 10.1523/JNEUROSCI.21-20-08222.2001.
- [44] C. M. Oddo *et al.*, “Intraneural stimulation elicits discrimination of textural features by artificial fingertip in intact and amputee humans,” *Elife*, vol. 5, Mar. 2016, doi: 10.7554/eLife.09148.
- [45] T. Yoshioka, B. Gibb, A. K. Dorsch, S. S. Hsiao, and K. O. Johnson, “Neural Coding Mechanisms Underlying Perceived Roughness of Finely Textured Surfaces,” *The Journal of Neuroscience*, vol. 21, no. 17, pp. 6905–6916, Sep. 2001, doi: 10.1523/JNEUROSCI.21-17-06905.2001.
- [46] MaxonMotor Group, “RE 35 Ø35 mm, Graphite Brushes, 90 Watt,” MaxonMotor Group.
- [47] ATI Industrial Automation, “Nano43, ATI IA Force/Torque Sensor System.” Accessed: Sep. 29, 2023. [Online]. Available: https://www.ati-ia.com/products/ft/ft_models.aspx?id=nano43
- [48] Maxon Group, “Encoder MR, Type L, 1024 CPT, 3 Channels, with Line Driver.” Accessed: Sep. 29, 2023. [Online]. Available: <https://www.maxongroup.com/maxon/view/product/225787>
- [49] SKF, “LTP 60.180.0804-02, SKF Multitec linear guide” Accessed: Sep. 29, 2023. [Online]. Available: <https://www.skf.com/pt>
- [50] National Instruments, “sbRIO-9637,” 2023 Accessed: Sep. 29, 2023. [Online]. Available: <https://www.apexwaves.com/pdfs/sbrio-9637-user-manual.pdf>
- [51] K. Sharma, “Instrumentation Subsystem,” in *Overview of Industrial Process Automation*, Elsevier, 2011, pp. 25–39. doi: 10.1016/B978-0-12-415779-8.00003-6.

- [52] P. Wilson, “Digital Circuits,” in *The Circuit Designer’s Companion*, Elsevier, 2017, pp. 259–320. doi: 10.1016/B978-0-08-101764-7.00006-2.
- [53] Quanser, “A12-437-1 Linear Current Amplifier Module LCAM-1,” 2023 Accessed: Sep. 29, 2023. [Online]. Available: <https://www.quanser.com/>
- [54] Texas Instruments, “OPA547T - Texas Instruments.” Accessed: Sep. 29, 2023. [Online]. Available: https://www.ti.com/lit/ds/symlink/opa547.pdf?HQS=dis-dk-null-digikeymode-dsf-pf-null-ww&ts=1695838602906&ref_url=https%253A%252F%252Fwww.ti.com%252Fgeneral%252Fdocs%252Fsuppproductinfo.tsp%253FdistId%253D10%2526gotoUrl%253Dhttps%253A%252F%252Fwww.ti.com%252Flit%252Fgpn%252Fopa547
- [55] Merlin Gerin, “MERLIN GERIN MULTI9 C60HB 25844 B16 16A 16 AMP MCB C ,” MCBs.UK. Accessed: Sep. 29, 2023. [Online]. Available: <https://www.mcbs.uk/mcbs/merlin-gerin-multi9-c60hb-25844-b16-16a-16-amp-mcb-circuit-breaker-type-b-detail.html>
- [56] ABB Electrification US, “Function and operation of circuit breakers.” Accessed: Sep. 29, 2023. [Online]. Available: <https://electrification.us.abb.com/circuit-breaker-basics>
- [57] Leela Prasad, “Ground vs Neutral | Learn the Differences between Ground and Neutral.” Accessed: Sep. 29, 2023. [Online]. Available: <https://www.electronicshub.org/ground-vs-neutral/>
- [58] Pragya Chauhan, “AC to DC Converters: Features, Design & Applications.” Accessed: Sep. 29, 2023. [Online]. Available: https://how2electronics.com/ac-to-dc-converters-features-design-applications/#google_vignette
- [59] Devan Thakur, “How to convert from AC to DC?” Accessed: Sep. 29, 2023. [Online]. Available: <https://www.geeksforgeeks.org/how-to-convert-from-ac-to-dc/>
- [60] D. H. Krantz, “Fundamental Measurement of Force and Newton’s First and Second Laws of Motion,” *Philos Sci*, vol. 40, no. 4, pp. 481–495, Dec. 1973, doi: 10.1086/288560.
- [61] C. A. Goldfarb, A. O. Gee, L. K. Heinze, and P. R. Manske, “Normative Values for Thumb Length, Girth, and Width in the Pediatric Population,” *J Hand Surg Am*, vol. 30, no. 5, pp. 1004–1008, Sep. 2005, doi: 10.1016/j.jhsa.2005.02.017.
- [62] M. J. Adams *et al.*, “Finger pad friction and its role in grip and touch,” *J R Soc Interface*, vol. 10, no. 80, p. 20120467, Mar. 2013, doi: 10.1098/rsif.2012.0467.

8. Appendix

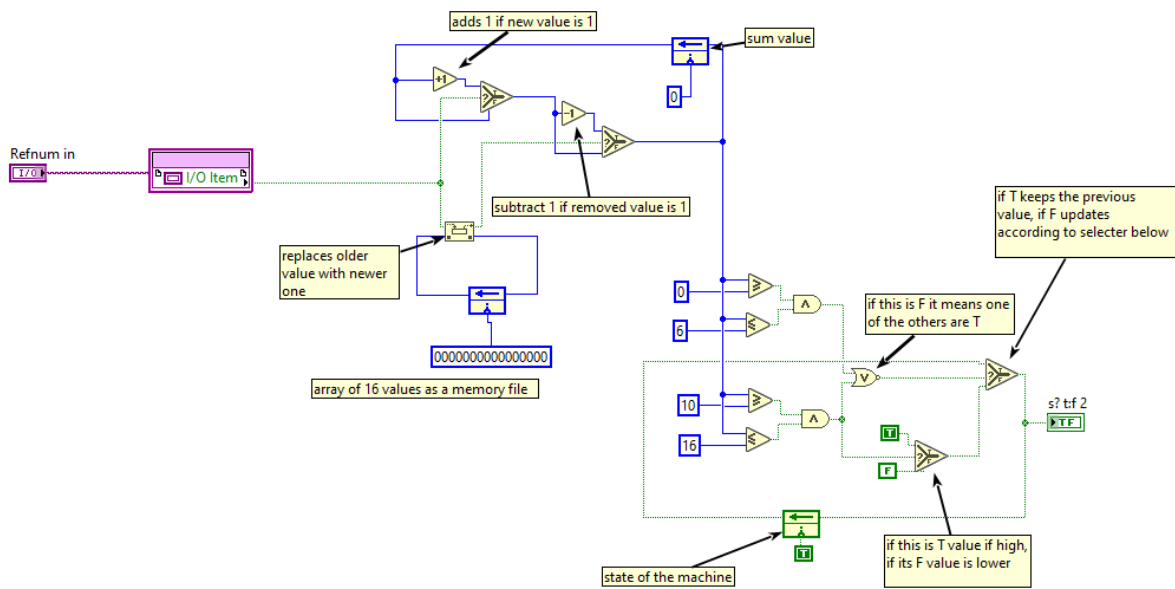


Figure 8-1 Code on LabVIEW to filter to remove random fluctuation in data. This filter adds the 16 latest values outputted by the encoder and relays the states the encoder is at depending on the thresholds implemented. Sum lower or equal to 6 is a low wave, higher or equal to 10 is a high wave, in the middle keeps the previous value until a threshold is meet.

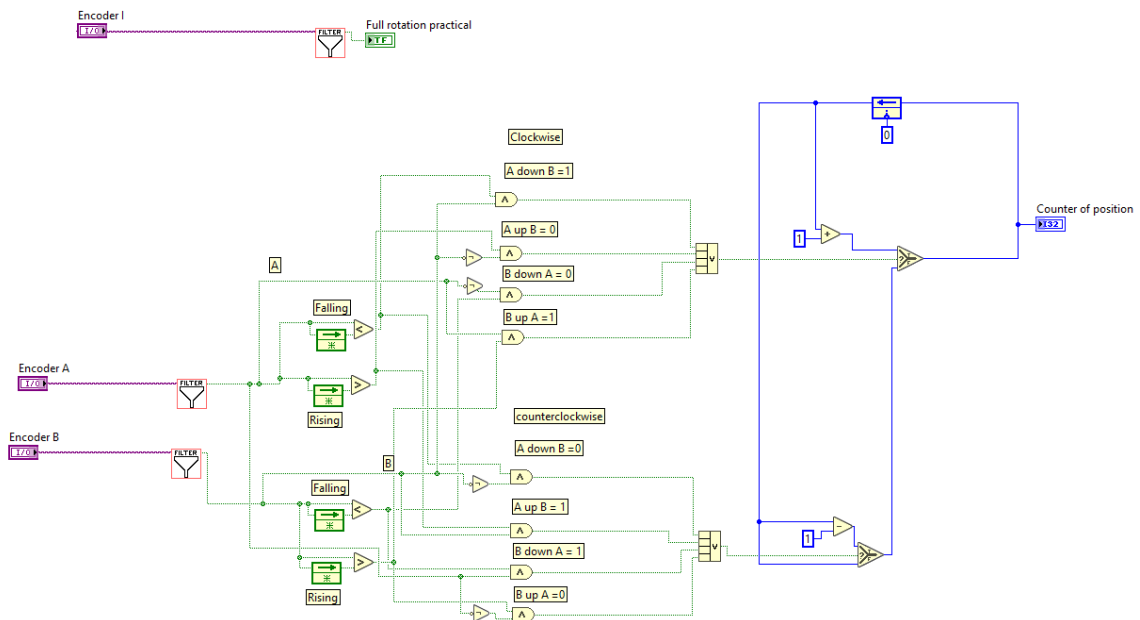


Figure 8-2 Code in LabVIEW for counter of elapsed states, this code adds one to a counter if a clockwise patten is meet and subtracts one if a counterclockwise patten in the square waves is meet.

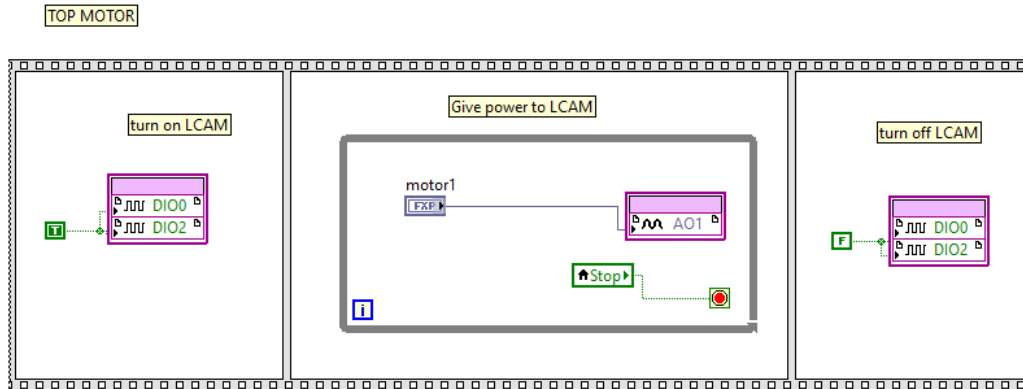


Figure 8-3 Sequence structure used in both controllers to output a signal voltage to the LCAM to power the drum motor. This sequence first enables the LCSM then powers the motor and latter disables it.

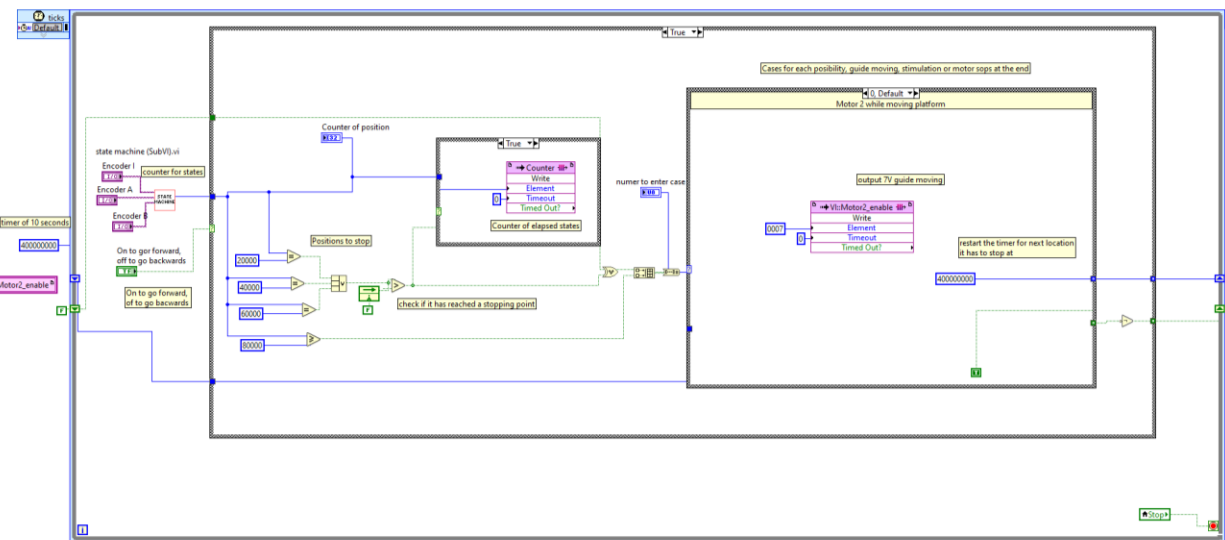


Figure 8-4 Sequential stimuli selector code on LabVIEW. This code moves the stimulator forward stopping at each preselected location for tactile stimulation to occur. At the end of the slider the stimulator returns to the begging position and the cycle repeats. This image displays the case where the motor moves forward.

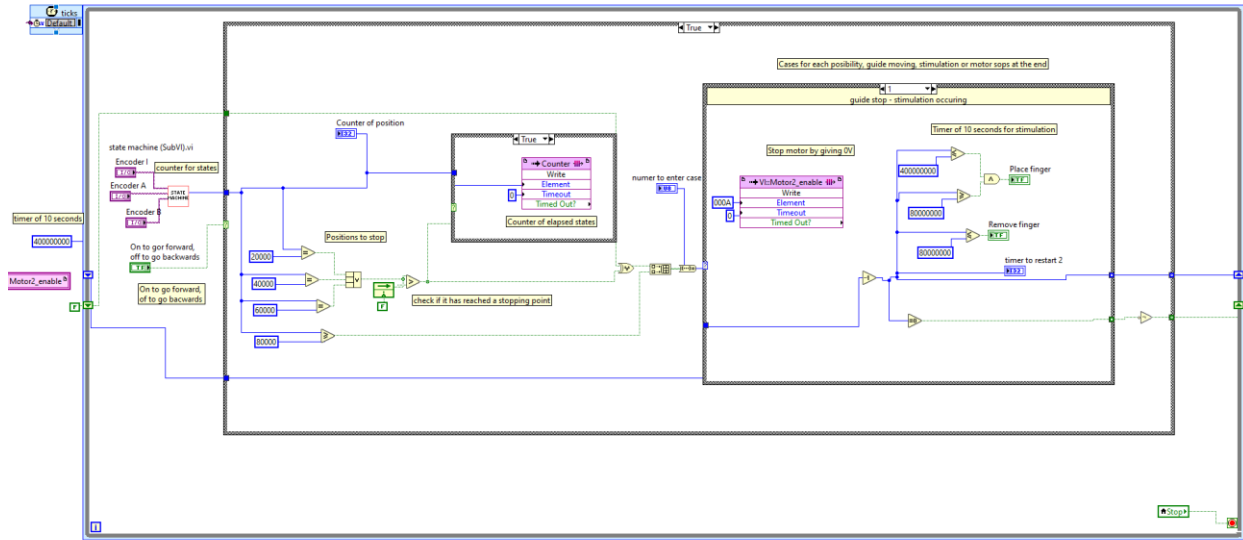


Figure 8-5 Sequential stimuli selector code on LabVIEW. This code moves the stimulator forward stopping at each preselected location for tactile stimulation to occur. At the end of the slider the stimulator returns to the beginning position and the cycle repeats. This image displays the case where the motor stops and stimulation occur.

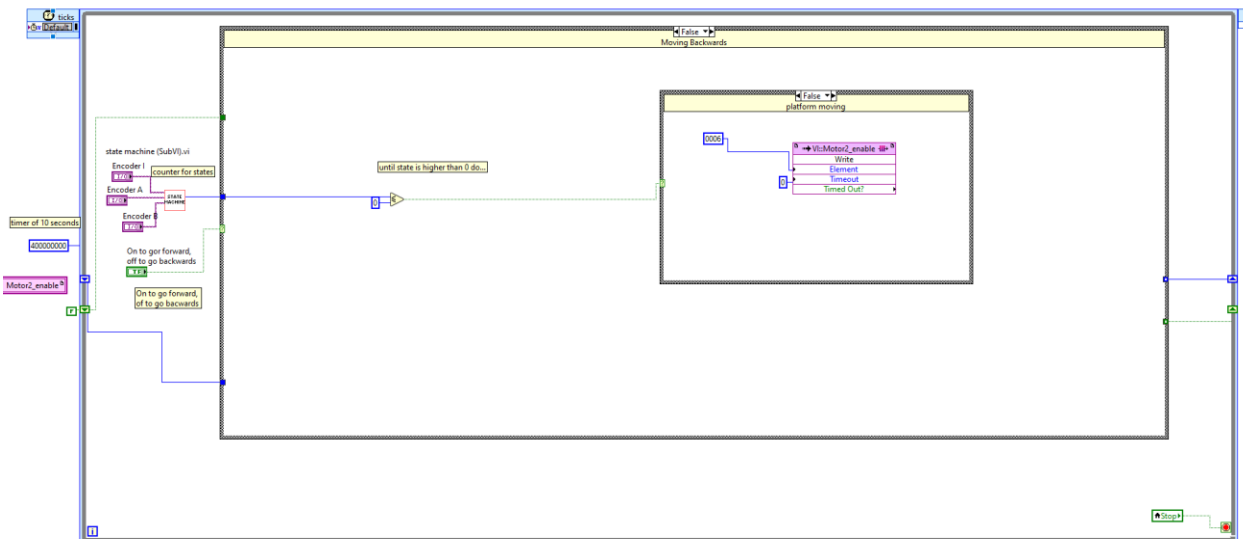


Figure 8-6 Sequential stimuli selector code on LabVIEW. This code moves the stimulator forward stopping at each preselected location for tactile stimulation to occur. At the end of the slider the stimulator returns to the beginning position and the cycle repeats. This image displays the case where the motor moves backwards.

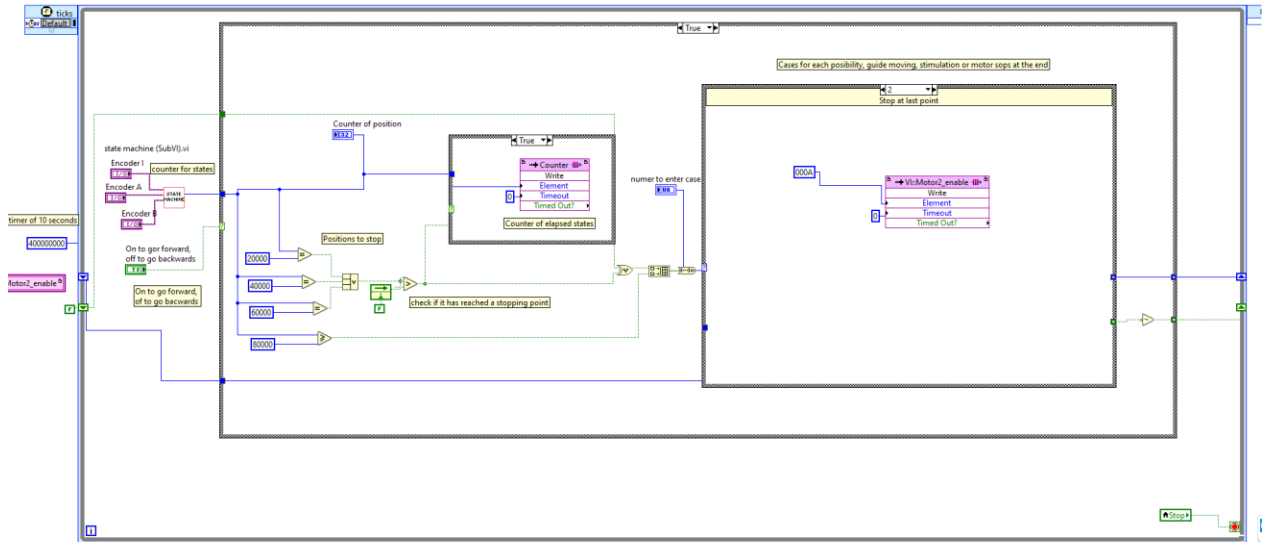


Figure 8-7 Sequential stimuli selector code on LabVIEW. This code moves the stimulator forward stopping at each preselected location for tactile stimulation to occur. At the end of the slider the stimulator returns to the beginning position and the cycle repeats. This image displays the case where the motor stops at the last marker.

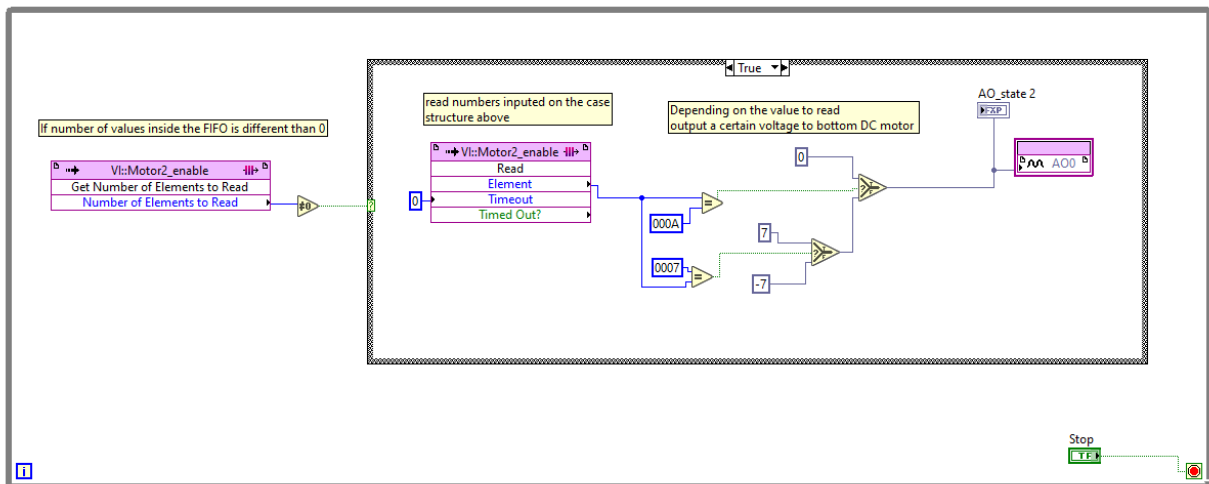


Figure 8-8 Parallel while loop used to output a signal voltage to the buffer which will power the guide motor. This code reads the values from a FIFO and depending on the value outputs a specific signal voltage to AO0. Used in “sequential stimuli selector”.

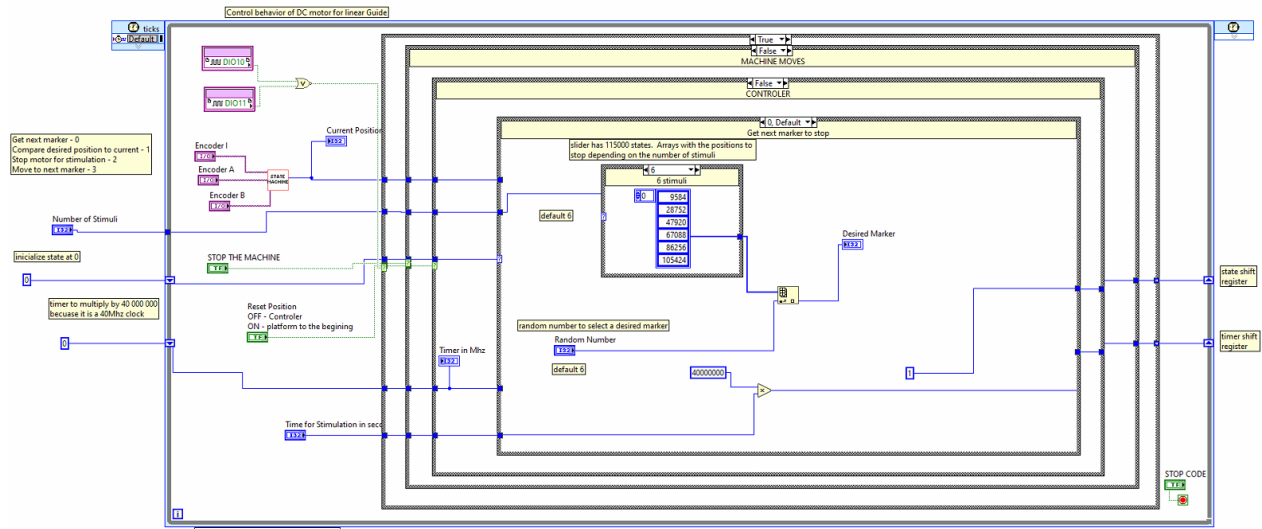


Figure 8-9 Random stimuli selector code done on LabVIEW. This codes randomly selects a stimulus to be used for stimulation, after this the controller verifies if the stimulator is in the right location considering the chosen stimulus. If not, it moves the stimulator until that position and then stops the motor for stimulation to occur. After this the controller gets a new random stimulus and the cycle repeats. This case displays the “get next random stimulus” structure.

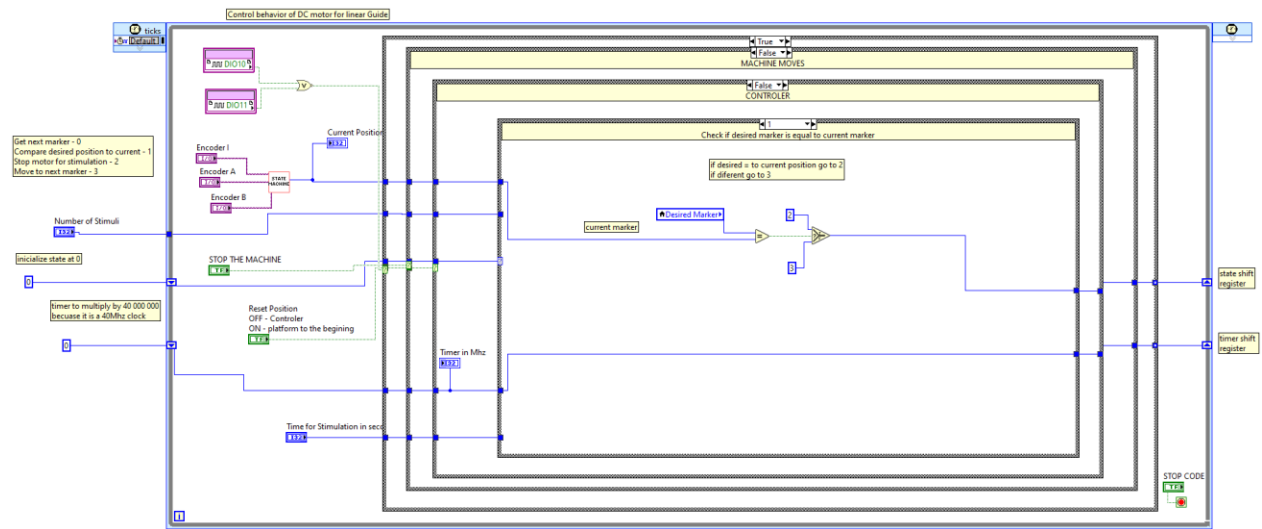


Figure 8-10 Random stimuli selector code done on LabVIEW. This codes randomly selects a stimulus to be used for stimulation, after this the controller verifies if the stimulator is in the right location considering the chosen stimulus. If not, it moves the stimulator until that position and then stops the motor for stimulation to occur. After this the controller gets a new random stimulus and the cycle repeats. This case displays the “compare current desired stimulus” structure.

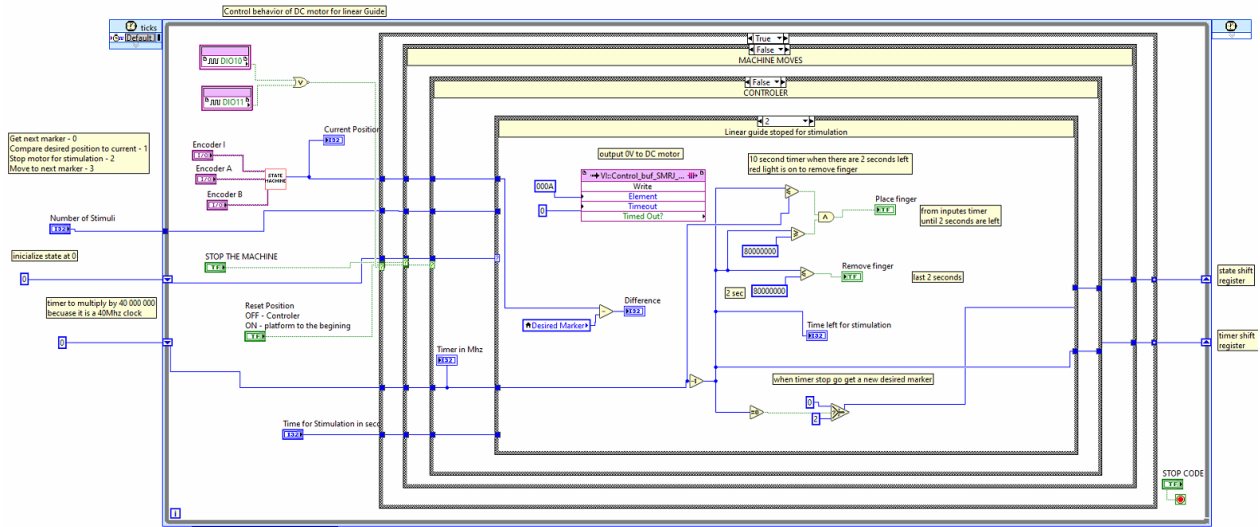


Figure 8-11 Random stimuli selector code done on LabVIEW. This codes randomly selects a stimulus to be used for stimulation, after this the controller verifies if the stimulator is in the right location considering the chosen stimulus. If not, it moves the stimulator until that position and then stops the motor for stimulation to occur. After this the controller gets a new random stimulus and the cycle repeats. This case displays the “stimulation case” structure.

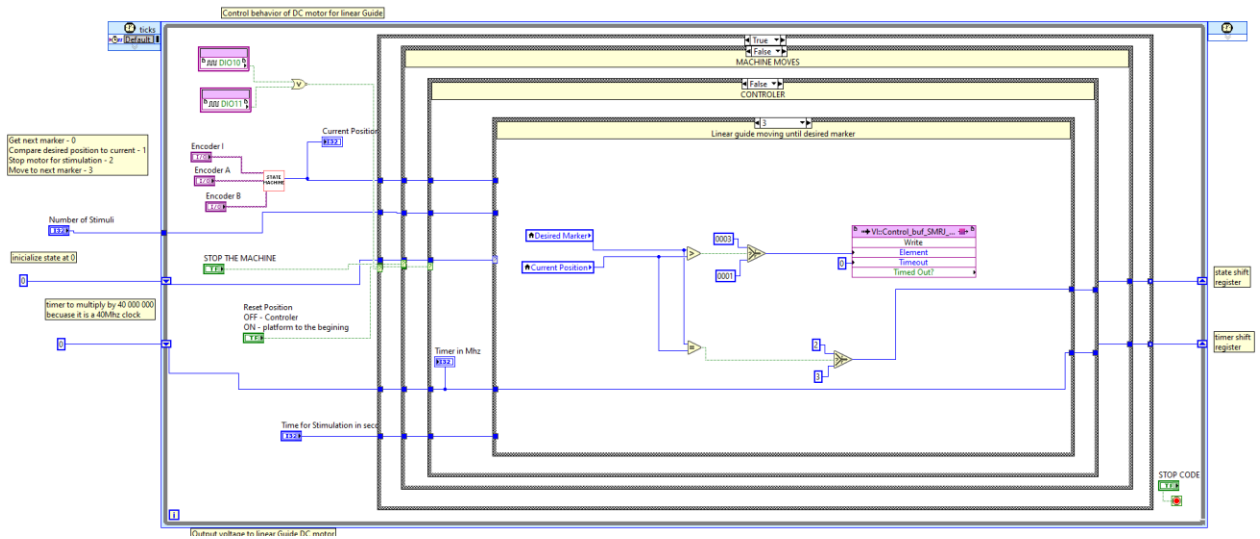


Figure 8-12 Random stimuli selector code done on LabVIEW. This codes randomly selects a stimulus to be used for stimulation, after this the controller verifies if the stimulator is in the right location considering the chosen stimulus. If not, it moves the stimulator until that position and then stops the motor for stimulation to occur. After this the controller gets a new random stimulus and the cycle repeats. This case displays the “move stimulator case” structure.

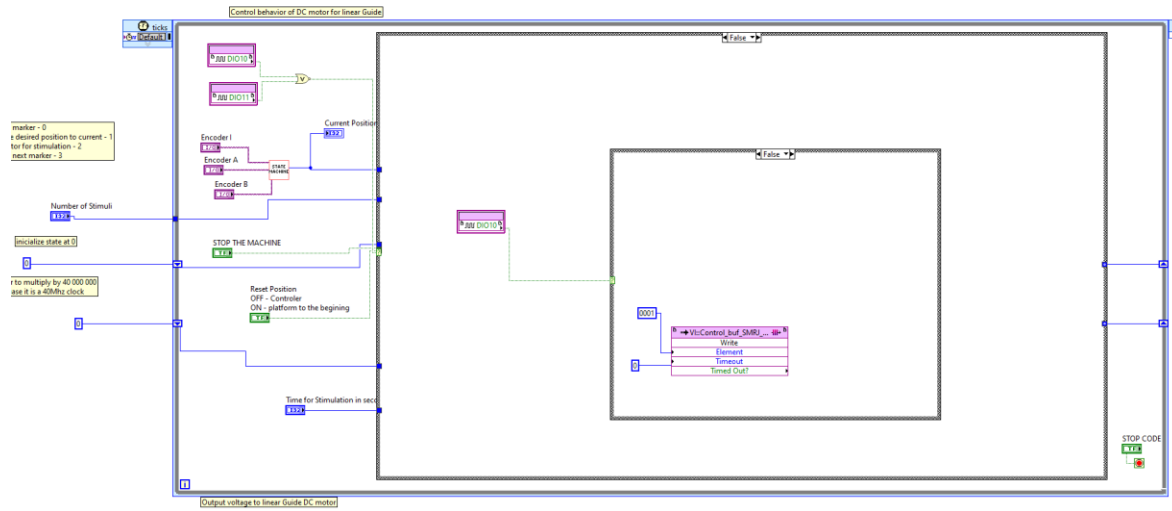


Figure 8-13 Random stimuli selector code done on LabVIEW. This codes randomly selects a stimulus to be used for stimulation, after this the controller verifies if the stimulator is in the right location considering the chosen stimulus. If not, it moves the stimulator until that position and then stops the motor for stimulation to occur. After this the controller gets a new random stimulus and the cycle repeats. This case displays the safety measure used to both initiate the platform always in the same position and to prevent it from going moving past the workspace delimited by the limit switches (the false case push the motor back not to touch the end point and the TRUE case forces it forward to not touch the start point).

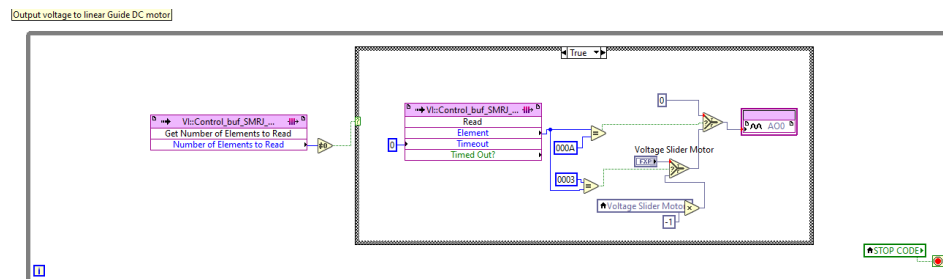


Figure 8-14 Parallel while loop used to output a signal voltage to the buffer which will power the guide motor. This code reads the values from a FIFO and depending on the value outputs a specific signal voltage to A00. Used in "random stimuli selector".

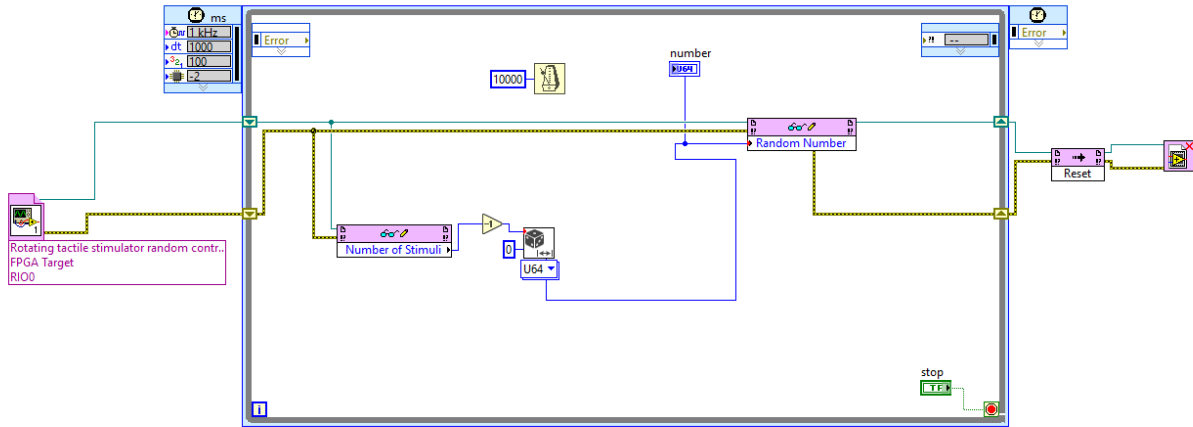


Figure 8-15 "random number generator V4.5" code. This code generates a random number from 0 to the specified in the "number of stimuli" control in the "random stimuli selector" code. This number is then sent to the "random stimulus selector" code and used to decide the next desired stimulus.

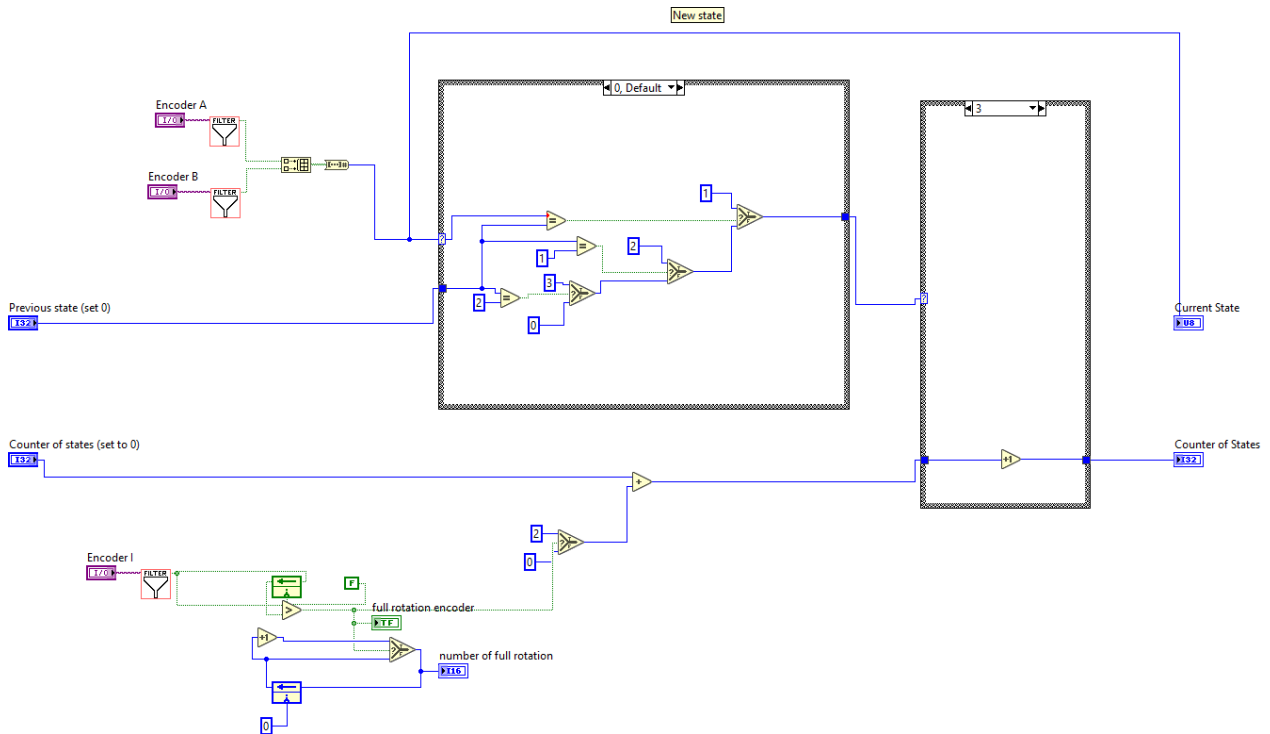


Figure 8-16 Alternative state counter, using a Boolean array converted to number to identify the state 00-0, 01-1, 11-3, 10-2. The current states are then compared to the previous state by equal functions and depending on this comparison the code will either increases one to a counter, subtract or do nothing. This variation in behavior is dependent on the direction of rotation, since the previous state to any current state can have to options, depending on the rotation.

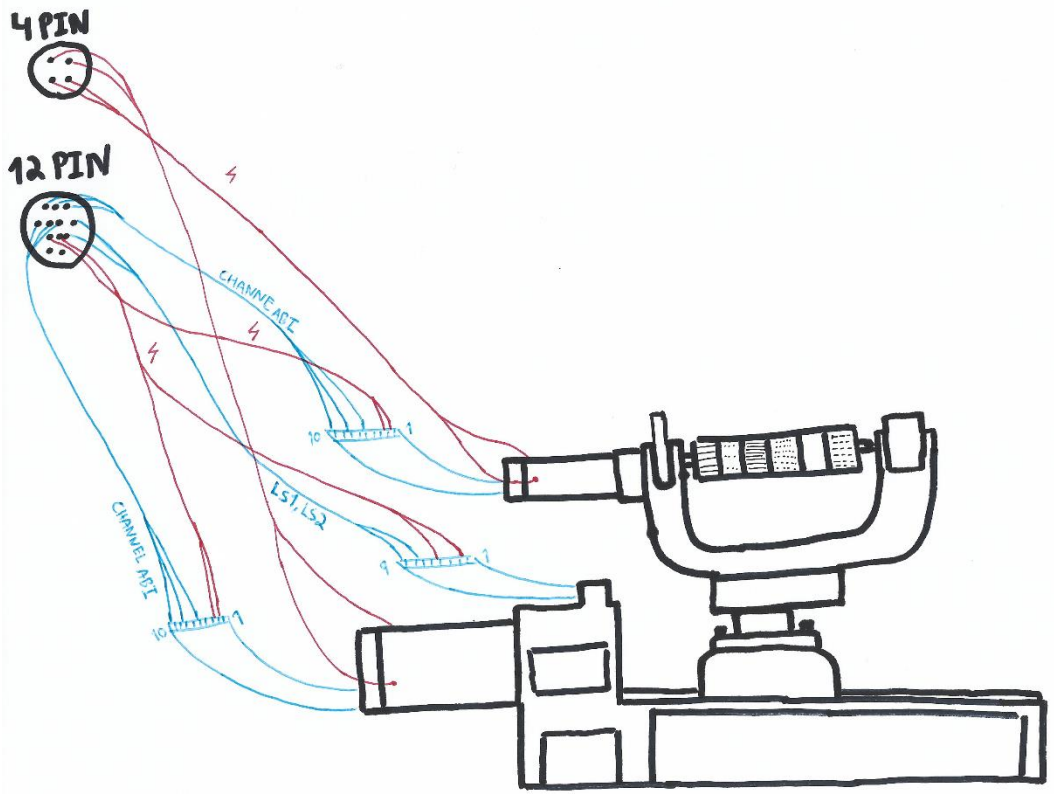
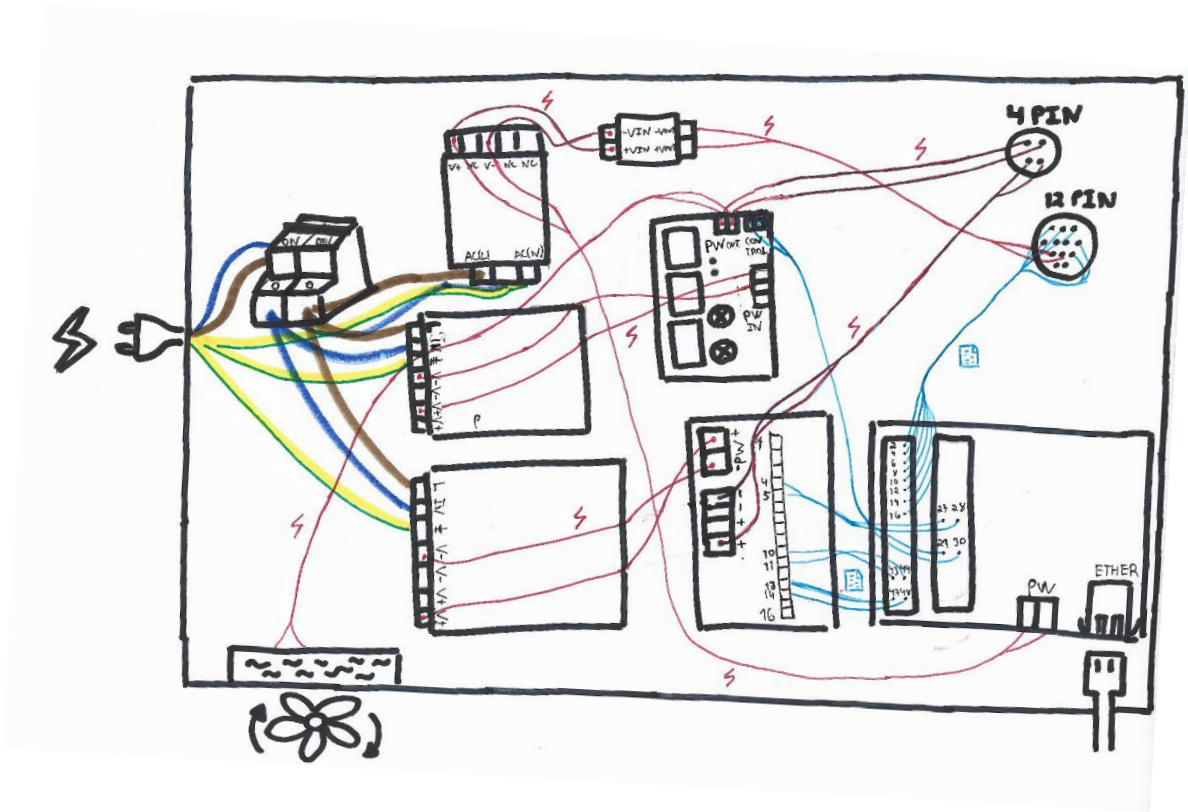


Figure 8-17 Manual drawing off all the power and data connections between components with the pins used for each connection.